Dynamics of Blockchain Mining and Painlevé Integrability

By

Cengiz Gazi

Supervised by Jan de Gier

Submitted in Partial Fulfilment
of the Requirements for the Degree
Master of Science in the
School of Mathematics and Statistics

University of Melbourne

October 2023

Abstract

We study a blockchain mining model that assumes the form of a nonlinear differential-difference equation. Numerical evidence indicates that at late times solutions converge to a travelling wave with constant speed. We conjecture a wave speed formula of this travelling wave which agrees with numerical evidence.

This model can be approximated by a modified non-linear Fisher-KPP differential equation, which provides further confirmation of our conjectured wave speed and also has an exact solution as a direct consequence of Painlevé integrability. The exact solution is shown to be a good approximation of the numerical blockchain solution in the fast mining regime. We elaborate on the relationship between the Painlevé equations and integrable systems. In particular, we detail the theory concerning isomondoromic deformations of meromorphic linear systems.

Acknowledgements

I would like to thank my supervisor, Professor Jan de Gier, for his patience, insight and consistent unwavering support. I have been quite lucky to work under such a mathematician who is well accomplsihed and knowledgable within their field.

I would also like to thank Professor Peter Taylor for his multiple helpful discussions concerning the mathematics of blockchain mining. Also thanks to Dr Hailon Guo for his recommendations and insight regarding numerical mathematics.

Contents

1 Introduction

We study a blockchain mining model that was introduced recently in [1] whereby the authors built upon previous models of the blockchain forking process [2, 3] to consider *fast mining* blockchains. In a *fast mining* blockchain the mean time to mine a block is faster than the time it takes for the block to be communicated to another miner and for that miner to validate it, termed *propagation delay*. The authors of [1] developed a simple continuous-time Markov chain (CTMC), which we denote *Model 1*, to examine whether the network of miners ever reach consensus. The numerical simulations of the algorithm described in [1] suggest that no matter how far the local blockchains diverge, they will almost surely return to consensus in finite expected time.

The accompanying talk [4] detailed a second model, which we denote *Model 2*, which models the time an arbitrary miner spends at each height of the blockchain. The model takes the form of an infinite system of nonlinear ODE's whose solutions are probability mass functions of local blockchain heights at time t. If one instead looks at the proportion of miners at time t with height at most n, or equivalently, the cumulative distribution function of local blockchain heights up to height n, then the solutions are wave fronts which propagate forward as one iterates through the system of equations. In [1, 4] it was conjectured that these wave fronts approach a limiting travelling wave that does not spread out for any rate of *propagation delay*. A direct consequence of this is that there exists a speed of travel of this limiting wave profile. We introduce the models described in [1, 4] which form a starting point for this thesis.

1.1 Model 1

We begin by describing a blockchain mining model, adapted from [1]. Consider a blockchain with N miners and suppose blocks are mined at uniformly randomly selected miners at the instants of a Poisson process with parameter $\lambda > 0$. Thus, each miner is mining at rate λ. We identify each newly mined block with a unique label $b \in \mathbb{Z}_{\geq 1}$, where at time t, the n^{th} miner has a sequence

$$B_n(t) = (b_1^{(n)}, ..., b_{j_n}^{(n)})$$

of connected blocks, $b_j^{(n)} \in \mathbb{Z}_{\geq 1}$, which we call its local blockchain. We say this miner has a local blockchain of j_n blocks which we call its height.

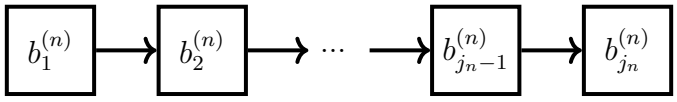

From this we define the state of the network of miners at time t as the N-tuple of local blockchains $B_i(t)$:

$$B(t) = (B_1(t), ..., B_N(t)).$$

As described in [1], miners are able to communicate their local blockchains to other miners. To be precise, we say each miner communicates their local blockchain to the network at rate $\omega > 0$. This represents the block propagating through the peer-to-peer network. Furthermore, we define the network of miners to be in consensus at time t when there exists a block $b \in \mathbb{Z}_{\geq 1}$ such that the last mined block of $B_i(t)$ is b for all $i = 1, ..., N$. This is basically saying that every miner acknowledges the last block mined hence in consensus.

Assuming the Markov property we define our transition rates as follows.

- The n^{th} miner mines a new block b

$$q((B_1, ..., B_n, ..., B_N), (B_1, ..., B_n + b, ..., B_N)) = \lambda,$$

  with b the extra block appended to B_n.

- The n^{th} miner communicates their block to the m^{th} miner

$$q((B_1, ..., B_n, ..., B_m, ..., B_N), (B_1, ..., B_n, ..., B_n, ..., B_N)) = \frac{\omega}{N-1},$$

  if B_n is longer than B_m.

- Return to consensus

$$q((B, ..., B, B_m, B, ..., B), (b, ..., b, b, b, ..., b)) = \omega,$$

  if B is longer than B_m where (b is the final block in B).

Remark 1.1. *When the n^{th} miner communicates their local blockchain to the m^{th} miner, the local blockchain of the m^{th} miner will become that of the n^{th} miner. For this reason, we only require the head block of each miner's local blockchain to model the system (including consensus). That is, the head block of each local blockchain is uniquely determined by the local blockchain and vice versa.*

There is always a sequence of at least one block at the beginning of each local blockchain that the network agrees on. We consider the last block of this sequence to be the highest block in the local blockchains when they were last in consensus. It follows that each state $B(t)$ corresponds to a tree, we denote the blocktree.

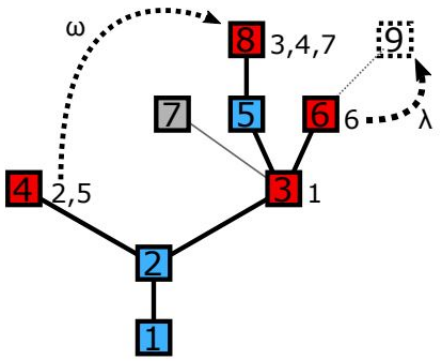

Figure 1.1: An example of a blocktree with mining and communication transition shown. Source: [1]. The local blockchains corresponding to this blocktree are presented in the following table.

Miner(s)	**Local Blockchain**	**Height**
1	1 2 3	3
2,5	1 2 4	3
3,4,7	1 2 3 5 8	5
6	1 2 3 6	4

Table 1.1: The local blockchains of the blocktree of Figure 1.1

In view of Remark 1.1, the corresponding state in the CTMC of Model 1 is

$$B(t) = (3, 4, 8, 8, 4, 6, 8)$$

Example 1. Suppose some time has passed and, in view of Figure 1.1, miner 6 mined block 9 while miner's 3,4 or 7 communicated their local blockchain to miner's 2 and 5. The resulting network will be

Miner(s)	**Local Blockchain**	**Height**
2,3,4,5,7	1 | 2 | 3 | 5 | 8	5
6	1 | 2 | 3 | 6 | 9	5
1	1 | 2 | 3	3

The corresponding state in the CTMC of Model 1 is

$$B(t) = (3, 8, 8, 8, 8, 9, 8).$$

Example 2. Now suppose, instead, miner's 3,4 or 7 communicated their local blockchain to miner's 1,2,5 and 6 before anything else happens. Then the blocktree of Figure 1.1 will collapse to a blockchain with every miner having the same local blockchain given by

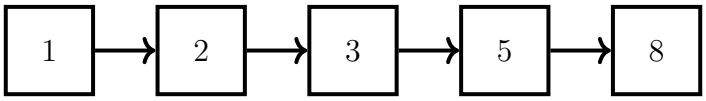

The corresponding state in the CTMC of Model 1 is

$$B(t) = (8, 8, 8, 8, 8, 8, 8),$$

which represents a consensus state.

A key result of [1] was that the consensus state of Model 1 is positive recurrent. Or put otherwise, the expected time to return to a consensus state is bounded above for all time $t > 0$.

Proposition 1.2. *Given $\omega > 0$ the consensus state in the CTMC of Model 1 is positive recurrent.*

Proof. See [1] □

Remark 1.3. *The proof of Proposition 1.2 follows by observing that whatever state the system is in, if one of the miner(s) with the longest local blockchain mines a new block and is able to communicate it to every other miner before anything else happens, then the model will be in consensus. This event has non-zero probability in every state and hence will occur in finite expected time.*

1.2 Model 2

Another way to study this model was discussed in [4]. Instead of looking at the transition rates between the N-tuple states of local blockchains, we can study the time each miner spends at each height of the blockchain. In this model we choose the convention to not include the first (genesis) block in this height. So for a local blockchain with n blocks (including the genesis block), we say this local blockchain has a height of $n - 1$.

1.2.1 The Probability Mass Function

We define for $i \geq 0$, $\theta_i(t)$ to be the proportion of miners, from N total miners, whose local blockchain has height equal to i at time t. So then the number of miners whose local blockchain has height equal to i at time t is given by $N\theta_i(t)$. Hence the state

$$\boldsymbol{\theta}(t) = (\theta_0(t), \theta_1(t), \theta_2(t), ...),$$

is a random variable that can be thought of as the (random) probability mass function of local blockchain heights at time t where each $\theta_i(t)$ is clearly a multiple of $1/N$. The probability normalisation $\sum_{i=0}^{\infty} \theta_i(t) = 1$ follows.

At time $t = 0$ every miner starts on the genesis block and has a local blockchain height of zero. Hence we have the initial condition

$$\boldsymbol{\theta}(0) = (\theta_0(0), \theta_1(0), \theta_2(0), ...) = (1, 0, 0, ...)$$

We define our Markov chain transition rates as follows.

- A miner of local blockchain height i mines a new block

$$q((\theta_0(t), ..., \theta_i(t), \theta_{i+1}(t), ...), (\theta_0(t), ..., \theta_i(t) - 1/N, \theta_{i+1}(t) + 1/N, ...)) = \lambda N\theta_i(t).$$

- A miner of local blockchain height i communicates their height to a miner with shorter local blockchain height j

$$q((\theta_0(t), ..., \theta_j(t), ..., \theta_i(t), ...), (\theta_0(t), ..., \theta_j(t) - 1/N, ..., \theta_i(t) + 1/N, ...)) = \frac{\omega}{N-1} N\theta_i(t) N\theta_j(t).$$

This is a density-dependent Markov chain.

Following [1], if we take $N \to \infty$, we can use some well known results of Kurtz [5] (for models with finitely-many compartments) and Barbour and Luczak [6](for the extension to countably-many compartments) to show that the sample paths of the sequence of Markov chains satisfy a Functional Law of Large Numbers, which takes the form of a deterministic set of ordinary differential equations

$$\frac{d\boldsymbol{\theta}(t)}{dt} = \sum_{i=0}^{\infty} \lambda\theta_i(t)(\boldsymbol{e}_{i+1} - \boldsymbol{e}_i) + \sum_{i=0}^{\infty} \sum_{j=i+1}^{\infty} \omega\theta_j(t)\theta_i(t)(\boldsymbol{e}_j - \boldsymbol{e}_i),$$

where $\boldsymbol{e}_i = (0, ..., 0, 1, 0, ...)$ is the $(i+1)^{th}$ unit vector and $\boldsymbol{\theta}(0) = (\theta_1(0), \theta_2(0), ...) = \boldsymbol{e}_1$.

The components of this infinite system of differential equations are

$$\frac{d\theta_0(t)}{dt} = -\lambda\theta_0(t) - \omega\theta_0(t) \sum_{j=1}^{\infty} \theta_j(t) = -\lambda\theta_0(t) - \omega\theta_0(t)(1 - \theta_0(t)), \tag{1.1}$$

and for $i \geq 1$

$$\frac{d\theta_i(t)}{dt} = \theta_i(t)[-\lambda - \omega \sum_{j=i+1}^{\infty} \theta_j(t)] + \lambda\theta_{i-1}(t) + \omega\theta_i(t) \sum_{j=1}^{i-1} \theta_j(t), \tag{1.2}$$

with initial conditions $\theta_0(0) = 1$ and $\theta_i(0) = 0$ for all $i \geq 1$.

No communication regime. Although difficult to analyse directly, a simplification occurs when we consider the regime of no communication between miners. In this regime we have $\omega = 0$ and so these equations (1.1),(1.2) reduce to

$$\frac{d\theta_0(t)}{dt} = -\lambda\theta_0(t), \tag{1.3}$$

and for $i \geq 1$

$$\frac{d\theta_i(t)}{dt} = -\lambda(\theta_i(t) - \theta_{i-1}(t)), \tag{1.4}$$

with initial conditions $\theta_0(0) = 1$, $\theta_i(0) = 0$ for $i \geq 1$ and $\theta_{-1}(t) = 0$ for $t \geq 0$.

An immediate application of proof by induction shows the solution is

$$\theta_n(t) = \frac{1}{n!}(\lambda t)^n e^{-\lambda t}, \tag{1.5}$$

which is the probability mass function of a Poisson random variable with mean λt and support $n \in \mathbb{N}_{\geq 0}$.

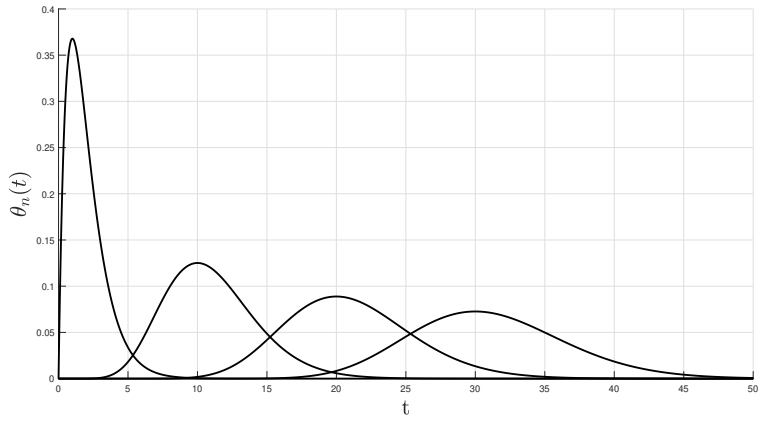

Figure 1.2: Plots of $\theta_n(t)$ for $n = 1, 10, 20, 30$ with $\lambda = 1, \omega = 0$. Solutions moving to the right for increasing n.

In Figure 1.2 we see that the distribution of miners at each height of their the local blockchains spreads out in the limit $t \to \infty$. As a function of time t, the mean of the distributions $\theta_n(t)$ travels with speed λ. The standard deviation is $\sqrt{\lambda t}$ which implies that the distribution spreads out at rate $\sqrt{t}$ during travel. Hence there is no convergence to a soliton solution which implies consensus will never be reached. Indeed, this behaviour is observed in Figure 1.2. In the language of the blocktree of Model 1 for finite many miners N, we would have N branches (local blockchains) continuously growing from the root node (genesis block) each mining a new block with rate λ. Each branch (local blockchain) of this tree thus represents a pure Poisson point process with jump rate λ.

We can extend the support of $\theta_n(t)$ to be non-negative real valued by defining

$$\theta_x(t) = \frac{1}{\Gamma(x+1)}(\lambda t)^x e^{-\lambda t}, \tag{1.6}$$

which in the limit of large t represents a travelling Gaussian centered around $x = \lambda t$. An interesting note is that an asymptotic expression of (1.6) exists which satisfies a Fokker-Planck equation.

Proposition 1.4. *Let $x = \lambda t(1+\delta)$ where $\delta \sim t^{-1/2}$ as $t \to \infty$. Then as $t \to \infty$ we have,*

$$\theta_x(t) \simeq \frac{1}{\sqrt{2\pi\lambda t}} e^{-\frac{(x-\lambda t)^2}{2\lambda t}} \tag{1.7}$$

Proof. We recall the solution (1.6) which gives,

$$\theta_x(t) = \frac{1}{\Gamma(x+1)}(\lambda t)^x e^{-\lambda t} = \frac{1}{x!} e^{x\ln(\lambda t)-\lambda t}.$$

Let $u = \lambda t$. We expand $\ln u$ about $u = x$ since $x \sim \lambda t = u$ as $t \to \infty$. Then,

$$\begin{aligned}
\ln \lambda t &= \ln x + \frac{1}{x}(\lambda t - x) - \frac{1}{2x^2}(\lambda t - x)^2 + \mathcal{O}((\lambda t - x)^3). \\
\Rightarrow \theta_x(t) &= \frac{1}{x!} e^{x(\ln x + \frac{1}{x}(\lambda t - x) - \frac{1}{2x^2}(\lambda t - x)^2 + \mathcal{O}((\lambda t - x)^3))} e^{-\lambda t} \\
&\sim \frac{1}{x!} e^{x(\ln x + \frac{1}{x}(\lambda t - x) - \frac{1}{2x^2}(\lambda t - x)^2)} e^{-\lambda t} \\
&= \frac{1}{x!} e^{x\ln x - x - \frac{1}{2x}(\lambda t - x)^2} \\
&\sim \frac{1}{\sqrt{2\pi x}(\frac{x}{e})^x} e^{x\ln x - x - \frac{1}{2x}(\lambda t - x)^2}, \quad \text{using Stirling's approximation,} \\
&= \frac{1}{\sqrt{2\pi\lambda t}} e^{x\ln e - x\ln x} e^{x\ln x - x - \frac{1}{2x}(\lambda t - x)^2} \\
&\sim \frac{1}{\sqrt{2\pi\lambda t}} e^{-\frac{(x-\lambda t)^2}{2\lambda t}}.
\end{aligned}$$

□

On the level of the differential difference equation (1.4), the asymptotic solution (1.7) can instead be derived by taking the Taylor series expansion of the difference term $\theta_{x-1}(t)$ to obtain

$$\frac{d\theta_x(t)}{dt} = \sum_{n=1}^{\infty} (-1)^n \frac{\partial^n}{\partial x^n}\Big(\frac{\lambda}{n!}\theta_x(t)\Big), \tag{1.8}$$

which is also known as the Kramers-Moyal expansion [7] of the master equation for $\theta_x(t)$. Of relevant importance is the Pawula theorem [8, 9], which states that the Kramers-Moyal expansion (1.8) either stops at the first or second terms or must contain an infinite number of terms. Truncating (1.8) at second order gives the Fokker-Planck equation (1.9) which has (1.7) as a solution.

Proposition 1.5. *The asymptotic solution* (1.7) *is a solution of the Fokker-Planck equation*

$$\frac{d\theta_x}{dt} = -\lambda\Big(\frac{\partial\theta_x}{\partial x} - \frac{1}{2}\frac{\partial^2\theta_x}{\partial x^2}\Big), \tag{1.9}$$

with boundary conditions $\theta_{\pm\infty} = 0$.

Proof. A simple substitution shows this is true. □

1.2.2 The Cumulative Distribution Function

Instead of studying the proportion of miners at height i at time t, given by $\theta_i(t)$, we can look at the proportion of miners at time t with height at most n. This is given by the cumulative distribution function

$$\varphi_n(t) := \sum_{i=0}^{n} \theta_i(t), \;\; \varphi_{-1}(t) = 0, \;\; \varphi_n(0) = 1 \text{ for } n \geq 0.$$

Proposition 1.6 (Blockchain equation)**.** *The cumulative distribution function $\varphi_n(t)$ satisfies the following system of equations*

$$\frac{\partial \varphi_0(t)}{\partial t} = -\lambda \varphi_0(t) - \omega \varphi_0(t)(1 - \varphi_0(t)), \tag{1.10}$$

and for $n \geq 1$

$$\frac{\varphi_n(t)}{dt} = -\lambda(\varphi_n(t) - \varphi_{n-1}(t)) - \omega \varphi_n(t)(1 - \varphi_n(t)), \tag{1.11}$$

with initial condition $\varphi_n(0) = 1$ for $n \geq 0$ and $\varphi_{-1}(t) = 0$ for $t \geq 0$.

Proof. For the $n = 0$ case we have $\varphi_0(t) = \theta_0(t)$ and so equation (1.1) gives (1.10).

We now consider $n \geq 1$ and recall equation (1.2) then

$$\begin{aligned}
\frac{d}{dt}\varphi_n(t) &= \sum_{i=0}^{n} \frac{d}{dt}\theta_i(t) \\
&= \sum_{i=0}^{n} \Big(\theta_i(t) \Big(-\lambda - \omega \sum_{j=i+1}^{\infty} \theta_j(t) \Big) + \lambda \theta_{i-1}(t) + \omega \theta_i(t) \sum_{j=0}^{i-1} \theta_j(t) \Big) \\
&= -\lambda \sum_{i=0}^{n} \theta_i(t) + \lambda \sum_{i=0}^{n} \theta_{i-1}(t) - \omega \sum_{i=0}^{n} \theta_i(t) \Big(\sum_{j=i+1}^{\infty} \theta_j(t) - \sum_{j=0}^{i-1} \theta_j(t) \Big) \\
&= -\lambda(\varphi_n(t) - \varphi_{n-1}(t)) - \omega \sum_{i=0}^{n} \theta_i(t) \Big(1 - \theta_i(t) - 2 \sum_{j=0}^{i-1} \theta_j(t) \Big) \\
&= -\lambda(\varphi_n(t) - \varphi_{n-1}(t)) - \omega \varphi_n(t) + \omega \Big(\sum_{i=0}^{n} \theta_i(t)^2 + 2 \sum_{i=1}^{n} \theta_i(t) \Big(\sum_{j=0}^{i-1} \theta_j(t) \Big) \Big) \\
&= -\lambda(\varphi_n(t) - \varphi_{n-1}(t)) - \omega \varphi_n(t) + \omega \Big(\sum_{i=0}^{n} \theta_i(t) \Big)^2 \\
&= -\lambda(\varphi_n(t) - \varphi_{n-1}(t)) - \omega \varphi_n(t)(1 - \varphi_n(t)),
\end{aligned}$$

which gives equation (1.11). □

Remark 1.7. *The Blockchain equation* (1.11) *will be the focal point of study in this thesis. Much of the work in Chapters 2 and 3 is devoted to this system of equations.*

No communication regime. In the regime of no communication between miners we have $\omega = 0$ and hence the Blockchain equation (1.11) reduces to

$$\frac{d\varphi_n(t)}{dt} = -\lambda(\varphi_n(t) - \varphi_{n-1}(t)), \tag{1.12}$$

with initial condition $\varphi_n(0) = 1$ for $n \geq 0$ and $\varphi_{-1}(t) = 0$. This equation (1.12) has an exact solution given by

$$\varphi_n(t) = e^{-\lambda t} \sum_{m=0}^{n} \frac{1}{m!} (\lambda t)^m, \tag{1.13}$$

which is the distribution function of a Poisson random variable with mean λt and support $n \in \mathbb{N}_{\geq 0}$.

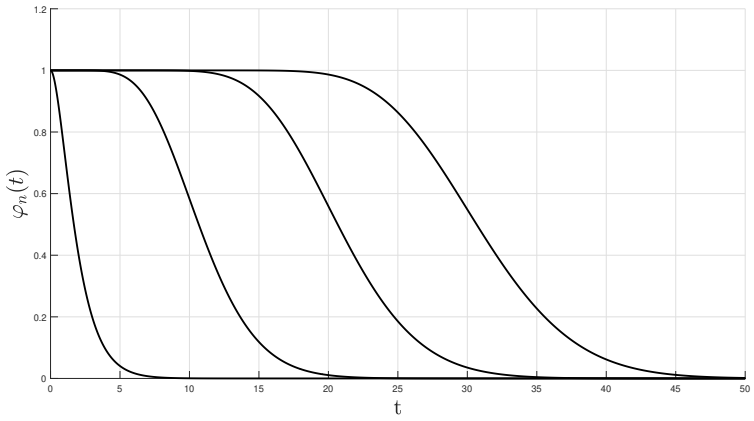

Figure 1.3: Plots of $\varphi_n(t)$ (1.13) for $n = 1, 10, 20, 30$ with $\lambda = 1, \omega = 0$. Solutions moving to the right for increasing n.

In view of Figure 1.3, we see that the distribution function of local blockchain heights flattens out as the miners mine further into the blockchain. The mean of this front, as a function of t, travels with speed λ and standard deviation $\sqrt{\lambda t}$ which implies that the front spreads out at rate $\sqrt{t}$ during travel. We later see that for positive $\omega > 0$ a travelling wave (front which does not deform) seems to form in the limit $n \to \infty$ which, if true, will imply consensus of local blockchains within a bounded distance of the longest local blockchain.

We now consider a solution $\varphi^*_x(t)$ of (1.12) with boundary conditions $\varphi^*_{-1}(t) = 0$ for all $t \geq 0$ and $\varphi^*_\infty = 1$. This solution corresponds to the integrated Poisson distribution of (1.6)

$$\varphi^*_x = \sum_{n=0}^{x} \theta_n = \frac{\Gamma(x+1; \lambda t)}{\Gamma(x+1)}, \tag{1.14}$$

where $\Gamma(x; \lambda t)$ is the incomplete gamma function

$$\Gamma(x+1; \lambda t) = \int_{\lambda t}^{\infty} s^x e^{-s} ds.$$

In the limit of large t, the solution (1.14) becomes a travelling front, which flattens out, given by the integrated Gaussian

$$\varphi^*_x \simeq \frac{1}{2} + \frac{1}{2} \mathrm{erf}\Big(\frac{x - \lambda t}{\sqrt{2\lambda t}}\Big), \tag{1.15}$$

where

$$\mathrm{erf}(z) = \frac{2}{\sqrt{\pi}} \int_0^z e^{-s^2} ds.$$

Proposition 1.8. *The asymptotic solution* (1.15) *is a solution of the Fokker-Planck equation*

$$\frac{d\varphi^*_x}{dt} = -\lambda \Big(\frac{\partial \varphi^*_x}{\partial x} - \frac{1}{2} \frac{\partial^2 \varphi^*_x}{\partial x^2} \Big), \tag{1.16}$$

with boundary conditions $\varphi^*_{-\infty} = 0$ *and* $\varphi^*_\infty = 1$.

No mining regime. In the regime of no mining we have $\lambda = 0$ and the difference term in the Blockchain equation (1.11) vanishes which gives

$$\frac{\varphi_n(t)}{dt} = -\omega\varphi_n(t)(1 - \varphi_n(t)),$$

where now the index n becomes extraneous and we consider the solution in the limit $n \to \infty$ which is given by

$$\frac{d\psi(\tau)}{d\tau} = -\omega\psi(\tau)(1 - \psi(\tau)), \;\; \psi(-\infty) = 1, \;\; \psi(\infty) = 0, \tag{1.17}$$

the well known logistic ODE which has many biological applications, for example, population growth [10]. An exact solution, satisfying $\psi(0) = \frac{1}{2}$, is given by

$$\psi(\tau) = \frac{1}{e^{\omega\tau} + 1}. \tag{1.18}$$

Although the *No Mining Regime* is degenerate, the exact solution (1.18) does give insight into what the limiting wave form $\varphi_n(t)$ should approach in the limit $\lambda \to 0$.

General regime. We now consider the general regime, $\lambda, \omega > 0$ in view of the Blockchain equation (1.11). Upon solving for the $n = 0$ solution, the φ_{-1} term vanishes and we obtain

$$\frac{\varphi_0(t)}{dt} = -\lambda\varphi_0(t) - \omega\varphi_0(t)(1 - \varphi_0(t)), \tag{1.19}$$

with initial condition $\varphi_0(0) = 1$, which has an exact solution given by

$$\varphi_0(t) = \frac{\lambda + \omega}{\omega + \lambda e^{t(\lambda+\omega)}}. \tag{1.20}$$

Attempting to solve for the $\varphi_1(t)$ solution proves difficult due to the non-linear term. Solving for $\varphi_1(t)$ via computer algebra produces a solution in the form of a large sum of hypergeometric functions with complex arguments. This leaves us with the suspicion that exact "nice" solutions of the Blockchain equation (1.11) do not exist for $n \geq 1$. In view of this, we provide numerical solutions of $\varphi_n(t)$ below:

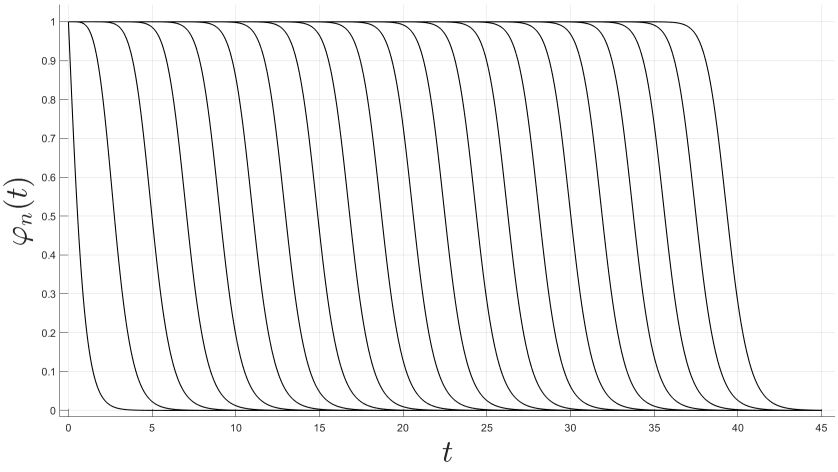

Figure 1.4: Plots of $\varphi_n(t)$ (1.11) for n = 0, 5, 10, 15, ..., 100 with $\lambda = 1, \omega = 1$. Solutions moving to the right for increasing n.

Remark 1.9. *The solutions of $\varphi_n(t)$ in Figure 1.4 were solved numerically using a 4^{th}-order explicit Runge Kutta integrator, the details of which can be found in Chapter 3.*

Indeed, by observation, a travelling wave seems to form as n increases. Taking n even further does show stability in solution. This leaves us with the suspicion that solutions $\varphi_n(t)$ of the Blockchain equation (1.11) do approach a travelling wave in the limit $n \to \infty$. This was conjectured in [1]. If this is true, it would mean that a blocktree with any positive rate of communication ω remains in consensus within a bounded distance of its maximum height for all time.

We conclude the introduction by proving boundedness and monotonicity properties of solutions $\varphi_n(t)$ of the Blockchain equation. We will make use of these results in Chapter 3.

Lemma 1.10 (Boundedness)**.** *It holds that $\varphi_n(t) \in [0,1]$ for $n \in \mathbb{N}_{\geq 0}$ and $t \geq 0$.*

Proof. We proceed by induction on $n \in \mathbb{N}_{\geq 0}$. The case $n = 0$ is clear from the exact solution (1.20). For the inductive step we suppose $\varphi_{n-1}(t) \in [0,1]$ for all $t \geq 0$ for some $n \in \mathbb{N}_{\geq 1}$. We want to show $\varphi_n(t) \in [0,1]$ for all $t \geq 0$. This can be done by looking at the derivative $\frac{\partial \varphi_n(t)}{\partial t}$ on the boundary of $[0,1]$. From the Blockchain equation (1.11) we have:

- $\frac{\partial \varphi_n}{\partial t} = -\lambda(1 - \varphi_{n-1}(t)) \in [-\lambda, 0]$ if $\varphi_n(t) = 1$,
- $\frac{\partial \varphi_n}{\partial t} = \lambda \varphi_{n-1}(t) \in [0, \lambda]$ if $\varphi_n(t) = 0$,

since $\varphi_{n-1}(t) \in [0,1]$ by induction hypothesis.

From the fist dot point, if $\varphi_n(t) = 1$ then $\varphi_n(t + \epsilon) \leq 1$ for some small ϵ. This gives $\varphi_n(t) \leq 1$ for all $t \geq 0$. From the second dot point, if $\varphi_n(t) = 0$ then $\varphi_n(t + \epsilon) \geq 0$ for some small ϵ. This gives $\varphi_n(t) \geq 0$ for all $t \geq 0$. We conclude $\varphi_n(t) \in [0,1]$ for all $t \geq 0$. The result extends to all of $n \in \mathbb{N}_{\geq 0}$ by induction. □

Lemma 1.11 (Monotonicity)**.** *For all $n \in \mathbb{N}_{\geq 0}$ we have $\varphi_n(t) - \varphi_{n-1}(t) \geq 0$ for all $t \geq 0$.*

Proof. Define $\delta_n(t) = \varphi_n(t) - \varphi_{n-1}(t)$. We prove $\delta_n(t) \geq 0$ for all $t \geq 0$ by induction on $n \in \mathbb{N}_{\geq 0}$. The case $\delta_0(t) \geq 0$ is clear from the exact solution (1.20) and $\varphi_{-1}(t) = 0$. For the inductive step suppose $\delta_{n-1}(t) \geq 0$ for all $t \geq 0$. We want to show $\delta_n(t) \geq 0$ for all $t \geq 0$. From the Blockchain equation (1.11), one can show

$$\dot{\delta_n}(t) = -(\lambda + \omega)\delta_n(t) + \lambda \delta_{n-1}(t) + \omega \delta_n(t)(\varphi_n(t) + \varphi_{n-1}(t)),$$

and so

$$\dot{\delta_n}(t) = \lambda \delta_{n-1}(t) \text{ if } \delta_n(t) = 0.$$

We know $\delta_n(0) = 0$ by the initial condition $\varphi_n(0) = 1$ for all $n \geq 0$. Suppose $\delta_n(t) = 0$, then $\dot{\delta_n}(t) = \lambda \delta_{n-1}(t) \geq 0$ since $\delta_{n-1}(t) \geq 0$ by inductive hypothesis. Hence $\delta_n(t) \geq 0$ for all $t \geq 0$. The result extends to all of $n \in \mathbb{N}_{\geq 0}$ by induction.

□

1.3 Thesis outline

In Chapter 2 we establish an asymptotic approximation of the Blockchain equation (1.11) which takes the form of a modified non-linear Fisher-KPP equation. Through a standard phase-plane analysis we show travelling wave solutions exist for a minimal speed, as a function of λ and ω. Building on this, the modified Fisher-KPP equation is shown to admit an exact solution, for a special speed, as a direct consequence of Painlevé integrability. Through numerical observation, this exact solution is shown to agree with the numerical Blockchain travelling wave solution, when their wave speeds coincide. This result can be seen as an extension of the exact solution of the original Fisher-KPP equation which was first solved by Ablowitz & Zeppetella, 1979 [11].

In Chapter 3 we conduct a detailed numerical study of the Blockchain equation (1.11). Through numerical inspection, we observe existence of travelling wave behaviour which was originally conjectured in [1, 4]. A wave speed formula of this travelling wave, as a function of λ and ω, is conjectured which is shown to agree with high accuracy to the numerically generated travelling wave speed of the Blockchain equation (1.11). In support of our conjecture we provide a detailed heuristic argument. This conjecture, and the various evidence supporting it, is the central original contribution of this thesis which directly builds on the earlier works of [1, 2, 3, 4].

In Chapter 4 we introduce the *Painlevé* equations and discuss their connection to integrable systems. In particular, we study the isomonodromy deformation of a Fuchsian system with four regular points. The Schlesinger equations are shown to be the conditions for the deformation of the Fuchsian system to be isomonodromic. As an application, we show that the *Painlevé VI* equation arises as a reduction of Schlesinger's equations in the case of four regular singular points.

2 Fisher-KPP Dynamics

In this chapter we study an asymptotic approximation of the Blockchain equation (1.11) introduced in Chapter 1. This asymptotic approximation takes the form of a modified Fisher-KPP equation, which shares a close resemblance to the well understood Fisher-KPP equation [12]. A direct consequence is that many of the analytical results for the Fisher-KPP equation can also be obtained for the modified Fisher-KPP equation, such as a minimal wave speed for a travelling wave solution [13, 12], and the existence of an exact solution for a special speed [11]. Much of the results in this section can be seen as a direct extension of the earlier works of Fisher 1937 [13], Kolmogorov 1937 [12] and Ablowitz 1979 [11], for their foundational contributions to the original Fisher-KPP equation. In conclusion, an exact solution for the modified Fisher-KPP equation is obtained by means of Painlevé integrability [11]. The exact solution is shown to be in close agreement with the numerical travelling wave solution of the Blockchain equation (1.11) when their wave speeds coincide.

2.1 Classic Fisher-KPP equation

Introduced in Fisher's seminal 1937 paper, *The Wave of Advance of Advantageous Genes* [13], was the second order non-linear partial differential equation

$$\frac{du}{dt} = D\frac{d^2u}{dx^2} + ru(1-u), \tag{2.1}$$

a simple reaction diffusion biological model for the propagation of a mutant gene. Mathematically this equation describes the diffusion of some substance u with rate D which reacts with itself via the non-linearity $u(1-u)$ with rate r. It is the most simple non-linear reaction-diffusion system and has been very well studied ever since [14, 15]. The main result found [13] was that a wave $u(z)$ of stationary form $z = x - vt$ advancing with velocity v exists for $v \geq 2\sqrt{Dr}$.

In the same year, 1937, Kolmogorov et al. [12] studied the more general form (now known as the Fisher-KPP equation)

$$u_t = u_{xx} + f(u), \;\; t \geq 0, \;\; x \in \mathbb{R}, \tag{2.2}$$

with conditions

$$\begin{aligned} &f(0) = f(1) = 0; \\ &f(u) > 0, \;\; 0 < u < 1; \\ &f'(0) = r > 0, \;\; f'(u) < r, \;\; 0 < u \leq 1. \end{aligned}$$

The prototypical example is a concave positive function f on (0, 1) which vanishes at 0 and 1, such as $f(u) = ru(1-u)$, which gives Fisher's equation (2.1) after rescaling the spatial coordinate by a factor of $\sqrt{D}$. The Fisher-KPP equation (2.2) was found to admit travelling wave solutions $g(x - vt) = u(x, t)$ for

$$v \geq 2\sqrt{\frac{df}{du}|_{u=0}}.$$

If one rescales (2.1) via

$$x \mapsto \sqrt{r/D}x \text{ and } t \mapsto rt,$$

we obtain the non-dimensionalised version of Fishers equation (2.1)

$$u_t = u_{xx} + u(1-u) \tag{2.3}$$

In 1979, Ablowitz et al. [11] found a one parameter family of travelling wave solutions to Fisher's (non-dimensionalised) equation (2.3) as

$$u(z) = \frac{1}{(1 + ae^{z/\sqrt{6}})^2}, \tag{2.4}$$

for some translation parameter $a > 0$ where $u(z) = u(x - vt)$ for the special speed $v = \frac{5}{\sqrt{6}}$. The existence of this exact solution was due to Fisher's (non-dimensionalised) equation (2.3) being Painlevé integrable when $v = \frac{5}{\sqrt{6}}$. In Chapter 4, we elaborate on the connection between integrable models and Painlevé integrability in the context of second order ordinary differential equations.

2.2 Modified Fisher-KPP equation

We recall the Blockchain equation

$$\frac{d\varphi_n(t)}{dt} = -\lambda(\varphi_n(t) - \varphi_{n-1}(t)) - \omega\varphi_n(t)(1 - \varphi_n(t)), \tag{2.5}$$

with $\varphi_n(0) = 1$ for $n \geq 0$ and $\varphi_{-1}(t) = 0$ for $t \geq 0$.

We make the assumption that in the limit of large n and t the solution $\varphi_n(t)$ becomes differentiable in the spatial variable n and hence an approximate solution can be obtained via a truncated Taylor series expansion.

From Taylor's theorem we write

$$\varphi_{x-1}(t) = \sum_{m=0}^{\infty} \frac{(-1)^m}{m!} \frac{\partial^m \varphi_x(t)}{\partial x^m},$$

or

$$\varphi_{x-1}(t) = \varphi_x(t) - \frac{\partial \varphi_x(t)}{\partial x} + \frac{1}{2}\frac{\partial^2 \varphi_x(t)}{\partial x^2} + R(x,t),$$

where the remainder term R is bounded as [16]

$$|R(x,t)| \leq \max_{\{b \in (-1, x-1)\}} \frac{1}{6}\frac{\partial^3 \varphi_b(t)}{\partial x^3}.$$

Truncating at second order, assuming the remainder term R to be small, we write $f(x,t) = \varphi_x(t)$ giving

$$\frac{\partial f}{\partial t} = -\lambda(\frac{\partial f}{\partial x} - \frac{1}{2}\frac{\partial^2 f}{\partial x^2}) - \omega f(1 - f). \tag{2.6}$$

We will refer to equation (2.6) as the modified Fisher-KPP equation. We assume this equation to be a good approximation of the Blockchain equation (2.5) in the asymptotic limit.

Remark 2.1. *The expansion to obtain* (2.6) *can be seen as analogous to the Kramers-Moyal expansion [7]. Again, the Pawula theorem [8, 9] says that truncating at second order is sufficient for the evolution of a probability density.*

2.3 Lower bound on travelling wave speed

As indicated earlier in Figure 1.4, we observed from the numerical solutions of the Blockchain equation (2.5) that a travelling wave seems to form in the asymptotic limit. Assuming the modified Fisher-KPP equation (2.6) is a good approximation of the Blockchain equation (2.5), we search for travelling wave solutions of (2.6).

In view of the modified Fisher-KPP equation (2.6), we assume a travelling wave solution $f(x,t) = g(z)$ advancing with velocity v where $z = x - vt$ to obtain

$$(v-\lambda)\frac{dg}{dz} + \frac{\lambda}{2}\frac{d^2g}{dz^2} = \omega g(1-g), \tag{2.7}$$

with boundary conditions $g(-\infty) = 0$ and $g(\infty) = 1$. These boundary conditions are a direct consequence of $\varphi_{-1} = 0$ and $\varphi_\infty = 1$. We will refer to (2.7) as the travelling wave form of the modified Fisher-KPP equation (2.6).

Alternative derivation. Equation (2.7) can be obtained in another way which we mention briefly. If we make the assumption that the Blockchain equation (2.5) approaches a travelling wave in the limit $n \to \infty$ then there must exist some $\tau := \tau(\lambda, \omega) > 0$ such that

$$\varphi_{n-1}(t) \longrightarrow \varphi_n(t+\tau)$$

(at least) pointwise as $n \to \infty$. The travelling wave speed is effectively $v := 1/\tau$.

Hence the Blockchain equation (2.5) reduces to the following in the limit of large n

$$\frac{d\varphi_n(t)}{dt} = -\lambda(\varphi_n(t) - \varphi_n(t+\tau)) - \omega\varphi_n(t)(1-\varphi_n(t)),$$

where the subscript n becomes extraneous and so we obtain

$$\frac{d\varphi(t)}{dt} = -\lambda(\varphi(t) - \varphi(t+\tau)) - \omega\varphi(t)(1-\varphi(t)), \tag{2.8}$$

with boundary conditions $\varphi(-\infty) = 1$ and $\varphi(\infty) = 0$. Equation (2.8) is a first order non-linear advanced ODE. These kinds of equations have applications in diverse areas such as biological networks [17]. The solutions of (2.8) are the travelling wave profiles of the Blockchain equation (2.5), where τ is a function of λ and ω and may also depend on the behaviour of the initial solution $\varphi_0(t)$, such as its rate of exponential decay in the limit $t \to \infty$ [12, 18].

Assuming $\varphi(t)$ in equation (2.8) is sufficiently differentiable, we write from Taylor's theorem

$$\varphi(t+\tau) = \sum_{m=0}^{\infty} \frac{\tau^m}{m!}\frac{\partial^m\varphi(t)}{\partial t^m},$$

then truncating at second order and substituting into (2.8) gives

$$(1-\lambda\tau)\frac{d\varphi(t)}{dt} = \frac{\lambda\tau^2}{2}\frac{d^2\varphi(t)}{dt^2} - \omega\varphi(t)(1-\varphi(t)). \tag{2.9}$$

We make the observation that equation (2.9) is equivalent to the modified Fisher-KPP equation (in travelling wave coordinates) (2.7) via the rescaling

$$t = -\tau z \text{ and } \tau = \frac{1}{v}. \tag{2.10}$$

Equation (2.9) is not easy to work with since the speed dependence $\tau = 1/v$ appears in front of both the first order and second order spatial derivatives. For this reason we will focus our study

on equation (2.7). Despite this, many of the results we obtain also hold true for equation (2.9) via the rescaling (2.10).

Phase-plane analysis. We recall the travelling wave form of the modified Fisher-KPP equation (2.7). Since the variable z does not appear explicitly we may write, for the solution gradient

$$\alpha h(g(z)) = g'(z),$$

which gives

$$\frac{d^2g}{dz^2} = \alpha \frac{dg}{dz}\frac{dh}{dg},$$

and obtain the first order ODE

$$h(g) + \frac{\alpha\lambda}{2(v-\lambda)} h(g)h'(g) = \frac{\omega}{\alpha(v-\lambda)} g(1-g).$$

Noting that $\alpha \in \mathbb{R}$ is arbitrary, we choose for convenience

$$\alpha = \frac{2(v-\lambda)}{\lambda},$$

and obtain the canonical form of the Abel equation of the second kind

$$h'(g)h(g) = -h(g) + \beta^2 g(1-g) \text{ where } \beta^2 = \frac{\omega\lambda}{2(v-\lambda)^2},$$

which gives

$$h'(g) = -1 + \frac{\beta^2 g(1-g)}{h(g)}. \tag{2.11}$$

This equation (2.11) governs the trajectories in the (g,h)-phase plane between the singular points $(0,0)$ and $(1,0)$, which correspond to the steady states. We can rewrite equation (2.11) as

$$\frac{dh}{dz} = -h(g(z)) + \beta^2 g(z)(1-g(z)), \tag{2.12a}$$

$$\frac{dg}{dz} = -h(g(z)). \tag{2.12b}$$

We wish to understand how the system behaves near these steady states so we linearize equations (2.12a), (2.12b) around the singular points which gives the following

$$\frac{d}{dz}\begin{pmatrix} h \\ g \end{pmatrix} = \begin{pmatrix} -1 & \beta^2 \\ 1 & 0 \end{pmatrix}_{(0,0)} \begin{pmatrix} h \\ g \end{pmatrix},$$

$$\frac{d}{dz}\begin{pmatrix} h \\ g \end{pmatrix} = \begin{pmatrix} -1 & -\beta^2 \\ 1 & 0 \end{pmatrix}_{(1,0)} \begin{pmatrix} h \\ g \end{pmatrix}.$$

If we denote the 2×2 matrices by $J_{(0,0)}$ and $J_{(1,0)}$ respectfully, then by the Hartman–Grobman theorem [16], the behaviour of the system near the steady states $(0,0)$ and $(1,0)$ is governed by the eigenvalues of $J_{(0,0)}$ and $J_{(1,0)}$, respectfully.

Recalling $\beta^2 = \frac{\omega\lambda}{2(v-\lambda)^2}$, the eigenvalues can be computed as

$$\mu^{\pm}_{(0,0)} = \frac{1}{2}\Big(-1 \pm \sqrt{1 + \frac{4\omega\lambda}{2(v-\lambda)^2}}\Big),$$

$$\mu^{\pm}_{(1,0)} = \frac{1}{2}\Big(-1 \pm \sqrt{1 - \frac{4\omega\lambda}{2(v-\lambda)^2}}\Big).$$

For a travelling wave solution $g(z)$, with boundary conditions $g(-\infty) = 0$ and $g(\infty) = 1$, we require $(1, 0)$ to be a stable steady state, and $(0, 0)$ to be an unstable steady state in the (g, h)-phase plane.

- The $\mu^{\pm}_{(0,0)}$ eigenvalue produces one positive and one negative eigenvalue for $v \geq \lambda + \sqrt{2\lambda\omega}$, thus, representing an unstable saddle point at $(0, 0)$.
- Similarly, the $\mu^{\pm}_{(1,0)}$ eigenvalue produces two negative eigenvalues for $v \geq \lambda + \sqrt{2\lambda\omega}$, thus, representing a stable node at $(1, 0)$.

We conclude that heteroclinic orbits $h_v(g)$ from $(0, 0)$ to $(1, 0)$ in the (g, h)-phase plane exist as long as $v \geq \lambda + \sqrt{2\lambda\omega}$. These heteroclinic orbits $h_v(g)$ correspond to travelling wave profiles $g(z)$ from $g(-\infty) = 0$ to $g(\infty) = 1$. This analysis gives a lower bound on the travelling wave speed v for travelling wave solutions $g(z)$ of (2.7).

Proposition 2.2. *The modified Fisher-KPP equation (2.6), admits travelling wave solutions $f(x, t) = g(x - vt)$ satisfying $g(-\infty) = 0$ and $g(\infty) = 1$, for wave speeds $v \geq \lambda + \sqrt{2\lambda\omega}$.*

Remark 2.3. *Indeed, this minimal wave speed should have been expected by observation of the Fisher equation* (2.1)*. The main difference is an additional λ term which comes from the λ-drift of the first order spatial derivative term in* (2.6) *which is not present in the Fisher equation* (2.1)*.*

Since the modified Fisher-KPP equation (2.6) is a second order approximation of the Blockchain equation (2.5), we would expect that the travelling wave speed of the Blockchain equation also be bounded below by $\lambda + \sqrt{2\lambda\omega}$. We later observe this to be true from from numerical results in Chapter 3.

2.4 An exact solution by Painlevé integrability

As mention in Chapter 1, the Blockchain equation (2.5) is integrable for $n = 0$ and for $n \geq 1$ no known analytic solution exists, as of current knowledge. For our purposes, we would like to understand the behaviour of solutions of the Blockchain equation (2.5) in the limit of large n, also known as travelling wave solutions. The solution in this limit will give us an idea of consensus in the blockchain for later times. In the language of the blocktree, introduced in Chapter 1, this late time travelling wave distribution will inform us of the strength of consensus, or put otherwise, the number of branches in the blocktree. For example, a steeper solution $\varphi_n(t)$ corresponds to few branches, whereas, a flatter solution $\varphi_n(t)$ corresponds to many branches. In both cases consensus occurs, however, consensus is weaker in the latter since the bounded distance between local blockchain heights is greater. This is due to the local blockchains disagreeing in a greater number of the last blocks, hence the greater number of branches in the blocktree.

We recall the modified Fisher-KPP equation in travelling wave coordinates

$$(v - \lambda)\frac{dg}{dz} + \frac{\lambda}{2}\frac{d^2g}{dz^2} = \omega g(1 - g), \tag{2.13}$$

with boundary conditions $g(-\infty) = 0$ and $g(\infty) = 1$.

We provide an exact analytic solution of (2.13) for a certain travelling wave speed $v := v(\lambda, \omega)$ by means of Painlevé integrability. This analytic solution will provide a second order approximation of the travelling wave solution of the Blockchain equation (2.5), when their wave speeds coincide. The calculation first involves showing that (2.13) is of Painlevé type, meaning, solutions of (2.13) admit only poles as movable singularities [19]. In doing so, we are able to capture values of v, as a function of λ and ω, for which equation (2.13) is integrable. The remaining part of the calculation involves linearizing around singular points in phase space, whereby, we are able to find a recursion for the coefficients of a series solution ansatz.

Calculation of exact solution. Inspired by the analysis of [11], we begin by determining what kind of pole a solution of (2.13) can have. If we take $g(z) \sim k(z-z_0)^{-\alpha}$, then the $\frac{\lambda}{2}g''(z)$ and $-\omega g(z)^2$ terms must balance and hence

$$\frac{\lambda}{2}g'' \sim \frac{\lambda}{2}k(-\alpha)(-\alpha-1)(z-z_0)^{-\alpha-2} = -\omega k^2(z-z_0)^{-2\alpha} \sim -\omega g^2.$$

This gives $\alpha = 2$ and $k = -\frac{3\lambda}{\omega}$ for a non-trivial solution. Then if the solutions are of Painlevé type it is a necessary condition that any Laurent series have coefficients well defined by the equation [19]. For this reason we look for a solution of the form

$$g(z) = \frac{k}{z^2} + \frac{a_{-1}}{z} + a_0 + a_1 z + ... \tag{2.14}$$

where the z_0 term vanishes due to the translation invariance of (2.13); since, if $g(z)$ is a travelling wave solution then $g(z+a)$ is also a travelling wave solution for all $a \in \mathbb{R}$. Now when (2.14) is substituted into (2.13) and the coefficients of $z^{-3}, z^{-2}, z^{-1}, z^0, z$ are successively equated to zero, we obtain expressions for $a_{-1}, a_0, a_1, a_2, a_3$:

$$\begin{aligned}
a_{-1} &= \frac{2k(v-\lambda)}{\lambda + 2k\omega},\\
a_0 &= \frac{1}{2k\omega}(\omega k - \omega a_{-1}^2 + a_{-1}(v-\lambda)),\\
a_1 &= \frac{1}{2k}(a_{-1} - 2a_0 a_{-1}),\\
a_2 &= \frac{1}{\lambda + 2k\omega}(-(v-\lambda)a_1 - \omega a_0^2 + \omega a_0 - 2\omega a_1 a_{-1}),\\
a_3 &= \frac{1}{3\lambda + 2\omega k}(-2(v-\lambda)a_2 - 2\omega a_0 a_1 + \omega a_1 - 2\omega a_2 a_{-1}).
\end{aligned}$$

However, we find that when equating the coefficient of z^2 to zero we obtain the equation

$$3(v-\lambda)a_3 + 6\lambda a_4 - \omega(-2ka_4 - a_1^2 - 2a_0 a_2 + a_2 - 2a_3 a_{-1}) = 0,$$

and using the already calculated $k = -\frac{3\lambda}{\omega}$ the a_4 terms vanish and hence the equation becomes

$$3(v-\lambda)a_3 + \omega a_1^2 + 2\omega a_0 a_2 - \omega a_2 + 2\omega a_3 a_{-1} = 0. \tag{2.15}$$

For the Laurent expansion (2.14) to be valid, v must satisfy (2.15). Using the expressions for $a_{-1}, a_0, a_1, a_2, a_3$ we find from (2.15)

$$v = \lambda \text{ or } \lambda \pm \frac{5}{6}\sqrt{\pm 3\lambda\omega}.$$

Remark 2.4. *If we added a logarithmic term to the expansion of $g(z)$ (2.14) then other wave speeds could be obtained, however, this would give a movable branch point at $z = z_0$ and so the solution is not of Painlevé type [19]. For $v = \lambda$, the modified Fisher-KPP equation (2.13) is completely integrable and admits a solution expressible in terms of elliptic functions. The solution of interest satisfies $g(-\infty) = 0$ and $g(\infty) = 1$ with a wave speed of $v \geq \lambda + \sqrt{2\lambda\omega}$. Hence we only consider the wave speed $v = \lambda + \frac{5}{6}\sqrt{3\lambda\omega}$.*

For convenience, we choose to transform as $\zeta(z) = 1 - g(z)$ where now $\zeta(z)$ satisfies $\zeta(-\infty) = 1$ and $\zeta(\infty) = 0$ which gives equation

$$(v-\lambda)\frac{d\zeta}{dz} + \frac{\lambda}{2}\frac{d^2\zeta}{dz^2} + \omega\zeta(1-\zeta) = 0. \tag{2.16}$$

If we linearize about the $(0,0)$ node in the (ζ,ζ')-phase plane we obtain

$$(v-\lambda)\frac{d\zeta}{dz}+\frac{\lambda}{2}\frac{d^2\zeta}{dz^2}+\omega\zeta=0, \tag{2.17}$$

which has general solution

$$\zeta(z)=c_1\exp\Big(\alpha_1 z\Big)+c_2\exp\Big(\alpha_2 z\Big),$$

where c_1, c_2 are integration constants.

If we substitute the general solution $\zeta(z)=\exp(\alpha z)$ form into the linearised equation (2.17) we obtain an algebraic equation for α as

$$\frac{\lambda}{2}\alpha^2+(v-\lambda)\alpha+\omega=0,$$

which gives two roots corresponding to α_1 and α_2 as

$$\alpha_1=\frac{1}{\lambda}(-(v-\lambda)+\sqrt{(v-\lambda)^2-2\lambda\omega}),$$
$$\alpha_2=\frac{1}{\lambda}(-(v-\lambda)-\sqrt{(v-\lambda)^2-2\lambda\omega}),$$

which are real valued for $v\geq\lambda+\sqrt{2\lambda\omega}$.

We now note that for any $v\geq\lambda+\sqrt{2\lambda\omega}$ we have $\alpha_1,\alpha_2<0$ and so $(0,0)$ is a stable node in the (ζ,ζ')-phase plane. This suggests a solution of the general non-linear equation (2.16) as

$$\zeta(z)=\sum_{m,n\geq 0, m+n\geq 1} a_{m,n}\exp\{(m\alpha_1+n\alpha_2)z\}. \tag{2.18}$$

For $v=\lambda+\frac{5}{6}\sqrt{3\lambda\omega}$ we get $\alpha_1=-2\sqrt{\frac{\omega}{3\lambda}}$ and $\alpha_2=-3\sqrt{\frac{\omega}{3\lambda}}$ and so (2.18) reduces to

$$\zeta(z)=\sum_{n=2}^{\infty}a_n\exp\Big(-n\sqrt{\frac{\omega}{3\lambda}}z\Big). \tag{2.19}$$

Setting $v=\lambda+\frac{5}{6}\sqrt{3\lambda\omega}$ and substituting (2.19) into (2.16) gives

$$\sum_{n=2}^{\infty}\Big(\frac{5}{6}\sqrt{3\lambda\omega}a_n\Big(-n\sqrt{\frac{\omega}{3\lambda}}\Big)+\frac{\lambda}{2}a_n n^2\frac{\omega}{3\lambda}+\omega a_n-\omega\sum_{l=2}^{n-2}a_l a_{n-l}\Big)\exp\Big(-n\sqrt{\frac{\omega}{3\lambda}}z\Big)=0, \tag{2.20}$$

where we made use of the Cauchy product of two power series to expand $\zeta(z)^2$. Upon equating the coefficients of the exponential term in (2.20) to zero we find that a_n must satisfy the recursion

$$a_n(n-2)(n-3)=6\sum_{l=2}^{n-2}a_l a_{n-l},\ \text{ for } n\geq 4. \tag{2.21}$$

From (2.21), a_2 and a_3 become arbitrary and we obtain a_n by recursion for $n\geq 4$. We require $\zeta(z)>0$ for all z, so we set $a_2=a^2$ for some arbitrary constant $a>0$. Choosing $a_3=a^3b_3$, recursion from (2.21) gives $a_n=a^n b_n$ where $b_2=1$ and

$$b_n=6\frac{\sum_{l=2}^{n-2}b_l b_{n-l}}{(n-2)(n-3)},\ \text{ for } n\geq 4. \tag{2.22}$$

The solution (2.19) becomes

$$\zeta(z) = \sum_{n=2}^{\infty} a^n b_n \exp\Big(- n\sqrt{\frac{\omega}{3\lambda}} z\Big) = \sum_{n=2}^{\infty} b_n \exp\Big(n\Big(\log(a) - \sqrt{\frac{\omega}{3\lambda}} z\Big)\Big),$$

which identifies $a > 0$ as a translation parameter.

We are left to decide the coefficients b_n. Using the recursion for b_n (2.22) we just need to fix a choice for b_3 and the rest will be generated. Different choices of b_3 will produce different trajectories in the (ζ, ζ')-phase plane emanating from the unstable node at $(1, 0)$ to the stable node at $(0, 0)$. The particular choice of $b_3 = -2$ gives $b_4 = 3$ and by induction from the recursion relation (2.22), $b_n = (-1)^n(n-1)$.

This gives the desired solution as

$$\begin{aligned} \zeta(z; a) &= \sum_{n=2}^{\infty} (-1)^n (n-1) \exp\Big(n\Big(log(a) - \sqrt{\frac{\omega}{3\lambda}} z\Big)\Big) \\ &= \frac{1}{\Big(1 + \exp\Big(log(a) + \sqrt{\frac{\omega}{3\lambda}} z\Big)\Big)^2}, \end{aligned} \tag{2.23}$$

which is valid provided $z > 0$ where we have made use of a Binomial series formula.

Remark 2.5. *We made clear that the equality in* (2.23) *is valid for $z > 0$. This was due to the Binomial series formula diverging for $z \leq 0$. Despite this, the equality can be extended to all of $z \in \mathbb{R}$ by analytic continuation. The result obtained* (2.23) *does indeed solve* (2.16) *by direct substitution.*

Transforming back to $g(z) = 1 - \zeta(z)$ we obtain from (2.23)

$$g(z; a) = 1 - \frac{1}{\Big(1 + \exp\Big(log(a) + \sqrt{\frac{\omega}{3\lambda}} z\Big)\Big)^2}, \tag{2.24}$$

which satisfies the boundary conditions $g(-\infty) = 0$ and $g(-\infty) = 1$ with a free translation parameter $a > 0$.

One can show, by direct substitution, that (2.24) solves the modified Fisher-KPP equation in travelling wave coordinates (2.13) for the specific wave speed $v = \lambda + \frac{5}{6}\sqrt{3\lambda\omega}$.

Proposition 2.6. *The modified Fisher-KPP equation in travelling wave coordinates* (2.13)*, has a one parameter family of exact solution given by* (2.24) *for the wave speed $v = \lambda + \frac{5}{6}\sqrt{3\lambda\omega}$.*

Remark 2.7. *Exact solutions of the modified Fisher-KPP equation in travelling wave coordinates* (2.13) *also exist for the other values $v = \lambda$ and $v = \lambda - \frac{5}{6}\sqrt{3\lambda\omega}$. However, these v values do not satisfy the minimal v value for a travelling wave solution, $v \geq \lambda + \sqrt{2\lambda\omega}$. Hence the blockchain relevant exact solution which is indicative of a travelling wave is given by* (2.24)*.*

2.5 Blockchain numerical comparison

We now compare the exact solution (2.24) of the modified Fisher-KPP equation in travelling wave coordinates (2.13), to the numerical solution $\varphi_n(t)$ of the Blockchain equation (2.5), for n sufficiently large enough such that $\varphi_n(t)$ is a travelling wave. The exact solution (2.24) was found for the travelling wave speed $v = \lambda + \frac{5}{6}\sqrt{3\lambda\omega}$. If we wish to compare the exact solution (2.24) to the numerical solution $\varphi_n(t)$ of the Blockchain equation we must do so when their wave speeds coincide. The trouble here is that a closed formula for the travelling wave speed for the Blockchain equation is currently unknown. A conjecture of this wave speed, as a function of λ

and ω, is provided in Chapter 3. For now we may, without loss of generality, set $\lambda = 1$, and vary ω until the speed $v = \lambda + \frac{5}{6}\sqrt{3\lambda\omega}$ coincides with the numerical travelling wave speed v_{bc} of solutions $\varphi_n(t)$.

By varying ω, through trial and error, we find that the speeds v_{bc} and $v = \lambda + \frac{5}{6}\sqrt{3\lambda\omega}$ indeed (approximately!) coincide for $\omega = 0.01075$ while noting that the travelling wave speed v_{bc} was approximately reached at height $N = 2400$ in the blockchain. Thus the numerical solution we will be comparing the exact solution (2.24) against is $\varphi_{2400}(t)$, for $\lambda = 1$ and $\omega = 0.01075$.

We choose to superimpose both solutions with respect to the time axis. The Blockchain equation (2.5) is numerically solved over the time axis, so we need to adjust our exact solution (2.24) to be variable with respect to time. Recalling our exact solution

$$g(z;a) = 1 - \frac{1}{(1 + a\exp(z\sqrt{\omega/3\lambda}))^2},$$

we write $z = x - vt$ and evaluate the speed $v = \lambda + \frac{5}{6}\sqrt{3\lambda\omega}$ at $\lambda = 1$ and $\omega = 0.01075$. Setting $x = N = 2400$ gives $z \simeq 2400 - 1.14965t$ and hence solution

$$g(t;a) := 1 - \frac{1}{(1 + a\exp((2400 - 1.14965t)\sqrt{0.01075/3})^2},$$

which as before still contains a free translation parameter, $a > 0$.

We plot the numerical Blockchain solution $\varphi_{2400}(t)$ superimposed with the exact solution $g(t;a)$ for $a = 17$. The choice of translation parameter $a = 17$, although arbitrary, was chosen to provide the best graphical comparison.

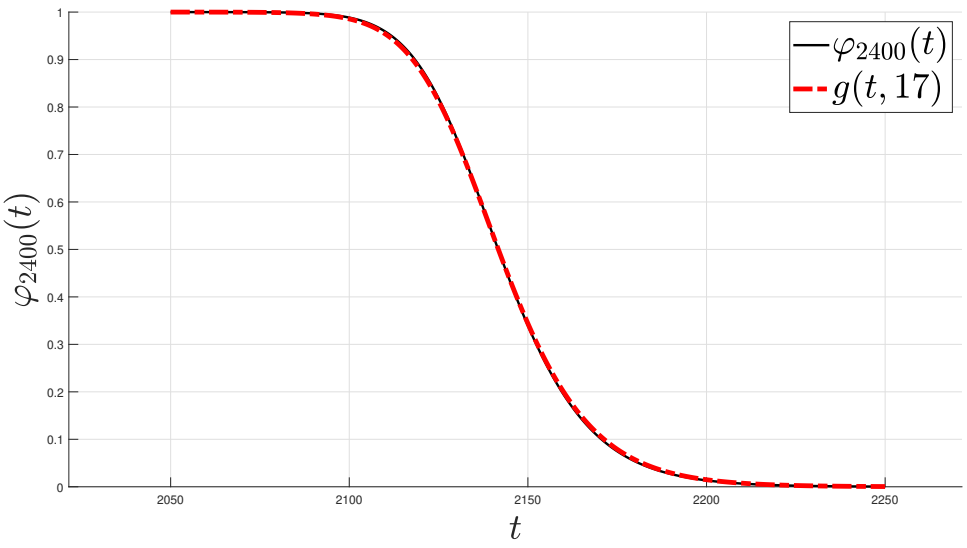

Figure 2.1: The numerical solution $\varphi_{2400}(t)$ of the Blockchain equation (2.5) (in Black) superimposed with the exact solution $g(t, 17)$, of the modified Fisher-KPP equation (2.13) (in Red). The mining and communication rates are $\lambda = 1$ and $\omega = 0.01075$ respectfully.

Graphically, there is strong agreement between the exact solution (2.24), of the modified Fisher-KPP equation in travelling wave coordinates (2.13), and the numerical travelling wave solution $\varphi_{2400}(t)$ of the Blockchain equation (2.5). Given that $\varphi_{2400}(t)$ is a travelling wave, the exact solution (2.24) will also approximate $\varphi_n(t)$ for all $n \geq 2400$, due to translation invariance. For $\omega \simeq 0.01075\lambda$, the exact solution (2.24) provides an answer to a question which was first asked in [1, 4], that is, what does the *shape* of the travelling wave $\varphi_n(t)$ look like?

3 Travelling Wave Speed Conjecture

It was conjectured that solutions φ_n of the Blockchain equation (2.5) approach a travelling wave in the limit of large n, [1, 4]. Indeed, if the consensus state in the CTMC model formulated in Chapter 1 is positive recurrent, then we expect the formation of a travelling wave for any choice of $\lambda, \omega > 0$. Proving, using rigorous analytical arguments, that solutions of (2.5) approach a travelling wave is quite difficult. We were able to show, in Chapter 2, that the modified Fisher-KPP equation (2.6) does admit travelling wave solutions for a minimal speed. Given that the modified Fisher-KPP equation approximates the Blockchain equation, it is very plausible that the Blockchain equation will approach a travelling wave.

The goal of this chapter is twofold. The first is providing numerical evidence that φ_n converges to a travelling wave in the limit of large n, for any $\lambda, \omega > 0$. This is in direct support of [1, 4] where the existence of a travelling wave was first conjectured. Secondly, from numerical observations we conjecture an exact wave speed formula of this travelling wave, as a function of λ and ω. We argue the validity of our conjecture through both numerical observation, and a heuristic argument. This conjecture, the numerical evidence surrounding it and the accompanying heuristic argument, forms the original key result of this thesis.

3.1 Numerical method for the Blockchain equation

Introduced in Chapter 2 was the Fisher-KPP equation (2.2), a reaction-diffusion PDE used for the modelling of many biologically relevant problems [14, 15]. Indeed the similarity between the Fisher-KPP equation and the Blockchain equation (2.5) is immediate.The Fisher-KPP equation admits a spatial diffusion term as opposed to the spatial difference term found in the Blockchain equation. There are many well understood numerical schemes to solve the Fisher-equation [20, 21, 22]. A common theme in the literature is the use of a Runge-Kutta integrator when solving over the discretized temporal lattice [23, 24, 25]. Some authors considered more exotic numerical methods such as the Petrov-Galerkin [26], the Sinc-Collocation [27] or a FTCS moving mesh [28]. The accuracy of the RK4 scheme when integrating over time was verified in [23, 24] and shown to be very accurate. A detailed tableau of the error's can be found therein. Given these conclusions and the similarity between the equations (2.2) and (2.5) we choose to adopt the classic Runge-Kutta Order 4 scheme as our numerical integrator of choice. A detailed analysis and implementation of the classic Runge-Kutta 4 can be found here [29].

RK4. We (numerically) solve the Blockchain equation,

$$\frac{d\varphi_n}{dt} = -\lambda(\varphi_n - \varphi_{n-1}) - w\varphi_n(1-\varphi_n), \quad \varphi_{-1}(t) = 0, \quad \varphi_n(0) = 1 \ \ \forall n \geq 0,$$

on $0 \leq t \leq T$ with T chosen sufficiently large such that the solutions $\varphi_n(t)$ have sufficient time to approach a travelling wave. We discretise the time domain with a uniform finite difference mesh, with spacing Δt. We use the notation that $\varphi_n^j = \varphi_n(j\Delta t)$, so that j indexes time and we approximate $\varphi_n(t)$ by φ_n^j for $t = j\Delta t$. The initial condition $\varphi_n(0) = 1$ is enforced by setting $\varphi_n^0 = 1$ for all $n \geq 0$.

The $n = 0$ solution is computed exactly as

$$\varphi_0^j = \frac{\lambda + \omega}{\omega + \lambda e^{j\Delta t(\lambda+\omega)}}.$$

For $n \geq 1$, the resulting system is integrating through time using the "classic" Runge-Kutta 4th order explicit scheme giving rise to

$$\frac{\varphi_n^{j+1} - \varphi_n^j}{\Delta t} = \frac{1}{6}(K_1 + 2K_2 + 2K_3 + K_4),$$

where the RK4 parameters are calculated as [29]

$$\begin{aligned}
K_1 &= -\lambda(\varphi_n^j - \varphi_{n-1}^j) - \omega\varphi_n^j(1 - \varphi_n^j) \\
K_2 &= -\lambda(\varphi_n^j + (\Delta t/2)K_1 - \varphi_{n-1}^j) - \omega(\varphi_n^j + (\Delta t/2)K_1)(1 - (\varphi_n^j + (\Delta t/2)K_1)) \\
K_3 &= -\lambda(\varphi_n^j + (\Delta t/2)K_2 - \varphi_{n-1}^j) - \omega(\varphi_n^j + (\Delta t/2)K_2)(1 - (\varphi_n^j + (\Delta t/2)K_2)) \\
K_4 &= -\lambda(\varphi_n^j + \Delta t K_3 - \varphi_{n-1}^j) - \omega(\varphi_n^j + \Delta t K_3)(1 - (\varphi_n^j + \Delta t K_3)).
\end{aligned}$$

The resulting system of equations are solved using $\Delta t = 10^{-6}$. We find that this choice leads to solutions and speed curve (to be defined soon) which are independent of the numerical discretisation.

BDF2. We find that when solving in the regime $\omega/\lambda \leq 0.4$, the Runge-Kutta solver, as outlined above, becomes unstable. This instability is observed both in solution and the resulting speed curve. To rectify this situation, we choose to switch to an implicit solver for $\omega/\lambda \leq 0.4$. In view of the analysis of [30], we choose the implicit second-order Backward Differentiation Formula 2 (BDF2) scheme, which gives rise to the system of algebraic equations

$$\varphi_n^{j+2} - \frac{4}{3}\varphi_n^{j+1} + \frac{1}{3}\varphi_n^j = \frac{2}{3}\Delta t\Big(- \lambda(\varphi_n^{j+2} - \varphi_{n-1}^{j+2}) - \omega\varphi_n^{j+2}(1 - \varphi_n^{j+2})\Big),$$

where φ_n^j and φ_n^{j+1} are solved using the standard explicit first-order Euler scheme. The algebraic equation for φ_n^{j+2} is solved using Newton-Raphson iteration with convergence tolerance ϵ. The resulting system of equations are solved using $\Delta t = 10^{-2}$ and $\epsilon = 10^{-12}$. We find that these choices lead to solutions and speed curve in agreement with the Runge-Kutta solver with $\Delta t = 10^{-6}$ when in the regime $\omega/\lambda > 0.4$.

Without loss of generality we set $\lambda = 1$ and consider variation in ω (unless otherwise specified). This is permissible since we can always re-scale time as $T = \lambda t$ and so the Blockchain equation (2.5) reduces to

$$\frac{d\varphi_n(T)}{dT} = -(\varphi_n(T) - \varphi_{n-1}(T)) - \frac{\omega}{\lambda}\varphi_n(T)(1 - \varphi_n(T)),$$

whose solutions depend explicitly on the ratio ω/λ.

Defining wave speed. Assuming solutions $\varphi_n(t)$ approach a travelling wave in the limit of large n, we define the speed of solution $\varphi_n(t)$ to be

$$s_n(p) = \frac{1}{\varphi_n^{-1}(p) - \varphi_{n-1}^{-1}(p)},$$

where $p \in (0, 1)$ is an arbitrary choice of percentile. If a travelling wave is approached in the limit of large n, then the choice of percentile $p \in (0, 1)$ does not matter, indeed, the asymptotic speed should be invariant under choice of measurement point. Hence the asymptotic speed (speed of the travelling wave), is given by

$$S(p) := \lim_{n\to\infty} s_n(p),$$

where $p \in (0, 1)$ is arbitrary.

Calculating wave speed. For our numerical study, we choose to set $p = 0.5$ arbitrarily. After solving each solution $\varphi_n(t)$, we use a standard linear interpolation to find $\varphi_n^{-1}(p)$, and hence

calculate the speed of solution $\varphi_n(t)$ as $s_n(p)$ where $\varphi_{n-1}^{-1}(p)$ would have been calculated in the previous solution. We recursively solve solutions $\varphi_n(t)$ until we reach some $n = N$ such $s_N(p) - s_{N-1}(p)$ is approximately zero. We assume this to be a sufficient indicator that a travelling wave has been reached. The value $s_N(p)$ is assumed to be a good approximation of the travelling wave speed $S(p)$ in the sense that

$$s_N(p) = S(p) - \epsilon_N(p),$$

for some $\epsilon_N(p) \geq 0$ where $\epsilon_N(p) \to 0$ as $N \to \infty$.

3.2 Numerical evidence of a travelling wave

In the plots that follow, we observe travelling wave behaviour for a variety of ω values. Secondly, the speed curve, defined by the sequence $(s_n(p))_{n\geq 1}$, is observed to flatten out indicating solutions approach a travelling wave as $n \to \infty$. For graphical presentation, we choose to plot every m^{th} solution, depending on how large N is. The travelling wave speed lower bound $v_{min} = \lambda + \sqrt{2\lambda\omega}$, as calculated in Chapter 2 for the modified Fisher-KPP equation, is juxtaposed with the speed curve $(s_n(p))_{n\geq 1}$ illustrating its validity for the Blockchain equation. Solutions $\varphi_n(t)$ are moving to the right for increasing n.

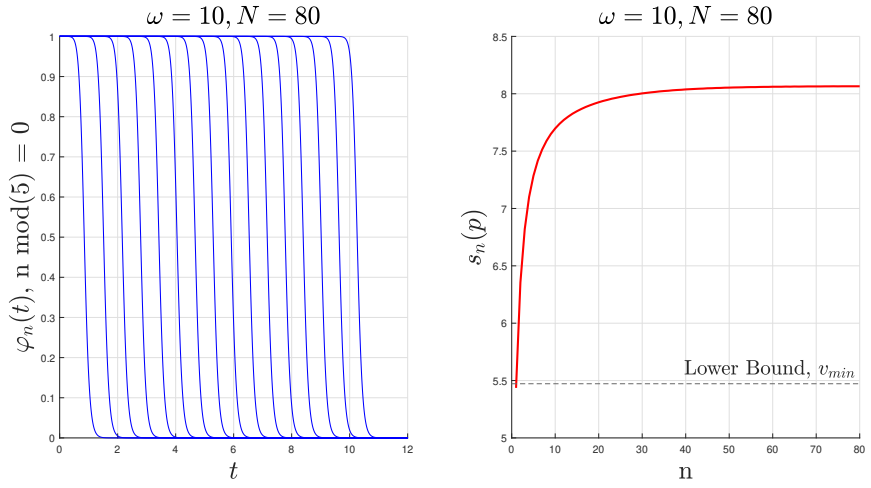

Figure 3.1: Left: Solutions $\varphi_n(t)$ and Right: Speed curve $s_n(p)$. $\lambda = 1$ and $\omega = 10$.

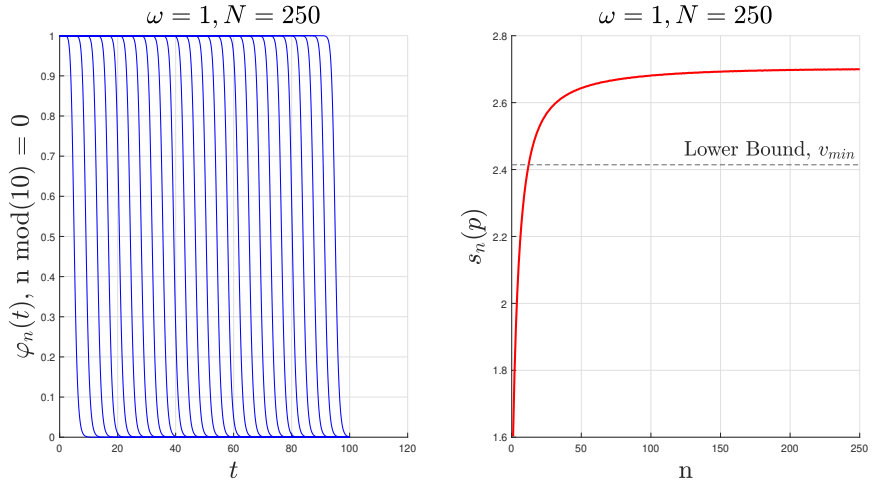

Figure 3.2: Left: Solutions $\varphi_n(t)$ and Right: Speed curve $s_n(p)$. $\lambda = 1$ and $\omega = 1$.

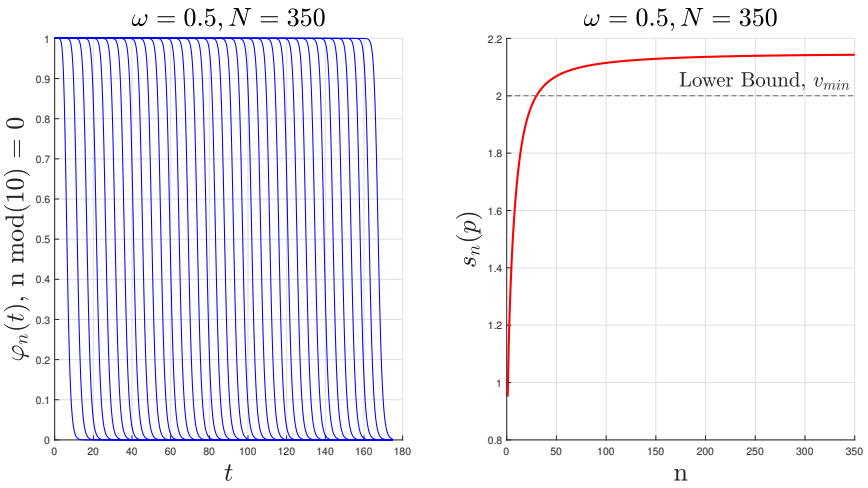

Figure 3.3: Left: Solutions $\varphi_n(t)$ and Right: Speed curve $s_n(p)$. $\lambda = 1$ and $\omega = 0.5$.

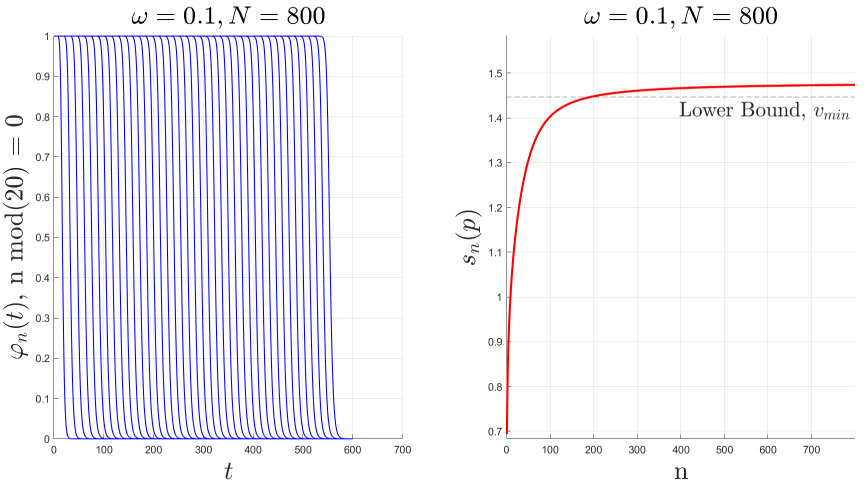

Figure 3.4: Left: Solutions $\varphi_n(t)$ and Right: Speed curve $s_n(p)$. $\lambda = 1$ and $\omega = 0.1$.

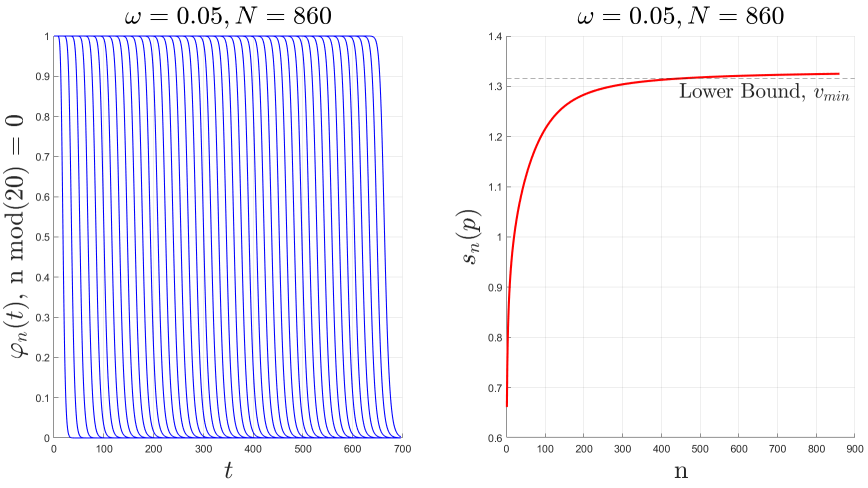

Figure 3.5: Left: Solutions $\varphi_n(t)$ and Right: Speed curve $s_n(p)$. $\lambda = 1$ and $\omega = 0.05$.

3.3 Numerical study of travelling wave speed

We established numerical evidence that solutions $\varphi_n(t)$ of the Blockchain equation converge to a travelling wave in the limit of large n. The observations of a travelling wave occurring indeed agree with the original conjecture of the existence of a travelling wave [1, 4]. In this section we will conduct a numerical study of the wave speed associated with this travelling wave. We recall the travelling wave speed was defined as $S(p) := \lim_{n\to\infty} s_n(p)$, where we approximate $S(p)$ with $s_N(p)$ for a suitably large N.

The main result of this section is a tight numerical bound on the travelling wave speed $S(p)$, as a function of λ and ω, which is observed to hold in the fast mining regime $\lambda \geq \omega$. In the slow mining regime $\lambda < \omega$, our numerical estimate acts as an upper bound.

Comparing lower bound. In Chapter 2, we provided an asymptotic approximation of the Blockchain equation (2.5) which gave us the modified Fisher-KPP equation (2.6). It was shown, using phase-plane analysis, that the modified Fisher-KPP equation admits travelling wave solutions for wave speeds at least

$$v_{min} := \lambda + \sqrt{2\lambda\omega}.$$

It is expected that the asymptotic speed $S(p)$ of the Blockchain equation (2.5) also be bounded below by v_{min}. We observe the validity of this lower bound in the following figure:

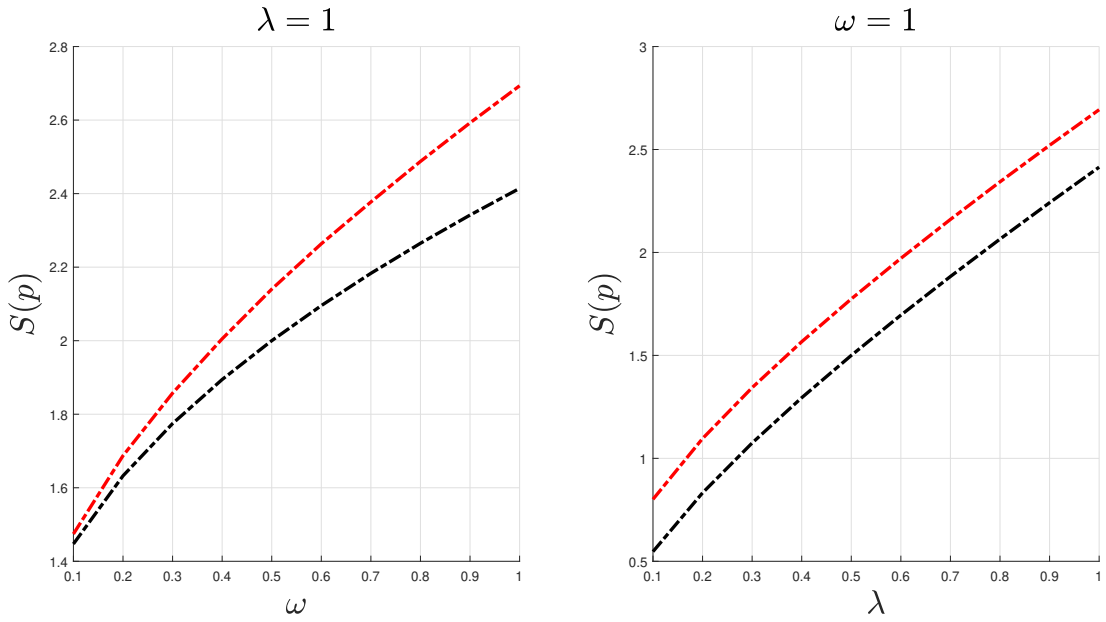

Figure 3.6: The red line is the numerically generated asymptotic speed $S(p)$, which was approximated by $s_N(p)$ for sufficiently large N. The black line is the lower bound formula $v_{min} = \lambda + \sqrt{2\lambda\omega}$.

By observation of Figure 3.6, there is clear numerical evidence that the lower bound v_{min} acts as a lower bound for the travelling wave speed $S(p)$ of the Blockchain equation (2.5). In view of these numerical observations, we assume v_{min} is a lower bound on the travelling wave speed of the Blockchain equation (2.5), and hence write this travelling wave speed as

$$S(p) = v_{min}(\lambda, \omega) + v_2(\lambda, \omega),$$

for some currently unknown $v_2(\lambda, \omega) \geq 0$.

In view of Figure 3.6, we can make two immediate observations about v_2. Namely, in the regime $\omega < \lambda$, v_2 seems to be an increasing function of ω. Whereas, in the regime $\lambda < \omega$, v_2 seems to be constant with respect to λ. We analyse these two cases separately.

Case 1. In view of Figure 3.6 ($\lambda = 1$), we write $v_2 = S(p) - v_{min}$ and hence obtain a numerical estimate of v_2. This generates the following points $(\omega, S(p) - v_{min})$,

$$(0.1, 0.0272), (0.2, 0.0548), (0.3, 0.0828), (0.4, 0.1107), (0.5, 0.1401),$$
$$(0.6, 0.1681), (0.7, 0.1950), (0.8, 0.2226), (0.9, 0.2508), (1.0, 0.2791),$$

from which when plotted gives:

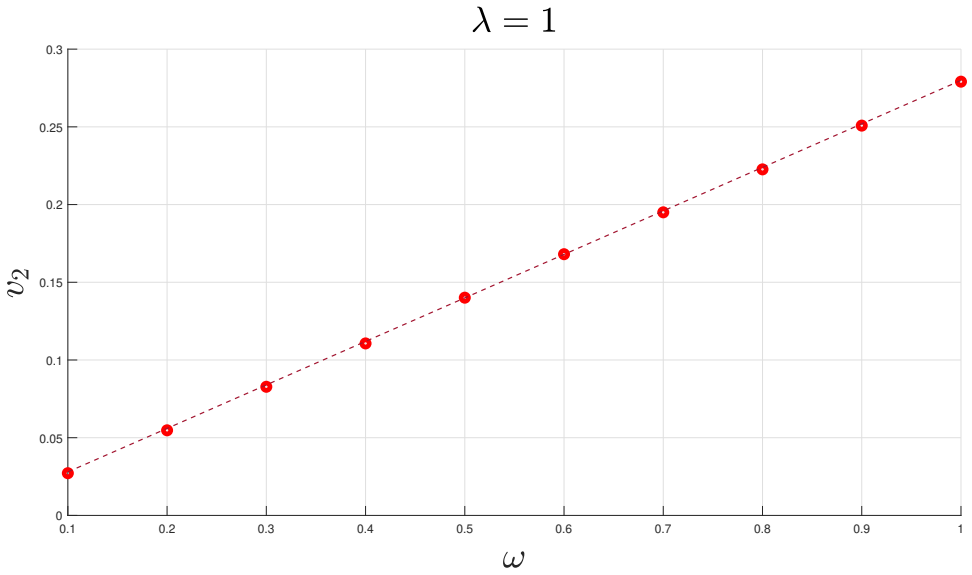

Figure 3.7: In red, $v_2 = S(p) - v_{min}$ for $\omega = 0.1, 0.2, ..., 1.0$ together with a line of best fit.

By observation of Figure 3.7, there is clear numerical evidence of a positive linear relationship between v_2 and ω. In view of this, we assume the form $S(p) = \lambda + \sqrt{2\lambda\omega} + \alpha\omega$ for some constant $\alpha > 0$, and perform a standard linear regression on the data points $(\omega, S(p) - v_{min})$. This gives a 95% confidence interval for α as

$$0.2785 < \alpha < 0.2814, \tag{3.1}$$

where the line of best fit, in Figure 3.7, has a slope of $\hat{\alpha} = 0.2799$.

We are left with the conclusion that the travelling wave speed $S(p)$ of the Blockchain equation (2.5) is exactly equal to

$$v_{bc} = \lambda + \sqrt{2\lambda\omega} + \alpha\omega,$$

when in the fast mining regime $\lambda \geq \omega$ for some $\alpha > 0$ which lies within the numerical estimated bound (3.1). To explore this further we will examine the case where $\omega > \lambda$.

Case 2. In view of Figure 3.6 ($\omega = 1$), the first observation is that v_2 is independent of λ. Indeed, the difference $S(p) - v_{min}$ looks constant over variation in λ. This behaviour breaks down however as we take $\lambda \to 0$. This can be observed in the following figure:

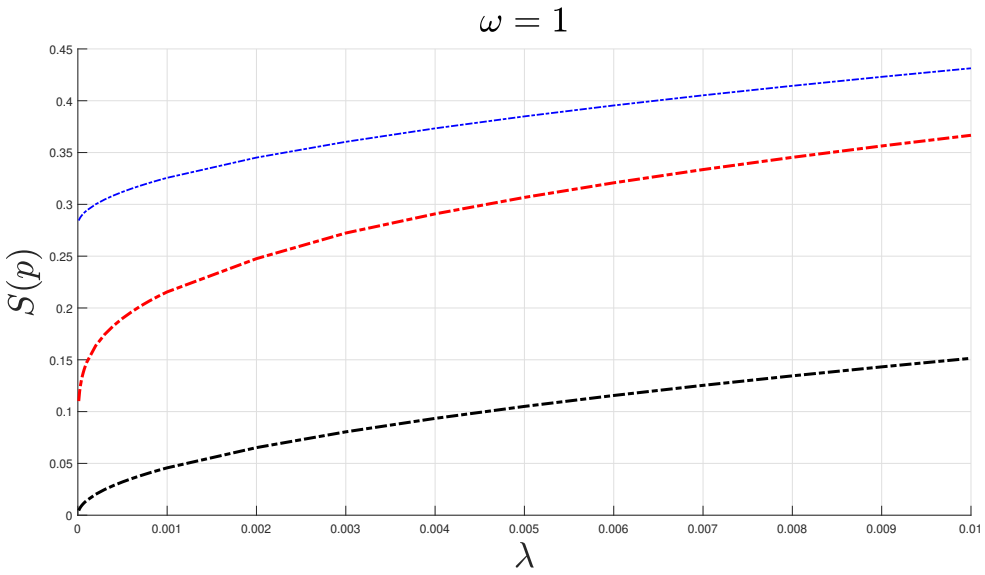

Figure 3.8: In black, $v_{min} = \lambda + \sqrt{2\lambda\omega}$ together with the numerically generated asymptotic speed $S(p)$, in red. The line in blue is $v_{bc} = \lambda + \sqrt{2\lambda\omega} + \hat{\alpha}\omega$ where $\hat{\alpha} = 0.2799$.

In Figure 3.6 ($\omega = 1$), we initially observed v_2 being independent of λ. In Figure 3.8, we have blown up the region near $\lambda = 0$. We can see that the speed $S(p)$ is below the speed $v_{bc} = \lambda + \sqrt{2\lambda\omega} + \hat{\alpha}\omega$, as $\lambda \to 0$ for $\hat{\alpha} = 0.2799$. In this case, the numerical estimate $v_{bc}(\lambda, \omega) = \lambda + \sqrt{2\lambda\omega} + \hat{\alpha}w$ (3.1) of the speed $S(p)$, must act as an upper bound in the regime $\omega > \lambda$. Indeed, this is observed in Figure 3.8. In summary, the numerical observation is that the travelling wave speed v is $v \simeq \lambda + \sqrt{2\lambda\omega} + \hat{\alpha}w$ when $\lambda \geq \omega$ and $v < \lambda + \sqrt{2\lambda\omega} + \hat{\alpha}w$ when $\lambda < \omega$.

Solution behaviour $\boldsymbol{\lambda/\omega \to 0}$. In the regime $\lambda/\omega \to 0$ we observe solutions $\varphi_n(t)$ approaching a step function. This is evident in the following figure, Figure 3.9. The difference term $\varphi_n(t) - \varphi_{n-1}(t)$ approaches an indicator function in the limit $\lambda/\omega \to 0$. We make extensive use of this observation in what follows.

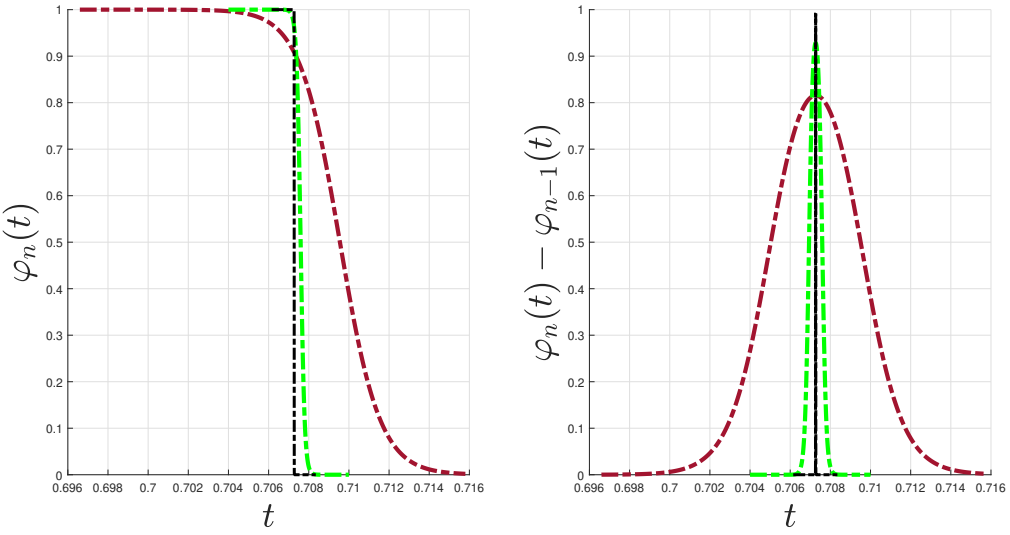

Figure 3.9: Superimposed (and translated) solutions of $\varphi_n(t)$ for large $n = N$. Regime $\lambda = 1$ and $\omega = 10^3$ (burgundy), $\omega = 10^4$ (green), $\omega = 10^6$ (black).

Conclusion. We have seen that the travelling wave speed of the Blockchain equation (2.5) seems to be exactly $v = \lambda + \sqrt{2\lambda\omega} + \alpha\omega$ when in the regime $\lambda \geq \omega$, where a numerically estimated bound on α was given in (3.1). This observation was covered in Figure 3.7. Furthermore, when considering $\omega > \lambda$, we saw in Figure 3.6 that the v_2 term seemed constant for $\lambda < \omega$. However, upon taking $\lambda << \omega$, we saw in Figure 3.8 that v_2 fails to behave as a constant with respect to λ, and in fact the speed $S(p)$ drops below the the numeric estimate $\lambda + \sqrt{2\lambda\omega} + \hat{\alpha}\omega$. As discussed earlier, if we re-scale time as $T = \lambda t$, the Blockchain equation (2.5) becomes explicitly dependent upon the ratio ω/λ. Hence, our observations in the regime of $\lambda \to 0$, should equivalently hold for instead $\omega \to \infty$. The conclusion is that the estimated speed $v_{bc} = \lambda + \sqrt{2\lambda\omega} + \hat{\alpha}\omega$ is observed to be valid in the regime $\lambda \geq \omega$. Upon taking $\lambda < \omega$, this estimated speed behaves as an upper bound of the travelling wave speed. We make the following assumption:

Assumption 3.1. *There exists an $\alpha > 0$ such that the travelling wave speed of the Blockchain equation (2.5) is exactly equal to or less than $v_{bc} = \lambda + \sqrt{2\lambda\omega} + \alpha\omega$, for all values of $\lambda, \omega > 0$.*

Furthermore, in the limit $\lambda/\omega \to 0$, we observed that the difference term $\varphi_n(t) - \varphi_{n-1}(t)$ approaches an indicator function for sufficiently large n. This was observed in Figure 3.9. We make the following assumption:

Assumption 3.2. *For all sufficiently large n, there exists a $t_n > 0$ such that $\varphi_n(t) - \varphi_{n-1}(t) \to \mathbf{1}_{t_n}(t)$ as $\lambda/\omega \to 0$. Where $\mathbf{1}_{t_n}(t) = 1$ if $t = t_n$ and zero otherwise.*

Remark 3.3. *These assumptions will be used in a heuristic argument in the next section. In particular, we conjecture an exact formula for the travelling wave speed which agrees with numerics when in the fast mining regime. In the slow mining regime, our formula acts as an upper bound.*

Connection to initial solution. Before we move on we should answer an immediate question. That is, why does the travelling wave speed behave differently in the regime $\omega > \lambda$? Indeed, we have observed that when $\lambda \geq \omega$ the travelling wave speed is behaves exactly as $v_{bc} = \lambda + \sqrt{2\lambda\omega} + \alpha\omega$ for some $\alpha > 0$. However, upon taking $\omega > \lambda$, the travelling wave speed seems to dip below this and the difference becomes progressively greater for decreasing λ, or equivalently, for increasing ω. There is an immediate connection between this behaviour of the travelling wave speed and the behaviour of the initial ($n = 0$) solution

$$\varphi_0(t) = \frac{\lambda + \omega}{\omega + \lambda e^{t(\lambda+\omega)}}. \tag{3.2}$$

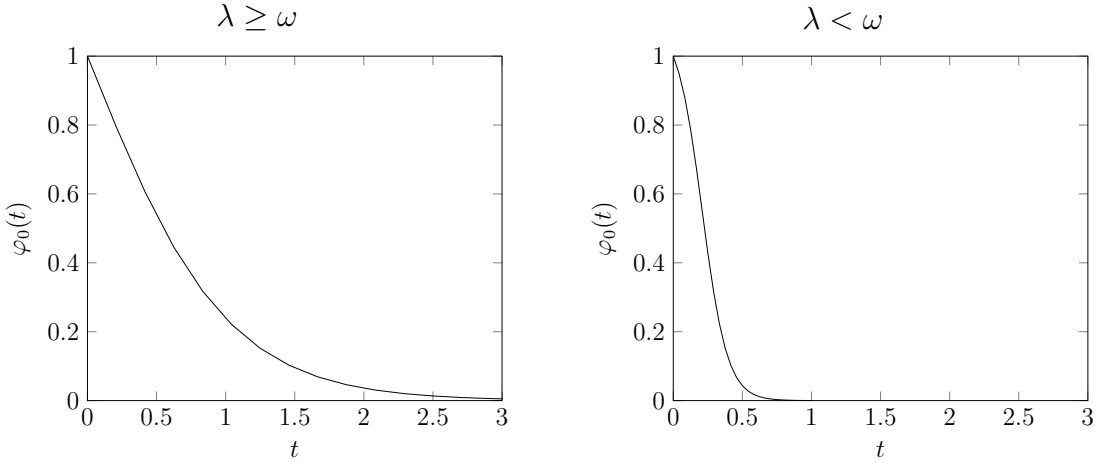

On the left, we have plotted $\varphi_0(t)$ for $\lambda = 1, \omega = 1$. On the right, we have plotted $\varphi_0(t)$ for $\lambda = 1, \omega = 10$. On the left, an inflection point is not observed for $t \geq 0$, whereas on the right, an inflection point is observed. This non-existence and existence of an inflection point,

for $t \geq 0$, is apparent in the regimes $\lambda \geq \omega$ and $\omega > \lambda$, respectfully. One can verify this is true analytically by taking derivatives of (3.2). When considering $\omega > \lambda$, the inflection point appears just below $\varphi_0 = 1$ which becomes progressively closer to $\varphi_0 = 0.5$ from above as $\omega/\lambda \to \infty$. Again, this can be verified analytically from (3.2). Given that the travelling wave speed also behaves differently in the regimes $\lambda \geq \omega$ versus $\lambda < \omega$, we believe that the travelling wave speed is directly influenced (non-trivially) by the dynamics of the initial solution $\varphi_0(t)$. Indeed, when in the regime $\omega > \lambda$, the initial solution $\varphi_0(t)$ is closer to a travelling wave form, and so one would expect a travelling wave to occur for smaller values of n. This was observed in the plots in section 3.2 where we only needed to solve up to $N = 80$ when $\omega = 10$ and $\lambda = 1$.

The connection between the travelling wave speed and the initial solution should have been expected. This connection was first observed by Kolmogorov et al. [12], with respect to travelling waves of the (non-dimensionalised) Fisher-KPP equation $u_t = u_{xx} + u(1-u)$ with conditions

$$u(x,0) = u_0(x), \quad u(x,t) \to 1 \text{ as } x \to -\infty, \quad u(x,t) \to 0 \text{ as } x \to \infty.$$

Kolmogorov et al. [12] proved that if $0 \leq u_0(x) \leq 1$ is any initial data such that for some $a < b$ we have $u_0(x) = 1$ for $x \leq a$ and $u_0(x) = 0$ for $x \geq b$, then the solution approaches a travelling wave with minimal speed $c = 2$. However, this result was noted to be sensitive to the spatial decay rate of the initial data into the stable steady state $u = 0$. To be explicit, suppose that

$$u_0(x) \sim Ce^{-\beta x},$$

as $x \to \infty$, where $\beta, C > 0$. If $\beta \geq 1$, then the solution approaches a travelling wave with speed $c = 2$. However, if the initial data decays more slowly as $0 < \beta < 1$ then the solution approaches a travelling wave with greater speed

$$c(\beta) = \beta + \frac{1}{\beta} > 2.$$

This connection between the initial data and the travelling wave speed, of a Fisher type equation, was also observed by Larson [18]. They constructed families of upper and lower bounds of solutions and compared the time-asymptotic convergence of these solutions towards travelling wave solutions. They showed that the convergence of the solution bounds to a travelling wave solution depends critically on the behavior of the initial data at infinity, that is, the rate of the exponential decay of the initial data at infinity.

In view of the Blockchain equation (2.5), the decay rate of the initial solution $\varphi_0(t)$ is dominated by the mining rate when in the fast mining regime $\lambda \geq \omega$ and decays as

$$\varphi_0(t) \sim e^{-\lambda t} \quad \text{as } t \to \infty,$$

whereas in the slow mining regime $\lambda < \omega$, the communication rate dominates and the initial solution decays as

$$\varphi_0(t) \sim e^{-\omega t} \quad \text{as } t \to \infty.$$

3.4 The wave speed conjecture

The formulation of an exact formula for the travelling wave speed of a reaction diffusion PDE for an arbitrary initial condition that evolves to a travelling wave is quite challenging. The current understanding is that the travelling wave speed is dependent upon the exponential decay rate of the initial condition. This was discussed in the previous section where we referenced the works of Kolmogorov [12] and Larson [18]. In this section we will propose, by means of a heuristic argument, an exact formula for the travelling wave speed of the Blockchain equation (2.5).

Heuristic argument

We conjecture an exact formula, as a function of λ and ω, for the travelling wave speed of the Blockchain equation (2.5). When comparing to numerics, our formula produces a travelling wave speed coinciding with the travelling wave speed observed in numerics when in the fast mining regime $\lambda \geq \omega$. In the slow mining regime $\lambda < \omega$, our formula acts as an upper bound for the travelling wave speed. Our argument will make use of the previous numerically motivated assumptions, namely, Assumption 3.1 and Assumption 3.2.

We begin our argument by recalling the Blockchain equation

$$\frac{d\varphi_n}{dt} = -\lambda(\varphi_n - \varphi_{n-1}) - \omega\varphi_n(1-\varphi_n), \quad \varphi_{-1} = 0, \quad \varphi_n(0) = 1 \text{ for all } n \geq 0, \tag{3.3}$$

the modified Fisher-KPP equation

$$\frac{\partial f}{\partial t} = -\lambda(\frac{\partial f}{\partial x} - \frac{1}{2}\frac{\partial^2 f}{\partial x^2}) - \omega f(1-f), \tag{3.4}$$

and the modified Fisher-KPP equation in travelling wave coordinates

$$-v\frac{dg}{dz} = -\lambda(\frac{dg}{dz} - \frac{1}{2}\frac{d^2 g}{dz^2}) - \omega g(1-g). \tag{3.5}$$

Derivative condition. We can write the Blockchain equation (3.3) in travelling wave coordinates $\psi(z) = \varphi_x(t)$ for $z = x - vt$ for some travelling wave speed v giving

$$-v\frac{d\psi}{dz} = -\lambda(\psi(z) - \psi(z-1)) - \omega\psi(z)(1-\psi(z)). \tag{3.6}$$

By the boundedness Lemma 1.10 and the monotonicity Lemma 1.11 from Chapter 1, the restriction $\varphi_n(t) - \varphi_{n-1}(t) \leq 1$ holds for all $n, t \geq 0$, which implies the restriction in travelling wave coordinates

$$\psi(z) - \psi(z-1) \leq 1 \quad \text{for all } z \in \mathbb{R},$$

from which follows

$$\frac{\partial g}{\partial z} - \frac{1}{2}\frac{\partial^2 g}{\partial z^2} \leq 1 \quad \text{for all } z \in \mathbb{R},$$

after equating (3.5) with (3.6) since (3.5) is a second order Taylor series approximation of (3.6).

Evaluating the last inequality at the inflection point $g = \bar{g}$ gives the derivative condition

$$0 < \frac{\partial \bar{g}}{\partial z} \leq 1. \tag{3.7}$$

Remark 3.4. *In general, solutions of the modified Fisher-KPP equation do not have to have a spatial inflection point derivative bounded above by* 1*. However, if we want solutions of the modified Fisher-KPP equation to be indicative of the Blockchain equation then we are required to make this restriction. Condition* (3.7) *can be seen as a trapping region in the* (g, g')*-phase plane; meaning, heteroclinic orbits* $h_v(g)$ *from* $(0,0)$ *to* $(1,0)$ *in* (g, g') *must satisfy* $0 < h_v(g) \leq 1$*.*

Renormalization. In view of Assumption 3.1, we make the ansatz that the travelling wave speed of the Blockchain equation is exactly equal to or less than

$$v_{bc}(\lambda, \omega) = \lambda + \sqrt{2\lambda\omega} + v_2(\omega), \tag{3.8}$$

where $v_2 \geq 0$ for all $\lambda, \omega > 0$ and $v_2(\omega)$ is independent of λ. Indeed, from numerical observation, $v_2 = \hat{\alpha}\omega$ (3.1) where $\hat{\alpha} \simeq 0.2799$, Figure 3.7.

We recall the minimal speed for a travelling wave solution of the modified Fisher-KPP equation (3.5) (in variables λ and ω)

$$v_{min}(\lambda,\omega) = \lambda + \sqrt{2\lambda\omega}. \tag{3.9}$$

We note that for any given $\omega > 0$ we have that $v_{min}(\lambda,\omega)$ is monotone increasing with respect to λ and $v_{min}(0,\omega) = 0$. In view of (3.8), we know $v_2(\omega)$ is independent of λ, so we must have for all $\lambda,\omega > 0$ there exists a $\delta(\omega) \geq 0$ such that $\gamma(\lambda,\omega) = \lambda + \delta(\omega)$ gives

$$v_{min}(\gamma(\lambda,\omega),\omega) = v_{bc}(\lambda,\omega). \tag{3.10}$$

Hence, a travelling wave solution of the Blockchain equation (3.3) (in variables λ and ω) travelling with speed $v_{bc}(\lambda,\omega)$, can be identified with a travelling wave solution of the Blockchain equation (3.3) (in variables γ and ω), travelling with speed $v_{min}(\gamma,\omega)$. This identification is through the equality of speed (3.10), where the Blockchain equation (in variables γ and ω) can be viewed as a renormalized version of the Blockchain equation (in variables λ and ω). We choose to work with this renormalized speed because we have an explicit expression for v_{min}.

We obtain the following identification of equations (in travelling wave coordinates) where the second row are the renormalized equations with respect to (3.10):

$$\begin{array}{ccc} \mathrm{BC}(v_{bc}(\lambda,\omega);\lambda,\omega) & \xrightarrow{\text{Taylor Series}} & \mathrm{mFKPP}(v_{bc}(\lambda,\omega);\lambda,\omega)) \\ \Big\downarrow (3.10) & & \Big\downarrow (3.10) \\ \mathrm{BC}(v_{min}(\gamma,\omega);\gamma,\omega) & \xrightarrow{\text{Taylor Series}} & \mathrm{mFKPP}(v_{min}(\gamma,\omega);\gamma,\omega)) \end{array}$$

where BC refers to the Blockchain equation in travelling wave coordinates (3.6), and mFKPP refers to the modified Fisher-KPP equation in travelling wave coordinates (3.5).

Limit $\boldsymbol{\lambda \to 0}$. Consider the travelling wave solution $g(z)$ of the modified Fisher-KPP equation (3.5) (in variables λ and ω) travelling with speed $v_{bc}(\lambda,\omega)$:

$$-(v_{bc}(\lambda,\omega))\frac{dg}{dz} = -\lambda(\frac{dg}{dz} - \frac{1}{2}\frac{d^2g}{dz^2}) - \omega g(1-g),$$

evaluating at the inflection point $z = \bar{z}$ gives

$$(\sqrt{2\lambda\omega} + v_2)\frac{\partial \bar{g}}{\partial z} = \omega\bar{g}(1-\bar{g}). \tag{3.11}$$

Similarly, consider the travelling wave solution $g_r(z)$ of the modified Fisher-KPP equation (3.5) (in variables γ and ω) travelling with speed $v_{min}(\gamma,\omega)$:

$$-(v_{min}(\gamma,\omega))\frac{dg_r}{dz} = -\gamma(\frac{dg_r}{dz} - \frac{1}{2}\frac{d^2g_r}{dz^2}) - \omega g_r(1-g_r),$$

evaluating at the inflection point $z = \bar{z}$ gives

$$\sqrt{2\gamma\omega}\frac{\partial \bar{g_r}}{\partial z} = \omega\bar{g_r}(1-\bar{g_r}), \tag{3.12}$$

which gives

$$\gamma = \frac{\omega\bar{g_r}^2(1-\bar{g_r})^2}{2(\bar{g_r}')}, \tag{3.13}$$

where we used notation $g_r(\bar{z}) = \bar{g_r}$ and $\frac{d\bar{g_r}}{dz} = \bar{g_r}'$.

Assuming equality of inflection points $\bar{g} = \bar{g_r}$ we obtain from (3.11) and (3.12)

$$(\sqrt{2\lambda\omega} + v_2)\frac{d\bar{g}}{dz} = \sqrt{2\gamma\omega}\frac{d\bar{g_r}}{dz}. \tag{3.14}$$

From the equality of speed (3.10) we obtain

$$\sqrt{2\lambda\omega} + v_2 = \gamma - \lambda + \sqrt{2\gamma\omega},$$

which gives

$$\sqrt{2\lambda\omega} + v_2 \geq \sqrt{2\gamma\omega},$$

for all $\lambda \geq 0$ since $\gamma \geq \lambda$. Hence from (3.14) we obtain the inequality

$$\frac{d\bar{g}}{dz} \leq \frac{d\bar{g_r}}{dz} \tag{3.15}$$

for all $\lambda \geq 0$. One can check, by a similar argument to before, that the derivative condition (3.7) also holds on the level of the renormalized mFKPP$(v_{min}(\gamma,\omega);\gamma,\omega)$, that is, $\bar{g_r}' \leq 1$. Hence inequality (3.15) becomes

$$\frac{d\bar{g}}{dz} \leq \frac{d\bar{g_r}}{dz} \leq 1 \tag{3.16}$$

Remark 3.5. *Inequality* (3.16) *can be seen as a trapping region for the heteroclinic orbit* $h_{v_{min}(\gamma,\omega)}(g_r)$ *from* $(0,0)$ *to* $(1,0)$ *in the* (g_r, g_r') *phase plane. To be specific, we have the following bound of heteroclinic orbits,* $h_{v_{bc}(\lambda,\omega)}(g_r) \leq h_{v_{min}(\gamma,\omega)}(g_r) \leq 1$*, when we superimpose the phase plane of* (g, g') *onto* (g_r, g_r') *and* $h_{v_{bc}(\lambda,\omega)}(g)$ *is the heteroclinic orbit of mFKPP*$(v_{bc}(\lambda,\omega);\lambda,\omega)$*.*

An implication of Assumption 3.2 and the derivative condition (3.7) is that if $\lambda \to 0$ (from above) then $\bar{g}' \to 1$ (from below) with respect to solutions $g(z)$ in mFKPP$(v_{bc}(\lambda,\omega);\lambda,\omega)$. Hence from inequality (3.16) we must have that $\bar{g_r}' \to 1$ as $\lambda \to 0$.

Hence in view of (3.13) we obtain in the limit $\lambda \to 0$

$$\gamma(\lambda,\omega) \to \gamma(0,\omega) = \frac{\omega}{2}\bar{g_r}^2(1-\bar{g_r})^2 = \delta(\omega).$$

We recall the equality of speed (3.10) which gives

$$\lambda + \sqrt{2\lambda\omega} + v_2 = \gamma + \sqrt{2\gamma\omega} = \lambda + \delta(\omega) + \sqrt{2(\lambda+\delta(\omega))\omega}$$

and so in the limit $\lambda \to 0$ gives

$$v_2 = \delta(\omega) + \sqrt{2\delta(\omega)\omega} = \frac{\omega}{2}\bar{g_r}^2(1-\bar{g_r})^2 + \omega\bar{g_r}(1-\bar{g_r}) \leq \frac{9}{32}\omega \tag{3.17}$$

since $\bar{g_r} \in (0,1)$ and maximum obtained when $\bar{g_r} = \frac{1}{2}$.

However, from Assumption 3.1 we know that v_2 is independent of λ. Hence the upper bound (3.17) should hold for all $\lambda > 0$. Adding $v_{min}(\lambda,\omega)$ to both sides of (3.17) gives

$$v_{bc}(\lambda,\omega) = \lambda + \sqrt{2\lambda\omega} + v_2 \leq \lambda + \sqrt{2\lambda\omega} + \frac{9}{32}\omega.$$

On the level of $v_{bc}(\lambda,\omega)$ we obtain in the limit $\lambda \to 0$

$$v_{bc}(0,\omega) \leq \frac{9}{32}\omega$$

which is indeed confirmed by numerics in Figure 3.8 (blue line), i.e., $\hat{\alpha} = 0.2799 < \frac{9}{32} = 0.28125$, where also $\frac{9}{32}$ lies within the numeric bound (3.1). We propose the following conjecture:

Conjecture 3.6. *(Wave Speed Conjecture) For all* $\lambda,\omega > 0$*, solutions* $\varphi_n(t)$ *of the Blockchain equation* (3.3) *approach a travelling wave in the sense; for all* $\lambda,\omega > 0$ *there exist a* $\tau(\lambda,\omega) > 0$ *such that* $\varphi_{n-1}(t) \to \varphi_n(t+\tau)$ *(at least) pointwise as* $n \to \infty$*. The speed of this travelling wave is bounded above by* $\lambda + \sqrt{2\lambda\omega} + \frac{9}{32}\omega$*. In the fast mining regime* $\lambda \geq \omega$ *this bound is sharp.*

3.5 Numerical evidence for the wave speed conjecture

To instil some confidence in Conjecture 3.6, we provide various numerically generated speed curves confirming the proposed speed formula. In the fast mining regime $\lambda \geq \omega$, these speed curves are observed to converge to our proposed formula $v = \lambda + \sqrt{2\lambda\omega} + \frac{9}{32}\omega$. In the slow mining regime $\omega > \lambda$, our formula acts as an upper bound.

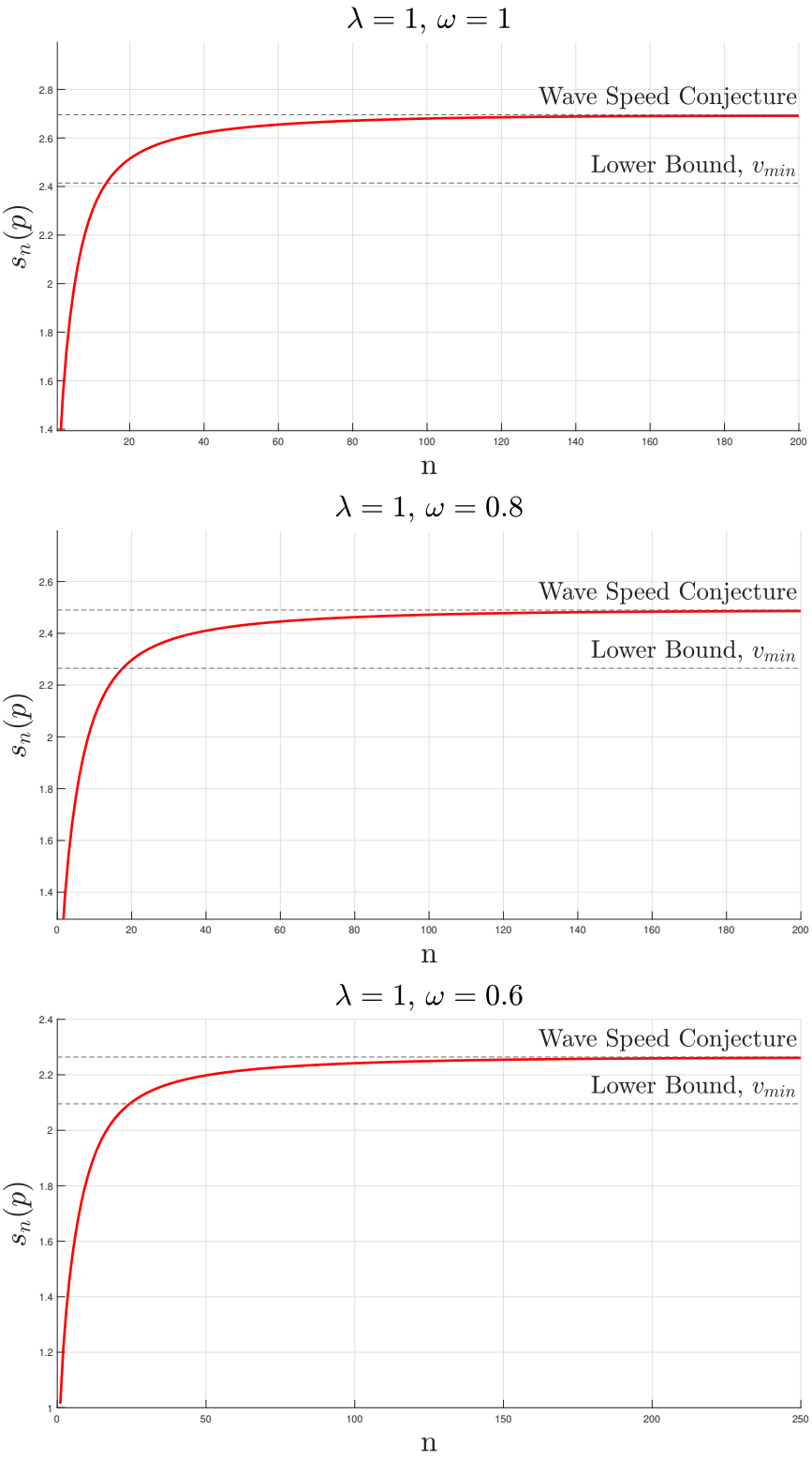

$\lambda = 1,\ \omega = 0.4$

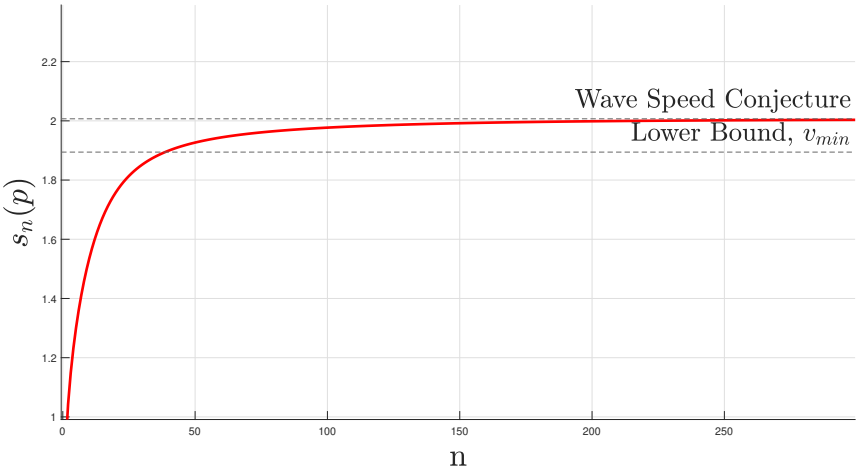

$\lambda = 1,\ \omega = 0.2$

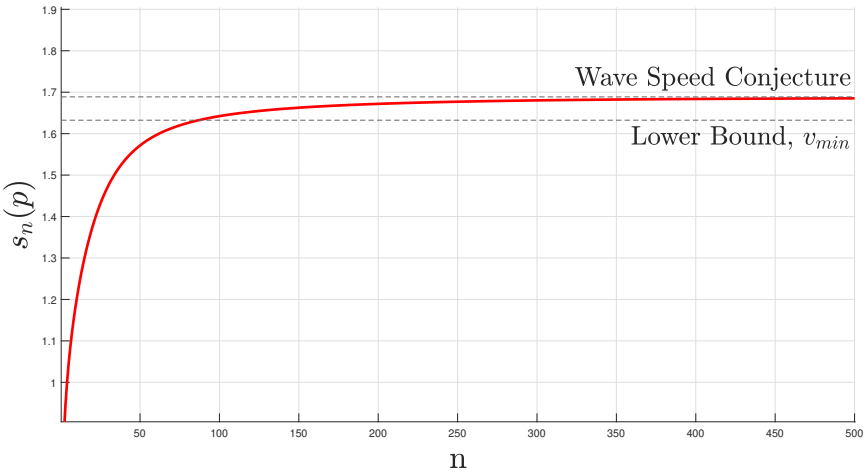

$\lambda = 1,\ \omega = 0.1$

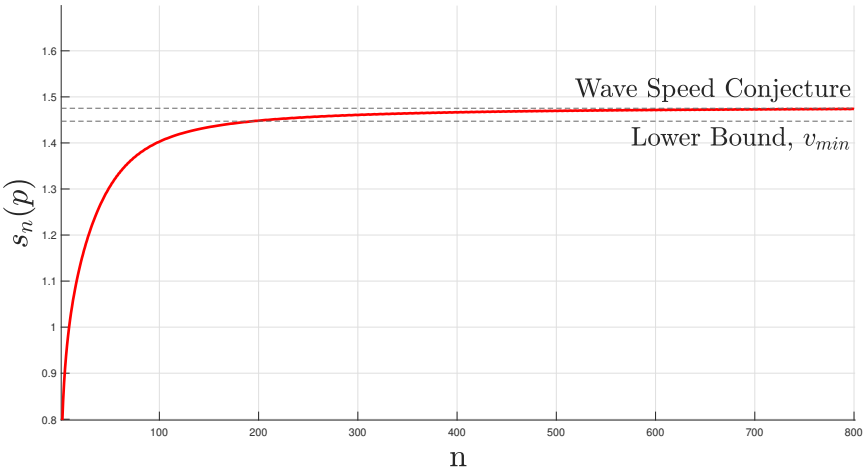

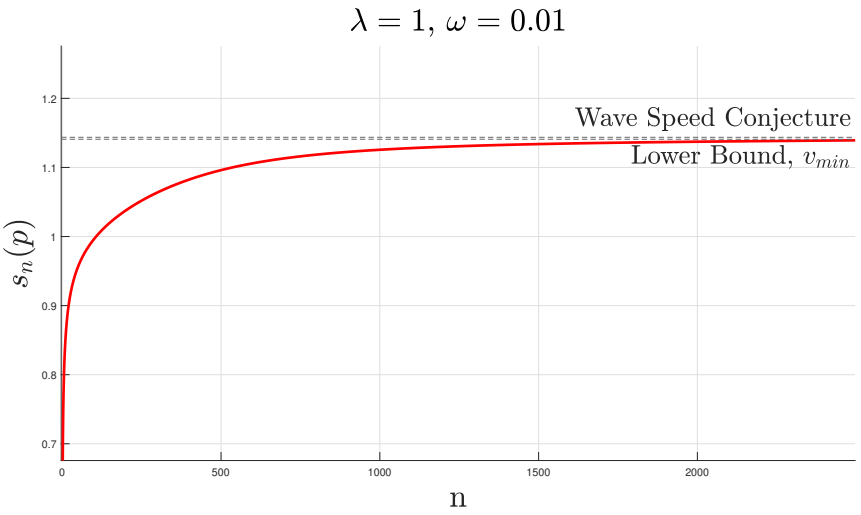

Figure 3.10: Speed curves $s_n(p)$ for $\lambda = 1$ and $\omega = 0.01, 0.1, 0.2, 0.4, 0.6, 0.8, 1$.

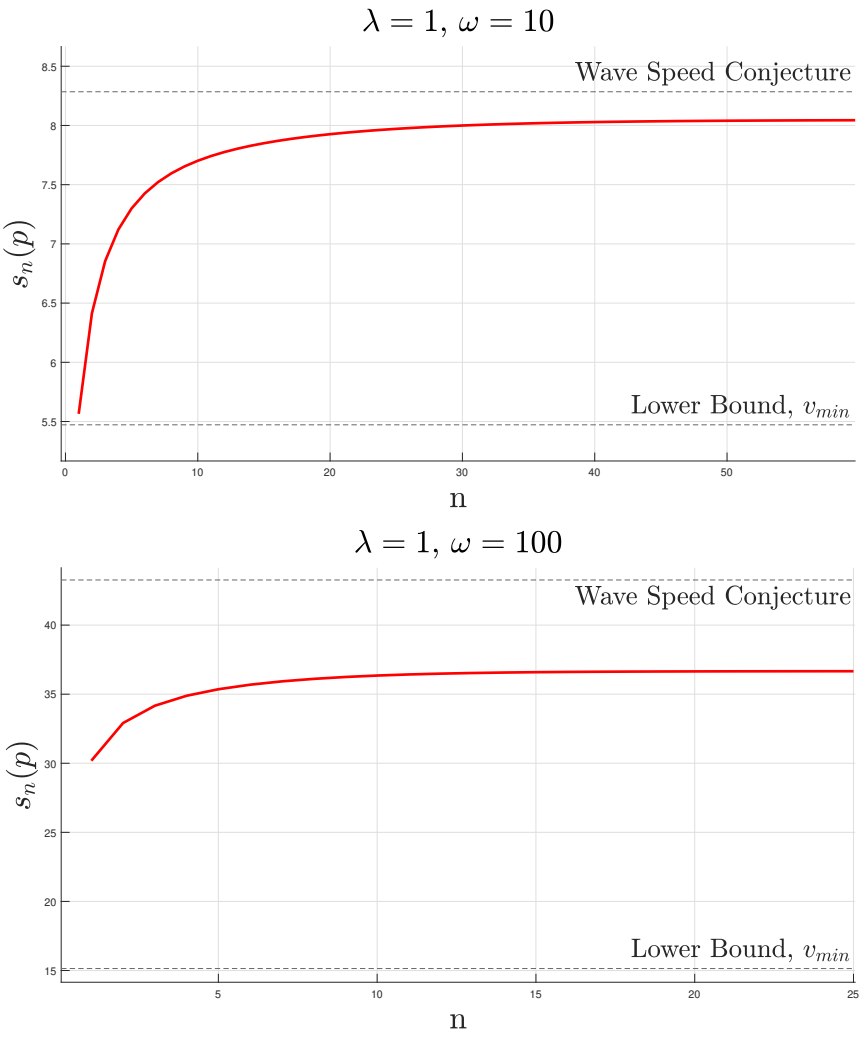

Figure 3.11: Speed curves $s_n(p)$ for $\lambda = 1$ and $\omega = 10, 100$.

3.6 An integral expression for the travelling wave speed

We recall that the speed of solutions of the Blockchain equation (2.5) can be obtained via choosing a percentile (measuring point) $p \in (0,1)$ and defining the speed of solution $\varphi_n(t)$ to be $s_n(p) = 1/(\varphi_n^{-1}(p) - \varphi_{n-1}^{-1}(p))$. The asymptotic (travelling wave) speed is thus $S(p) = \lim_{n\to\infty} s_n(p)$. If solutions do approach a travelling wave then the asymptotic speed $S(p)$ should be invariant under choice of percentile $p \in (0,1)$. We will use the notation that $\tau = \lim_{n\to\infty} \varphi_n^{-1}(p) - \varphi_{n-1}^{-1}(p)$ where the asymptotic (travelling wave) speed is effectively $v = 1/\tau$.

Proposition 3.7. *Let $\varphi_n(t)$ be a solution of the Blockchain equation (2.5) for some $n \geq 1$ then the following equality of integrals holds,*

$$\int_0^1 \varphi_n^{-1}(p) - \varphi_{n-1}^{-1}(p)dp = \int_0^\infty \varphi_n(t) - \varphi_{n-1}(t)dt \tag{3.18}$$

Proof. The quantity obtained, integral on right-hand-side, is the area bounded between $\varphi_n(t)$ and $\varphi_{n-1}(t)$ over the $t-$axis. The integral exists since $\varphi_n(0) = 1$ for all $n \geq 0$, lemmas 1.10 and 1.11 imply $\varphi_n(t) - \varphi_{n-1}(t) \in (0,1)$ for all $n, t \geq 0$ and that solutions $\varphi_n(t)$ decay exponentially in the large t limit. The exponential decay can be checked by linearizing the Blockchain equation (2.5) around $\varphi_n = 0$ which is then solvable with an exponentially decaying solution in the limit $t \to \infty$. The integral on the left-hand-side gives the same area if one switches the axis and instead integrates over percentiles $p \in (0,1)$. □

If the solutions $\varphi_n(t)$ approach a travelling wave in the limit $n \to \infty$ then

$$\tau = \lim_{n\to\infty} \int_0^\infty \varphi_n(t) - \varphi_{n-1}(t)dt. \tag{3.19}$$

To see why this is true we recall $\tau = \lim_{n\to\infty} \varphi_n^{-1}(p) - \varphi_{n-1}^{-1}(p)$ is a constant up to choice of λ and ω. Integrating $\tau = \lim_{n\to\infty} \varphi_n^{-1}(p) - \varphi_{n-1}^{-1}(p)$ with respect to p over $p \in (0,1)$ just gives τ, which is true since τ is the inverse of the travelling wave speed v which is invariant under choice of percentile $p \in (0,1)$. Then use the equality of integrals (3.18) to get the result (3.19).

Rearranging the Blockchain equation (2.5) gives

$$\varphi_n(t) - \varphi_{n-1}(t) = \frac{1}{\lambda}\Big(- \frac{\partial \varphi_n}{\partial t} - \omega\varphi_n(t)(1 - \varphi_n(t))\Big),$$

then integrating both sides with respect to t from 0 to ∞ gives

$$\int_0^\infty \varphi_n(t) - \varphi_{n-1}(t)dt = \frac{1}{\lambda}\Big(1 - \omega\int_0^\infty \varphi_n(t)(1 - \varphi_n(t))dt\Big),$$

then taking the limit $n \to \infty$ of both sides and using (3.19) we obtain a formula for the asymptotic (travelling wave) speed

$$v := 1/\tau = \frac{\lambda}{1 - \omega \lim_{n\to\infty} \int_0^\infty \varphi_n(t)(1 - \varphi_n(t))dt}. \tag{3.20}$$

Comment. We see that taking $\omega \to 0$ gives $v = \lambda$ which agrees with the speed of the flattening front solution of the Blockchain equation (2.5) with $\omega = 0$ as discussed in Chapter 1. The travelling wave formula (3.20) is not particularly useful, indeed, we do not have an analytic form for $\varphi_n(t)$ in the limit $n \to \infty$. However, if in future works one is able to find analytic approximations of $\varphi_n(t)$ in the limit $n \to \infty$, then (3.20) will provide a way to estimate the travelling wave speed. Furthermore, the formula (3.20) provides another way to numerically calculate the travelling wave speed. A solution $\varphi_n(t)$ with a sufficiently large n will suffice.

4 Painlevé Equations and Isomonodromic Deformations

4.1 Introduction to the Painlevé equations and integrability

We saw in Chapter 2 that the modified Fisher-KPP equation (2.6) was of Painlevé type and consequentially admitted an exact solution. This result draws us to study in detail the relationship between integrable systems and the Painlevé equations. We introduce the Painlevé equations, their singularity and Hamiltonian structure, and their symmetries via Bäcklund transformations. For completeness we illustrate the Painlevé coalescence cascade which shows that the Painlevé equations I-V are degeneration's of Painlevé VI. Following this, we discuss the relationship between the Painlevé equations and integrable systems. We will focus our attention to integrability in the sense of monodromy preserving deformations and in the sense of the existence of a similarity reduction.

4.1.1 The Painlevé equations

Before the formulation of the Painleve equations much research was devoted to the study of differential equations which admitted solutions with the following property: *The only movable singularities are poles*, which is now known as the Painlevé property [19]. The seminal 1884 work of Poincare and Fuchs showed that first order equations, with the Painlevé property, of the form

$$y' = R(z, y),$$

where R is locally analytic in z and rational in y, can be reduced to a Weierstrass elliptic function or the Riccati equation. This result motivated research for the classification of second order ODE's.

In the early 1900s, Painlevé, Gambier and Fuchs [31, 32, 33, 34] investigated a possible classification of all second order differential equations of the form

$$y'' = R(z, y, y'),$$

where R is rational in y, y' and locally analytic in z, with the Painlevé property. Their investigation found that there were 50 canonical equations (listed in Ince, 1956 [35]) of this form up to a Möbius transformation of the dependent variable y and analytic changes in the independent variable z. Painlevé found that 44 of these equations were reducible and solvable in terms of known functions, which left 6 of these equations whose solutions must be transcendental. These six nonlinear second-order ODE's are now known as the Painlevé equations and their solutions, the Painlevé transcendents:

$$\begin{aligned}
\mathrm{P_I}: &\quad \frac{d^2y}{dz^2} = 6y^2 + z \\
\mathrm{P_{II}}: &\quad \frac{d^2y}{dz^2} = 2y^3 + zy + \alpha \\
\mathrm{P_{III}}: &\quad \frac{d^2y}{dz^2} = \frac{1}{y}\Big(\frac{dy}{dz}\Big)^2 - \frac{1}{z}\frac{dy}{dz} + \frac{\alpha y^2 + \beta}{z} + \gamma y^3 + \frac{\delta}{y} \\
\mathrm{P_{IV}}: &\quad \frac{d^2y}{dz^2} = \frac{1}{2y}\Big(\frac{dy}{dz}\Big)^2 + \frac{3}{2}y^3 + 4zy^2 + 2(z^2 - \alpha)y + \frac{\beta}{y} \\
\mathrm{P_V}: &\quad \frac{d^2y}{dz^2} = \Big(\frac{1}{2y} + \frac{1}{y-1}\Big)\Big(\frac{dy}{dz}\Big)^2 - \frac{1}{z}\frac{dy}{dz} + \frac{(y-1)^2}{z^2}\Big(\alpha y + \frac{\beta}{y}\Big) + \frac{\gamma y}{z} + \frac{\delta y(y+1)}{y-1}
\end{aligned}$$

$$\mathrm{P_{VI}}: \quad \frac{d^2y}{dz^2} = \frac{1}{2}\Big(\frac{1}{y} + \frac{1}{y-1} + \frac{1}{y-z}\Big)\Big(\frac{dy}{dz}\Big)^2 - \Big(\frac{1}{z} + \frac{1}{z-1} + \frac{1}{y-z}\Big)\frac{dy}{dz} + \frac{y(y-1)(y-z)}{z^2(z-1)^2}\Big(\alpha + \frac{\beta z}{y^2} + \frac{\gamma(z-1)}{(y-1)^2} + \frac{\delta z(z-1)}{(y-z)^2}\Big),$$

where $\alpha, \beta, \gamma, \delta$ are arbitrary complex constants.

Remark 4.1. *Solutions of $P_I - P_{VI}$ are transcendental for arbitrary values of the parameters $\alpha, \beta, \gamma, \delta$. However, for certain values of the parameters, rational and special function solutions can be obtained which are outlined in [36]. For example, the P_{II} equation admits a unique rational solution for each $\alpha \in \mathbb{Z}$ which can be generated by Bäcklund transformations.*

Singularity structure. Each Painlevé equation admits a finite number of isolated singularities. For example, the locations of the fixed singularities are $\{\infty\}$ for $\mathrm{P_I}, \mathrm{P_{II}}, \mathrm{P_{IV}}$, $\{0, \infty\}$ for $\mathrm{P_{III}}, \mathrm{P_V}$ and $\{0, 1, \infty\}$ for $\mathrm{P_{VI}}$. Hence we can always find a Riemann surface where each solution of $\mathrm{P_J}$ is single-valued on its cover. If we remove the isolated singularities of each equation $\mathrm{P_J}$ we obtain a subset $Q_J \subset \bar{\mathbb{C}} := \mathbb{C} \cup \{\infty\}$ which has a covering space where all solutions are meromorphic:

$$Q_I = \bar{\mathbb{C}} \setminus \{\infty\}, \;\; Q_{II} = \bar{\mathbb{C}} \setminus \{\infty\}, \;\; Q_{III} = \bar{\mathbb{C}} \setminus \{0, \infty\},$$
$$Q_{IV} = \bar{\mathbb{C}} \setminus \{\infty\}, \;\; Q_V = \bar{\mathbb{C}} \setminus \{0, \infty\}, \;\; Q_{VI} = \bar{\mathbb{C}} \setminus \{0, 1, \infty\}.$$

An implication is that each solution of $\mathrm{P_J}$ defines a single-valued function on a Riemann surface covering $\mathrm{Q_J}$. It is in this sense that the Painlevé transcendents are accepted as new special functions.

Hamiltonian structure. Following [36], each of the Painlevé equations $\mathrm{P_I} - \mathrm{P_{VI}}$ can be written as a Hamiltonian system:

$$\frac{Dq}{Dz} = \frac{\partial H_J}{\partial p}, \qquad \frac{Dp}{Dz} = -\frac{\partial H_J}{\partial q},$$

where the derivative D/Dz is given by

$$\frac{D}{Dz} = \frac{d}{dz}, \qquad \text{for } J = I, II, V,$$
$$\frac{D}{Dz} = z\frac{d}{dz}, \qquad \text{for } J = III, V,$$
$$\frac{D}{Dz} = z(z-1)\frac{d}{dz}, \qquad \text{for } J = VI,$$

for a suitable Hamiltonian function $H_J(q, p, z)$. If one defines $\sigma(z) = H_J(q, p, z)$, then $\sigma(z)$ satisfies a second order ODE whose solution is expressible in terms of the associated Painlevé equation $\mathrm{P_J}$. We illustrate the case of $\mathrm{P_I}$:

The Hamiltonian for $\mathrm{P_I}$ is

$$H_I(q, p, z) = \frac{1}{2}p^2 - 2q^3 - zq, \tag{4.1}$$

where

$$q' = p, \qquad p' = 6q^2 + z. \tag{4.2}$$

It is easy to check that $q = y$ satisfies $\mathrm{P_1}$. Furthermore, the function $\sigma(z) = H_1(q, p, z)$ given by (4.1) satisfies

$$(\sigma'')^2 + 4(\sigma')^3 + 2z\sigma' - 2\sigma = 0. \tag{4.3}$$

Conversely, if σ is a solution of (4.3) then

$$q = -\sigma', \qquad p = -\sigma'',$$

are solutions of (4.2).

The Hamiltonian functions $\sigma = H_J$ have many applications, for example: random matrix theory (Tracy and Widom [37, 38]) and statistical physics (Jimbo, Miwa, Mori and Sato, [39]). For the Hamiltonian structure of $\mathrm{P_{II}}$ see [36] and for $\mathrm{P_{III}} - \mathrm{P_{VI}}$ see Okamoto [40, 41, 42, 43].

4.1.2 Bäcklund transformations

Each Painlevé equation $\mathrm{P_{II}} - \mathrm{P_{VI}}$ admits a Bäcklund transformation of the independent parameter. These transformations relate one solution to another of the same equation, or relate one solution to another of a different equation. These Bäcklund transformations are outlined in detail in [36]. We illustrate the simplest case, the Bäcklund transformations for $\mathrm{P_{II}}$. We recall the $\mathrm{P_{II}}$ equation with dependent variable $\alpha \in \mathbb{C}$:

$$\mathrm{P_{II}}(\alpha): \quad \frac{d^2y}{dz^2} = 2y^3 + zy + \alpha.$$

Then the following Bäcklund transformations T_+ and T_- map a solution of $\mathrm{P_{II}}(\alpha)$ to a solution of $\mathrm{P_{II}}(\alpha+1)$ and $\mathrm{P_{II}}(\alpha-1)$ respectively, for any $\alpha \in \mathbb{C}$:

$$T_+(\alpha, y) = -y - \frac{\alpha + \frac{1}{2}}{y' + y^2 + \frac{z}{2}},$$
$$T_-(\alpha, y) = -y + \frac{\alpha - \frac{1}{2}}{y' - y^2 - \frac{z}{2}},$$

where we also have the involution transformation given by:

$$S(\alpha, y) = -y,$$

which sends a solution of $\mathrm{P_{II}}(\alpha)$ to $\mathrm{P_{II}}(-\alpha)$.

If we consider $\mathrm{P_{II}}(0)$ which has the unique rational solution $y = 0$ then applying T_+ and T_- gives

$$T_+(0,0) = -0 - \frac{0 + \frac{1}{2}}{0 + 0^2 + \frac{z}{2}} = -\frac{1}{z},$$
$$T_-(0,0) = -0 + \frac{0 - \frac{1}{2}}{0 - 0^2 - \frac{z}{2}} = \frac{1}{z},$$

which are the unique rational solutions of $\mathrm{P_{II}}(1)$ and $\mathrm{P_{II}}(-1)$ respectively. If we apply T_+ and T_- to $\mathrm{P_{II}}(1)$ and $\mathrm{P_{II}}(-1)$ respectively, we then obtain

$$T_+(1, -\frac{1}{z}) = -\Big(-\frac{1}{z}\Big) - \frac{1 + \frac{1}{2}}{\Big(-\frac{1}{z}\Big)' + \Big(-\frac{1}{z}\Big)^2 + \frac{z}{2}} = \frac{1}{z} - \frac{3}{2\Big(\frac{z}{2} + \frac{2}{z^2}\Big)},$$
$$T_-(-1, \frac{1}{z}) = -\Big(\frac{1}{z}\Big) + \frac{1 - \frac{1}{2}}{\Big(\frac{1}{z}\Big)' - \Big(\frac{1}{z}\Big)^2 - \frac{z}{2}} = -\frac{1}{z} + \frac{3}{2\Big(\frac{z}{2} + \frac{2}{z^2}\Big)},$$

which are the unique rational solutions of $\mathrm{P_{II}}(2)$ and $\mathrm{P_{II}}(-2)$ respectively. Continuing this process, we are able to iterate through all the unique rational solutions of $\mathrm{P_{II}}(\alpha)$ for $\alpha \in \mathbb{Z}$:

$$\begin{array}{ccccccccc}
 & & \mathrm{P_{II}}(1) & \xrightarrow{T_+} & \mathrm{P_{II}}(2) & \xrightarrow{T_+} & \mathrm{P_{II}}(3) & \xrightarrow{T_+} & \cdots \\
 & \overset{T_+}{\nearrow} & \downarrow S & & \downarrow S & & \downarrow S & & \\
\mathrm{P_{II}}(0) & & & & & & & & \\
 & \underset{T_-}{\searrow} & & & & & & & \\
 & & \mathrm{P_{II}}(-1) & \xrightarrow[T_-]{} & \mathrm{P_{II}}(-2) & \xrightarrow[T_-]{} & \mathrm{P_{II}}(-3) & \xrightarrow[T_-]{} & \cdots
\end{array}$$

Theorem 4.2 ([36]). *1. For every $\alpha = n \in \mathbb{Z}$ there exists a unique rational solution of P_{II}. For every $\alpha = n + \frac{1}{2}$, with $n \in \mathbb{Z}$, there exists a unique one-parameter family of classical solutions of P_{II}, each of which is rationally written in terms of Airy functions. For all other values of $\alpha \in \mathbb{C}$, the solution of P_{II} is transcendental.*

Similar theorems for the other Painlevé equations $\mathrm{P_{III}} - \mathrm{P_{VI}}$ exists and are outlined in [36].

4.1.3 The coalescence cascade

Paul Painlevé [31] found that is was possible to connect the six Painlevé equations $\mathrm{P_I} - \mathrm{P_{VI}}$ by a transformation of variables and parameters. More specifically, he introduced an artificial parameter ϵ and considered a mapping which included this artificial parameter in such a way that taking $\epsilon \to 0$ will transform one Painlevé equation into another. This process can be seen as a degeneration of one Painlevé equation into another. The $\mathrm{P_{VI}}$ equation is viewed as the master equation of this transformation process, since it degenerates into the other five Painlevé equations $\mathrm{P_{II}} - \mathrm{P_{VI}}$. When viewed as a diagram, we have what is now known as the Painlevé coalescence cascade [19]:

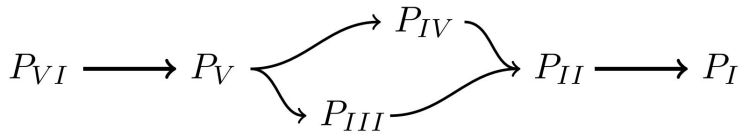

Starting with the $\mathrm{P_{VI}}$ equation we have

$$\mathrm{P_{VI}}: \quad \frac{d^2y}{dz^2} = \frac{1}{2}\Big(\frac{1}{y} + \frac{1}{y-1} + \frac{1}{y-z}\Big)\Big(\frac{dy}{dz}\Big)^2 - \Big(\frac{1}{z} + \frac{1}{z-1} + \frac{1}{y-z}\Big)\frac{dy}{dz} + \frac{y(y-1)(y-z)}{z^2(z-1)^2}\Big(\alpha + \frac{\beta z}{y^2} + \frac{\gamma(z-1)}{(y-1)^2} + \frac{\delta z(z-1)}{(y-z)^2}\Big),$$

with transformation

$$y(z) \mapsto y(z), \quad z \mapsto 1 + \epsilon z, \quad \alpha \mapsto \alpha, \quad \beta \mapsto \beta, \quad \gamma \mapsto \frac{\gamma}{\epsilon} - \frac{\delta}{\epsilon^2}, \quad \delta \mapsto \frac{\delta}{\epsilon},$$

upon taking $\epsilon \to 0$ degenerates into the $\mathrm{P_V}$ equation:

$$\mathrm{P_V}: \quad \frac{d^2y}{dz^2} = \Big(\frac{1}{2y} + \frac{1}{y-1}\Big)\Big(\frac{dy}{dz}\Big)^2 - \frac{1}{z}\frac{dy}{dz} + \frac{(y-1)^2}{z^2}\Big(\alpha y + \frac{\beta}{y}\Big) + \frac{\gamma y}{z} + \frac{\delta y(y+1)}{y-1}. \tag{4.4}$$

Depending on choice of transformation, the $\mathrm{P_V}$ (4.4) equation can degenerate into to either the $\mathrm{P_{IV}}$ equation or the $\mathrm{P_{III}}$ equation. The $\mathrm{P_V}$ (4.4) equation with the transformation

$$y(z) \mapsto \frac{\epsilon y(z)}{\sqrt{2}}, \quad z \mapsto 1 + \sqrt{2}\epsilon z, \quad \alpha \mapsto \frac{1}{2\epsilon^4}, \quad \beta \mapsto \frac{\beta}{4}, \quad \gamma \mapsto -\frac{1}{\epsilon^4}, \quad \delta \mapsto \frac{\alpha}{\epsilon^2} - \frac{1}{2\epsilon^4},$$

upon taking $\epsilon \to 0$ degenerates into the $\mathrm{P_{IV}}$ equation:

$$\mathrm{P_{IV}}: \quad \frac{d^2y}{dz^2} = \frac{1}{2y}\Big(\frac{dy}{dz}\Big)^2 + \frac{3}{2}y^3 + 4zy^2 + 2(z^2 - \alpha)y + \frac{\beta}{y}. \tag{4.5}$$

The $\mathrm{P_V}$ (4.4) equation with the transformation

$$y(z) \mapsto 1 + \epsilon z y(z), \quad z \mapsto z^2, \quad \alpha \mapsto \frac{\alpha}{4\epsilon} + \frac{\gamma}{8\epsilon^2}, \quad \beta \mapsto -\frac{\gamma}{8\epsilon^2}, \quad \gamma \mapsto \frac{\epsilon\beta}{4}, \quad \delta \mapsto \frac{\delta\epsilon^2}{8},$$

upon taking $\epsilon \to 0$ degenerates into the $\mathrm{P_{III}}$ equation:

$$\mathrm{P_{III}}: \quad \frac{d^2y}{dz^2} = \frac{1}{y}\Big(\frac{dy}{dz}\Big)^2 - \frac{1}{z}\frac{dy}{dz} + \frac{\alpha y^2 + \beta}{z} + \gamma y^3 + \frac{\delta}{y}. \tag{4.6}$$

The $\mathrm{P_{IV}}$ (4.5) equation with transformation

$$y(z) \mapsto \frac{2^{\frac{2}{3}} y(z)}{\epsilon} + \frac{1}{\epsilon^3}, \quad z \mapsto 2^{-\frac{2}{3}}\epsilon z - \frac{1}{\epsilon^3}, \quad \alpha \mapsto -2\alpha - \frac{1}{2\epsilon^6}, \quad \beta \mapsto -\frac{1}{2\epsilon^{12}},$$

upon taking $\epsilon \to 0$ degenerates into the $\mathrm{P_{II}}$ equation:

$$\mathrm{P_{II}}: \quad \frac{d^2y}{dz^2} = 2y^3 + zy + \alpha \tag{4.7}$$

The $\mathrm{P_{III}}$ (4.6) equation with transformation

$$y(z) \mapsto 1 + 2\epsilon y(z), \quad z \mapsto 1 + \epsilon^2 z, \quad \alpha \mapsto -\frac{1}{2\epsilon^6}, \quad \beta \mapsto \frac{1}{2\epsilon^6} + \frac{2\alpha}{\epsilon^3}, \quad \gamma \mapsto \frac{1}{4\epsilon^6}, \quad \delta \mapsto -\frac{1}{4\epsilon^6},$$

upon taking $\epsilon \to 0$ degenerates into the $\mathrm{P_{II}}$ equation (4.7).

The $\mathrm{P_{II}}$ (4.7) equation with transformation

$$y(z) \mapsto \epsilon y(z) + \frac{1}{\epsilon^5}, \quad z \mapsto \epsilon^2 z - \frac{6}{\epsilon^{10}}, \quad \alpha \mapsto \frac{4}{\epsilon^{15}},$$

upon taking $\epsilon \to 0$ degenerates into the $\mathrm{P_I}$ equation:

$$\mathrm{P_I}: \quad \frac{d^2y}{dz^2} = 6y^2 + z.$$

4.1.4 Connection to integrable systems

We now discuss the connection between integrable systems and the Painlevé equations. The general consensus is that there is no one definition of integrability. The notion of integrability is synonymous with certain properties that the system must admit. For example, the existence of a Hamiltonian structure, a Lax pair or the conservation of infinitely many quantities are an indication of integrability [44]. The Painlevé equations indeed admit some properties of integrability which we outline now.

Monodromy deformation. One connection to integrable PDE's is that each Painlevé equation admits a Lax representation. In this sense they arise as the compatibility condition for an associated pair of linear systems of differential equations. This is a direct result of the theory of monodromy-preserving deformations of linear systems. Following the original results of Flaschka and Newell [45], we present the associated linear problem for the $\mathrm{P_{II}}$ equation as illustrated in [46].

Consider the coupled system of linear differential equations for $\boldsymbol{u}(z,t) = (u_1(z,t), u_2(z,t))^T$:

$$\boldsymbol{u}_t = \begin{pmatrix} -i(4t^2 + 2y^2 + z) & 4ty + 2iy' + \alpha/t \\ 4ty - 2iy' + \alpha/t & i(4t^2 + 2y^2 + z) \end{pmatrix} \boldsymbol{u}, \tag{4.8a}$$

$$\boldsymbol{u}_z = \begin{pmatrix} -it & y \\ y & it \end{pmatrix} \boldsymbol{u}, \tag{4.8b}$$

where $y = y(z)$ and $\alpha \in \mathbb{C}$. Enforcing the compatibility condition of this pair of equations, or $\boldsymbol{u}_{zt} = \boldsymbol{u}_{tz}$, gives $y(z)$ satisfying $\mathrm{P_{II}}$ with parameter α.

If one considers the monodromy of the system of equations (4.8a), then equation (4.8b) is the condition on a deformation of the solution $\boldsymbol{u}$ in variable z to preserve the monodromy data for the singular points $t = 0$ and $t = \infty$, [46, 45, 47].

Remark 4.3. *Monodromy is the study of how objects behave as they run around a singularity. In the context of differential equations, monodromy would be understanding how solutions behave as we evaluate the solution around a singularity. A precise definition of monodromy data and deformation of solution will be made clear in the isomonodromic deformations section.*

This is the connection to the theory of monodromy preserving deformations of linear systems. In fact, each of the six Painlevé equations arises via this monodromy-preserving deformation process. For example, $\mathrm{P_{VI}}$ was obtained by R.Fuchs, [33, 34], as the condition for the monodromy preserving deformation of a Fuchsian system with four regular singular points. We explore this result in detail in the isomonodromic deformations section.

Similarity reduction. Furthermore, each Painlevé equation can be obtained as a similarity reduction of an integrable PDE. Following [46], we illustrate this with the Korteweg-de Vries equation, a well known integrable PDE [48]

$$\phi_t + 6\phi\phi_x + \phi_{xxx} = 0. \tag{4.9}$$

We consider the following similarity reduction

$$\phi(x,t) = \frac{\eta(z)}{(3t)^{\frac{2}{3}}}, \quad z = \frac{x}{(3t)^{\frac{1}{3}}},$$

then equation (4.9) gives,

$$\eta''' + 6\eta'\eta - z\eta' - 2\eta = 0. \tag{4.10}$$

Consider a solution $y(z)$ of $\mathrm{P_{II}}$ for an arbitrary $\alpha \in \mathbb{C}$, then by a direct calculation one can show that

$$\eta(z) = -(y'(z) + y(z)^2) \tag{4.11}$$

satisfies equation (4.10). Another route would be substituting equation (4.11) into equation (4.10) and then integrate to obtain $\mathrm{P_{II}}$ with a constant of integration α.

There are similarity reductions of other well-known integrable PDEs, such as the sine-Gordon equation and Boussinesq equations. These equations have been shown to reduce to cases of the remaining Painlevé equations, [[49, 50, 51, 46, 52]. These reductions, of known integrable equations, to Painlevé equations lead to the following conjecture by Ablowitz et al. in the late 70s.

Conjecture 4.4 (Ablowitz-Ramani-Segur, 1978 [53])**.** *Every exact reduction of a PDE which is integrable (in the sense of being solvable by the inverse scattering transform) yields an ODE with the Painlevé property, possibly after a change of variables.*

4.2 Isomonodromic deformations

This section provides a brief introduction to the theory of isomonodromic deformations of meromorphic linear systems of ordinary differential equations. We introduce the monodromy matrices associated with a meromorphic linear system defined on the Riemann sphere and the associated monodromy representation. In particular, the special case of a Fuchsian system with four regular points is discussed, which leads to a derivation of the *Painleve VI* equation via an application of *Schlesinger's Theorem*. Much of this chapter follows a sequence of ideas as presented in [54]. For a more deeper understanding of isomonodromic deformations; we refer the reader to [55] for the symplectic description of the isomonodromic deformation equations of Jimbo, Miwa and Ueno, and [56] for the geometric isomonodromic deformations which arise from the moduli spaces of elliptic surfaces over $\mathbb{P}^1$.

4.2.1 The monodromy representation

We start with a homogeneous linear ODE of order N

$$a_N(x)\frac{d^N y}{dx^N} + ... + a_1(x)\frac{dy}{dx} + a_0(x)y(x) = 0,$$

where each $a_n(x)$ term is rational in x. We can now rewrite this as a set of N coupled first-order linear ODE's

$$\frac{d}{dx}\boldsymbol{y}(x) = A(x)\boldsymbol{y}(x),$$

where $\boldsymbol{y}(x)$ is an N-component vector and $A(x)$ an $N \times N$ matrix rational in x.

We define the fundamental matrix solution $Y(x)$, to be an $N \times N$ matrix built from a given set of N linearly independent vector solutions, which give the columns of $Y(x)$. By linearity, $Y(x)$ satisfies the same equation

$$\frac{d}{dx}Y(x) = A(x)Y(x). \tag{4.12}$$

Remark 4.5. *We note that if the Wronskian*

$$W(Y;x) = \det Y(x),$$

does not vanish identically, then the N vector solutions are linearly independent. A different set of linearly independent solutions constitutes to multiplying $Y(x)$ on the right by a nonsingular constant matrix.

Proposition 4.6. *[16] If $A(x)$ is analytic at $x = x_0$ then $Y(x)$ is analytic at $x = x_0$. However, the converse is not necessarily true.*

Let the poles of $A(x)$ be localised at the points $\{a_i\}_{i=1,...,n}$ and at $a_\infty = \infty$. An immediate consequence of Proposition 4.6 is that all the singularities of $Y(x)$ belong to the set $\{a_i\}_{i=1,...,n} \cup \{a_\infty\}$.

Definition 4.7 (Branch Point)**.** *[16] Let $f(z)$ be a complex multi-valued function. The point z_0 is called a branch point of $f(z)$ if $f(z)$ is n-valued at that point then all neighbourhoods containing z_0 contain a point z' such $f(z')$ has more than n-values.*

In general, the singularities of $Y(x)$ are branch points. For this reason $Y(x)$ is multivalued when in a punctured neighbourhood of a branch point. Hence in order to understand the monodromy of our differential system near these branch points we make use of the following objects:

- $\mathbb{P}^1_a$: The complex projective line (Riemann Sphere) deprived of the singular points $\{a_i\}_{i=1,...,n}$.
- $\bar{\mathbb{P}^1_a}$: The universal covering of $\mathbb{P}^1_a$.
- $\pi : \bar{\mathbb{P}^1_a} \to \mathbb{P}^1_a$: The universal covering map.

We want to understand how solutions $Y(x)$ behave when evaluated along a path $\gamma_i \in \bar{\mathbb{P}^1_a}$ around an arbitrary branch point a_i. The monodromy representation of our system will tells us this behaviour.

Let γ be a path in $\bar{\mathbb{P}^1_a}$ starting at some arbitrary base point x and ending at some point x_γ such that $\pi(x_\gamma) = \pi(x)$. Then $\pi(\gamma)$ is a closed path in $\mathbb{P}^1_a$. We evaluate the fundamental matrix solution $Y(x)$ at the point x_γ which amounts to choosing a specific linear combination of the N vector solutions for each column solution of $Y(x)$. Clearly the matrix $Y(x_\gamma)$ satisfies our differential system and hence (by Remark 4.5) there exists a nonsingular constant matrix $M_\gamma \in GL(N, \mathbb{C})$ such that

$$Y(x_\gamma) = Y(x)M_\gamma,$$

where M_γ is a function of the homotopy class $[\gamma]$ of the path γ.

Remark 4.8. *The fact that M_γ is a function of the homotopy class $[\gamma]$ of the path γ is clear from realising that M_γ is invariant under a homotopy of path $\gamma \to \mu$ as long as the end points are fixed as x and $x_\mu = x_\gamma$.*

Definition 4.9. *The map $[\gamma] \to M_\gamma$ defines a representation of the fundamental homotopy group of $\mathbb{P}^1_a$. Also called the monodromy representation associated with the differential system* (4.12).

In view of the monodromy representation $[\gamma] \to M_\gamma$, let us fix a base point $x \in \bar{\mathbb{P}^1_a}$ and choose for each singular point $a_v \in \{a_i\}_{i=1,...,n} \cup \{a_\infty\} \subset \bar{\mathbb{P}^1_a}$, a path γ_v with end points x and x_v which encircles a_v once counterclockwise where $\pi(x) = \pi(x_\gamma)$. These loops generate the fundamental homotopy of $\mathbb{P}^1_a$ since any other loop in $\mathbb{P}^1_a$ is either homotopic to a point or homotopic to a product of the $\{[\gamma_v]\}_{v=1,2,...,n,\infty}$ loops.

Using the monodromy representation $[\gamma_v] \to M_v$ the monodromy matrices M_v are defined by

$$Y(x_v) = Y(x)M_v, \;\; (v = 1, ..., n, \infty),$$

where the points x and x_v are connected via γ_v such that $\pi(x) = \pi(x_v)$.

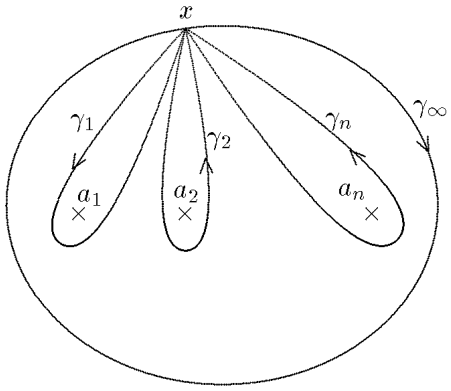

Figure 4.1: Graphical illustration of the homotopy paths $\{[\gamma_i]\}_{i=1,,,n,\infty}$ in the base space $\mathbb{P}^1_a$ each encircling their respective singular points a_i. Each path $[\gamma_i]$ has end points x and x_{γ_i} which are all identified under π which gives rise to the paths being loops as illustrated. Source: [54]

Remark 4.10. *The fact that the path γ_∞ encircling the singular point a_∞ is travelling clockwise is clear from viewing the space $\mathbb{C} \cup \{\infty\}$ as the Riemann sphere. The north pole of the Riemann sphere is identified with the point at infinity $a_\infty \in \mathbb{C} \cup \{\infty\}$ under the standard stereographic projection. A closed anti-clockwise directed path around the north pole of the Riemann sphere $\mathbb{C} \cup \{\infty\}$ becomes homotopic to a closed clockwise directed path around any $x \in \mathbb{C}$ when projected onto $\mathbb{C}$ via the standard stereographic projection.*

In view of Figure 4.1 it is always possible to choose the paths γ_v's in such a way that their product path be homotopic to a point

$$\gamma_1 * ... * \gamma_n * \gamma_\infty \simeq \{*\}.$$

To see this, consider the two paths γ_1 and γ_2 encircling the singularities a_1 and a_2 respectfully. If we take their product we get a path $\gamma_1 * \gamma_2$ which is homotopic to a path which encircles the set $\{a_1, a_2\}$. Now taking the path γ_3 we see that the product $\gamma_1 * \gamma_2 * \gamma_3$ becomes homotopic to a path encircling the set $\{a_1, a_2, a_3\}$. Iterating this procedure up to n gives the product path $\gamma_1 * \gamma_2 * ... * \gamma_n$ homotopic to a path encircling the set $\{a_1, a_2, ..., a_n\}$. Finally, the product path $\gamma_1 * \gamma_2 * ... * \gamma_n * \gamma_\infty$ becomes homotopic to a path which does not encircle any of the singularities $\{a_i\}_{i=1,...,n,\infty}$. This is clear from the fact that, at this point, the path γ_∞ is just the homotopic

inverse of the product path $\gamma_1 * \gamma_2 * ... * \gamma_n$. Hence by the definition of homotopy, the product path $\gamma_1 * \gamma_2 * ... * \gamma_n * \gamma_\infty$ must be homotopic to a point which gives the result.

Using the monodromy representation $[\gamma] \to M_\gamma$ on the product path we obtain the *monodromy constraint*

$$M_1 ... M_n M_\infty = \mathbf{1}.$$

This is clear from

$$\gamma_1 * ... * \gamma_n * \gamma_\infty \simeq \{*\} \Rightarrow [\gamma_1 * ... * \gamma_n * \gamma_\infty] = [\{*\}] \Rightarrow [\gamma_1] ... [\gamma_n][\gamma_\infty] = \mathbf{1}.$$

What the monodromy constraint tells us is that if we fix some base point $x \in \bar{\mathbb{P}^1_a}$ and traverse the product path around every singularity we will end up with the same solution. This is equivalent to multiplying the fundamental matrix solution $Y(x)$ on the right by the monodromy matrix M_i for each path γ_i traversed. Traversing every path is thus equivalent to multiplying the fundamental matrix solution $Y(x)$ by the monodromy constraint which is just multiplication by the identity matrix. We illustrate this in the following example:

Example 4.11. *Consider the following differential equation*

$$\frac{d}{dx} y(x) = \frac{1}{2x} y(x),$$

which has solution

$$y(x) = \begin{cases} \pm\sqrt{x} & x \neq 0 \\ 0 & x = 0 \end{cases}$$

The solution has branch points at $x = 0$ and $x = \infty$. We choose a path $\gamma_0 : [0, 1] \to \mathbb{C} \;\; \theta \mapsto e^{2\pi i \theta}$ which encircles the branch point $x = 0$ anti-clockwise and path $\gamma_\infty : [0, 1] \to \mathbb{C} \;\; \theta \mapsto e^{-2\pi i \theta}$ which encircles the branch point $x = \infty$ clockwise.

Defining $x_{\gamma_0} = x \cdot \gamma_0(1)$ for some $x \notin \mathbb{C} \setminus \{0, \infty\}$ we get,

$$y(x_{\gamma_0}) = y(x \cdot \gamma_0(1)) = y(x) e^{\pi i} = -y(x),$$

which gives the monodromy matrix $M_{\gamma_0} = -1$ associated to the path γ_0. Similarly for $x_{\gamma_\infty} = x \cdot \gamma_\infty(1)$ we get $M_{\gamma_\infty} = -1$. Traversing the product path $\gamma_0 * \gamma_\infty$ gives,

$$y(x \cdot \gamma_0(1) \cdot \gamma_\infty(1)) = y(x \cdot \gamma_0(1)) M_{\gamma_\infty} = y(x) M_{\gamma_\infty} M_{\gamma_0} = y(x),$$

where also the monodromy constraint is satisfied,

$$M_{\gamma_0} M_{\gamma_\infty} = \mathbf{1}.$$

4.2.2 Isomonodromic deformations of Fuchsian systems

Thus far we have established the monodromy representation of a differential system defined on the punctured Riemann sphere $\mathbb{P}^1_a$. In this section we will consider an isomonodromic deformation of a Fuchsian system. The monodromy representation will play an important role here. For now, we assume some definitions:

Definition 4.12 (Fuchsian singularity)**.** *[57] A singular point $x = x^*$ of matrix $A(x)$ of system $\frac{d}{dx} Y(x) = A(x) Y(x)$ is called Fuchsian if the matrix of coefficients $A(x)$ defined in a punctured neighbourhood $\mathbb{C} \setminus \{x^*\}$ of the point x^* has a first order pole at this point.*

Definition 4.13 (Fuchsian system)**.** *[57] An ODE, or a differential system, is called Fuchsian when all its singularities are Fuchsian.*

Definition 4.14 (Deformation of differential system)**.** *[58] Let*

$$\frac{d}{dx}y(x) = A(x,t)y(x)$$

be a system of N equations, where $x \in \mathbb{C}$, $t \in \mathbb{C}^m$. The system is called a deformation of a system where $t = t_0$ is fixed.

Moving forward, we consider the following Fuchsian system

$$\frac{d}{dx}Y(x) = A(x)Y(x), \tag{4.13}$$

and we define

$$A(x) = \sum_{v=1}^{n} \frac{A_v}{x - a_v} \quad \text{where } A_v \in GL(N, \mathbb{C})$$
$$A_\infty = -\sum_{v=1}^{n} A_v.$$

We state the deformation problem:

Given the Fuchsian differential system (4.13)*, is it possible to deform it, while preserving its monodromy representation?*

Definition 4.15. *[59] A deformation of a differential system* (4.13) *is isomonodromic if and only if it leaves all the monodromy matrices M_v invariant.*

Hence the deformation problem amounts to finding conditions on $Y(x)$ or $A(x)$, if any, such that the deformation is isomonodromic. This was solved by Schlesinger, 1912 [60] in the case of Fuchsian systems. His conclusion was that such a Fuchsian system exhibits an isomonodromic deformation, if $Y(x)$, as a function of the deformation parameters, satisfies a system of linear partial differential equations, or equivalently, $A(x)$, as a function of the same deformation parameters, satisfies a set of completely integrable nonlinear differential equations. Ultimately this result is the *Schlesinger Theorem* which we will state and prove soon. For now, we provide some mathematical foundations, which will explain why we can only deform the singularities $\{a_i\}_{i=1,\dots,n,\infty}$ for a deformation of system (4.13) to be isomonodromic.

Assumption 4.16. *All the matrices A_v are diagonalizable as $A_0^{(v)} = G_v^{-1} A_v G_v$, $v \in \{1, ..., n, \infty\}$ for some invertible G_v. Without loss of generality, A_∞ is diagonal, meaning $G_\infty = \mathbf{1}$.*

Assumption 4.17. *All the eigenvalues of the matrices A_v, $v \in \{1, ..., n, \infty\}$, are distinct modulo the nonzero integers. Meaning the difference of any two eigenvalues cannot be a non-zero integer.*

In view of the Fuchsian system (4.13), the singularities a_v are of order one and so the singular part of any solution around a_v will be contained in a factor of $(x - a_v)^{A_v}$ or $(1/x)^{A_\infty}$. Hence we can define particular solutions $Y^{(v)}(x)$, which around a_v expand as,

$$Y^{(v)}(x) = G_v\Big(1 + \sum_{j=1}^{\infty} Y_j^{(v)} (x_v)^j\Big)(x_v)^{A_0^{(v)}}, \tag{4.14}$$

where $(x_v) = (x - a_v)$, $v \in \{1, ..., n, \infty\}$, and $(x_\infty) = 1/x$.

Remark 4.18. *Assumption 4.16 and Assumption 4.17 imply that the series expansion* (4.14) *is well defined.*

We note that any solution of (4.13) can be written as $Y^{(v)}(x)C_v$, with C_v some invertible constant matrix. If we choose $Y^{(\infty)}(x)$ as the fundamental matrix solution then the connection matrices $C_v \in GL(N, \mathbb{C})$ can be defined as connecting any particular solution $Y^{(v)}(x)$ to the fundamental matrix solution $Y^{(\infty)}(x)$ via right multiplication

$$Y(x) = Y^{(\infty)}(x) = Y^{(v)}(x)C_v, \ \ (v = 1, ..., n). \tag{4.15}$$

In view of expansion (4.14), a transformation $x \to x_v$ along a path γ_v around a singularity a_v will transform $Y^{(v)}(x)$ into

$$Y^{(v)}(x_v) = Y^{(v)}(x)e^{2\pi i A_0^{(v)}}, \tag{4.16}$$

and hence $Y(x_v)$ becomes

$$Y(x_v) = Y(x)M_v, \tag{4.17}$$

where the *Monodromy Matrix* is given by

$$M_v = C_v^{-1} e^{2\pi i A_0^{(v)}} C_v. \tag{4.18}$$

We now have an explicit formula for the monodromy matrices of our Fuchsian system (4.13). By Definition 4.15 we require that these monodromy matrices be left invariant during a deformation of the Fuchsian system (4.13) for such a deformation to be isomonodromic. We must now search for some parameter, or group of parameters of our system, which when subjected to deformation, leave our monodromy matrices invariant. First we must define some data which we would like to track during the deformation.

Definition 4.19 (Singularity data)**.** *The set of data which specifies the system*

$$SD = \{a_v, A_0^{(v)}, G_v; v = 1, ..., n\},$$

where $\sum_{v=1}^{n} G_v A_0^{(v)} G_v^{-1}$ *is diagonal.*

Definition 4.20 (Monodromy data)**.** *The set of data which characterizes the monodromy properties of the fundamental matrix solution* $Y(x)$

$$MD = \{a_v, A_0^{(v)}, C_v; v = 1, ..., n, \infty\},$$

where $a_\infty = \infty$, $C_\infty = \mathbf{1}$.

Definition 4.21 (Partial monodromy data)**.** *The set of data which characterizes the monodromy matrices of the fundamental matrix solution* $Y(x)$

$$PMD = \{A_0^{(v)}, C_v; v = 1, ..., n, \infty; C_\infty = 1\}$$

The fact that the singularity data, SD, explicitly specifies the Fuchsian system (4.13) is quite clear from the diagonalization Assumption 4.16. Furthermore, the monodromy data, MD, explicitly gives the information for the construction of the monodromy matrix (4.18) but also the location of the singularities $\{a_i\}_{i=1,...,n,\infty}$. The partial monodromy data, PMD, is different in the sense that it does not tell us the location of the singularities $\{a_i\}_{i=1,...,n,\infty}$, but does give the information for the construction of the monodromy matrices M_v. Hence, if we ask for an isomonodromic deformation of (4.13) then we must require the partial monodromy data, PMD, be left invariant.

Hence we can recast the deformation problem as:

Can we continuously deform the singularity data while preserving the partial monodromy data?

A deformation of the singularity data, SD, would involve a deformation of any of the following:

$$a_v,\ \ A_0^{(v)},\ \ G_v.$$

However, we cannot deform the $A_0^{(v)}$'s, as this would involve a deformation of the partial monodromy data. Likewise, a deformation of the G_v's would involve a deformation of the $A_0^{(v)}$'s via the diagonalization Assumption 4.16. The location of the singularities $\{a_i\}_{i=1,...,n,\infty}$ do not influence the $A_0^{(v)}$'s or the C_v's and hence, its the only parameter we can independently deform while preserving the partial monodromy data. Thus, for an isomonodromic deformation of system (4.13), the only parameters we can deform are the singularities $\{a_i\}_{i=1,...,n,\infty}$.

It may not be quite clear intuitively why a deformation of the location of the singularities $\{a_i\}_{i=1,...,n,\infty}$ would leave the monodromy matrices (4.18) invariant. We provide a topological description: We recall that the monodromy matrices were defined up to a path homotopy encircling a particular singularity. The fact that is was defined up to a path homotopy is the key point. If we vary the location of the singularity then we may require a variation in the path. Given that this variation in singularity can never coincide with another singularity we must have that the variation in path encircling this singularity must remain in the same homotopy class of all paths encircling this singularity. Hence a variation in location of singularity coincides with a possible variation of path within the same homotopy class of paths. It is thus clear that varying the singularity location does not change the homotopy class of path encircling it, and so the monodromy matrix associated to that singularity should remain invariant.

Remark 4.22. *Since the only parameters we can deform independently are the location of singularities a_v's, we assume the functions $Y(x)$ and G_v's become functions of the a_v's, so become $Y(x,a)$ and $G_v(a)$, respectively. Similarly, the matrices A_v become functions of the a_v's.*

4.2.3 Schlesinger's theorem

Here we state and prove a key theorem in the isomonodromic deformation problem for Fuchsian systems. An immediate application of this theorem is the derivation of the *Painleve VI* equation. Much of the arguments in proof follows ideas in [54], however, the former paper leaves plenty of detail to the reader to prove and or understand without much explanation. For this reason, we provide an explicit and complete analysis of proof, hence providing a more comprehensive substantiation in argument. For organisation, we break up the proof of Theorem 4.23 into four propositions; namely, Propositions 4.24, 4.25, 4.26, 4.27.

Theorem 4.23 (Schlesinger, 1921 [60])**.** *The deformations of the system of linear differential equations*

$$\frac{\partial}{\partial x}Y(x,a)=\sum_{v=1}^{n}\frac{A_v(a)}{x-a_v}Y(x,a), \tag{4.19}$$

are isomonodromic if and only if $Y(x,a)$ satisfies the following set of linear PDE

$$\frac{\partial}{\partial a_v}Y(x,a)=-\frac{A_v(a)}{x-a_v}Y(x,a),\ \ (v=1,...,n). \tag{4.20}$$

An equivalent condition is that the $A_v(a)$'s satisfy the integrability conditions of (4.19) *and* (4.20)*, namely, the completely integrable set of nonlinear PDE*

$$\frac{\partial}{\partial a_\mu}A_v=\frac{[A_\mu,A_v]}{a_\mu-a_v}\ \ (\mu\neq v),\ \ \frac{\partial}{\partial a_v}A_v=-\sum_{\substack{\mu=1,...,n\\ \mu\neq v}}\frac{[A_\mu,A_v]}{a_\mu-a_v}. \tag{4.21}$$

Proposition 4.24. *If the system of linear differential equations* (4.19) *are isomonodromic then* $Y(x,a)$ *must satisfy the set of linear PDE* (4.20).

Proof. We denote $\boldsymbol{\delta}$ the exterior derivative with respect to the a_v's

$$\boldsymbol{\delta} = \sum_{v=1}^{n} da_v \frac{\partial}{\partial a_v}$$

Consider the matrix of 1-forms

$$\Omega(x,a) = [\boldsymbol{\delta} Y(x,a)] Y(x,a)^{-1},$$

which is well defined since $Y(x,a)$ invertible due to linearly independent columns. Since $Y(x,a)$ is holomorphic in variable x in $\bar{\mathbb{P}}^1_a$, $\Omega(x,a)$ is also holomorphic in variable x in $\bar{\mathbb{P}}^1_a$.

We assume the deformation of system (4.19) is isomonodromic which amounts to the PMD being independent of a. Then using the monodromy matrix equation (4.18) we obtain

$$\boldsymbol{\delta} Y(x_v,a) = \boldsymbol{\delta} Y(x,a) M_v,$$

which implies $\Omega(x,a)$ is single valued in $\mathbb{P}^1_a$. To see this, we calculate

$$\begin{aligned}
\Omega(x_v,a) &= [\boldsymbol{\delta} Y(x_v,a)] Y(x_v,a)^{-1} \\
&= [\boldsymbol{\delta} Y(x,a) M_v][Y(x,a)M_v]^{-1} \\
&= [\boldsymbol{\delta} Y(x,a) M_v] M_v^{-1} Y(x,a)^{-1} \\
&= [\boldsymbol{\delta} Y(x,a)] Y(x,a)^{-1} \\
&= \Omega(x,a)
\end{aligned}$$

Now we expand $\Omega(x,a)$ about the singularity a_v using the expansion (4.14). Keeping only the divergent terms we get

$$\Omega(x,a) = \begin{cases} -\frac{A_v}{x-a_v} da_v + \mathcal{O}(1) & v = 1,...,n \\ \mathcal{O}(1/x) & v = \infty \end{cases} \tag{4.22}$$

Since $\Omega(x,a)$ goes to zero at infinity we must have

$$\Omega(x,a) = -\sum_{v=1}^{n} \frac{A_v(a)}{x-a_v} da_v, \tag{4.23}$$

then multiplying both sides on the right by $Y(x,a)$ gives

$$\boldsymbol{\delta} Y(x,a) = \sum_{v=1}^{n} \frac{\partial}{\partial a_v} Y(x,a) da_v = -\sum_{v=1}^{n} \frac{A_v(a)}{x-a_v} Y(x,a) da_v,$$

identifying the coefficients of da_v for $v = 1,...,n$ gives the result (4.20). □

Proposition 4.25. *The set of nonlinear PDE given by* (4.21) *can be re-written as*

$$\boldsymbol{\delta} A_v = \sum_{\substack{\mu=1,...,n \\ \mu \neq v}} [A_\mu, A_v] \frac{da_\mu - da_v}{a_\mu - a_v}, \quad v = 1,...,n \tag{4.24}$$

Proof. Applying the exterior derivative $\boldsymbol{\delta}$ to A_v gives

$$\begin{aligned}
\boldsymbol{\delta} A_v &= \sum_{\mu=1}^{n} da_\mu \frac{\partial A_v}{\partial a_\mu} \\
&= da_v \frac{\partial A_v}{\partial a_v} + \sum_{\substack{\mu=1,\dots,n \\ \mu\neq v}}^{n} da_\mu \frac{\partial A_v}{\partial a_\mu} \\
&= -da_v \sum_{\substack{\mu=1,\dots,n \\ \mu\neq v}}^{n} \frac{[A_\mu, A_v]}{a_\mu - a_v} + \sum_{\substack{\mu=1,\dots,n \\ \mu\neq v}}^{n} da_\mu \frac{[A_\mu, A_v]}{a_\mu - a_v} \\
&= \sum_{\substack{\mu=1,\dots,n \\ \mu\neq v}} [A_\mu, A_v] \frac{da_\mu - da_v}{a_\mu - a_v}.
\end{aligned}$$

□

Proposition 4.26. *An equivalent condition for a deformation of the system of linear differential equations* (4.19) *to be isomonodromic is that the $A_v(a)$'s satisfy the integrability conditions of* (4.19) *and* (4.20)*, namely the completely integrable set of nonlinear PDE given by* (4.21)*.*

Proof. For integrability of (4.19) and (4.20) we require that the partial derivatives commute as follows

$$\frac{\partial^2 Y(x,a)}{\partial a_\mu \partial x} = \frac{\partial^2 Y(x,a)}{\partial x \partial a_\mu} \quad \forall \mu = 1, ..., n.$$

Calculating the left-hand side gives

$$\frac{\partial^2 Y(x,a)}{\partial a_\mu \partial x} = \Big(\frac{1}{(x-a_\mu)^2} A_\mu(a) + \sum_{v=1}^{n} \frac{1}{x-a_v} \frac{\partial}{\partial a_\mu} A_v(a) \Big) Y(x,a) - \Big(\sum_{v=1}^{n} \frac{A_v(a)}{x-a_v} \Big) \frac{A_\mu(a)}{x-a_\mu} Y(x,a)$$

Calculating the right-hand side gives

$$\frac{\partial^2 Y(x,a)}{\partial x \partial a_\mu} = \frac{A_\mu(a)}{(x-a_\mu)^2} Y(x,a) - \frac{A_\mu(a)}{x-a_\mu} \Big(\sum_{v=1}^{n} \frac{A_v(a)}{x-a_v} \Big) Y(x,a)$$

Equating both sides and dropping the $Y(x,a)$ gives

$$\frac{A_\mu(a)}{(x-a_\mu)^2} + \sum_{v=1}^{n} \frac{1}{x-a_v} \frac{\partial}{\partial a_\mu} A_v(a) - \Big(\sum_{v=1}^{n} \frac{A_v(a)}{x-a_v} \Big) \frac{A_\mu(a)}{x-a_\mu} = \frac{A_\mu(a)}{(x-a_\mu)^2} - \frac{A_\mu(a)}{x-a_\mu} \Big(\sum_{v=1}^{n} \frac{A_v(a)}{x-a_v} \Big),$$

which simplifies to

$$\sum_{v=1}^{n} \frac{1}{x-a_v} \frac{\partial}{\partial a_\mu} A_v(a) - \Big(\sum_{\substack{v=1,\dots,n \\ v\neq\mu}}^{n} \frac{A_v(a)}{x-a_v} \Big) \frac{A_\mu(a)}{x-a_\mu} = -\frac{A_\mu(a)}{x-a_\mu} \Big(\sum_{\substack{v=1,\dots,n \\ v\neq\mu}}^{n} \frac{A_v(a)}{x-a_v} \Big),$$

When taking $x \to a_v$ for an arbitrary $v \neq \mu$ we see that the terms $1/(x-a_v)$ blow up and hence we obtain

$$\frac{1}{x-a_v} \Big(\frac{\partial}{\partial a_\mu} A_v(a) - \frac{A_v(a) A_\mu(a)}{a_v - a_\mu} \Big) + \mathcal{O}(1) = \frac{1}{x-a_v} \Big(- \frac{A_\mu(a) A_v(a)}{a_v - a_\mu} \Big) + \mathcal{O}(1),$$

from which follows the first equation of (4.21)

$$\frac{\partial}{\partial a_\mu}A_v(a) = \frac{A_v(a)A_\mu(a)}{a_v - a_\mu} - \frac{A_\mu(a)A_v(a)}{a_v - a_\mu} = \frac{[A_\mu, A_v]}{a_\mu - a_v}.$$

To get the second equation of (4.21) we instead take $x \to a_\mu$ and see that the terms $1/(x - a_\mu)$ blow up and hence we obtain

$$\frac{1}{x - a_\mu}\Big(\sum_{v=1}^{n}\frac{x - a_\mu}{x - a_v}\frac{\partial A_v(a)}{\partial a_\mu} - \sum_{\substack{v=1,\dots,n\\ v\neq\mu}}^{n}\frac{A_v(a)A_\mu(a)}{a_\mu - a_v}\Big) = \frac{1}{x - a_\mu}\Big(-A_\mu(a)\sum_{\substack{v=1,\dots,n\\ v\neq\mu}}^{n}\frac{A_v(a)}{a_\mu - a_v}\Big).$$

The first sum on the left-hand side is equates to $\partial A_\mu(a)/\partial a_\mu$ for $v = \mu$ and otherwise equates to 0 for $v \neq \mu$ since we are in the limit $x \to a_\mu$

$$\frac{1}{x - a_\mu}\Big(\frac{\partial A_v(a)}{\partial a_\mu} - \sum_{\substack{v=1,\dots,n\\ v\neq\mu}}^{n}\frac{A_v(a)A_\mu(a)}{a_\mu - a_v}\Big) = \frac{1}{x - a_\mu}\Big(-A_\mu(a)\sum_{\substack{v=1,\dots,n\\ v\neq\mu}}^{n}\frac{A_v(a)}{a_\mu - a_v}\Big),$$

from which follows the second equation of (4.21) after a change of notation $v \leftrightarrow \mu$

$$\frac{\partial A_v(a)}{\partial a_v} = \sum_{\substack{\mu=1,\dots,n\\ \mu\neq v}}^{n}\frac{A_\mu(a)A_v(a)}{a_v - a_\mu} - \sum_{\substack{\mu=1,\dots,n\\ \mu\neq v}}^{n}\frac{A_v(a)A_\mu(a)}{a_v - a_\mu} = -\sum_{\substack{\mu=1,\dots,n\\ \mu\neq v}}^{n}\frac{[A_\mu, A_v]}{a_\mu - a_v}.$$

Furthermore, the compatibility conditions of the set of PDE (4.21) are satisfied. This amounts to say that the 1-forms $\boldsymbol{\delta}A_v$ are closed or $\boldsymbol{\delta}\boldsymbol{\delta}A_v \equiv 0$. We check this now.

Applying the exterior derivative $\boldsymbol{\delta}$ to equation (5.12) gives

$$\boldsymbol{\delta}\boldsymbol{\delta}A_v = \sum_{v=1}^{n} da_v \frac{\partial}{\partial a_v}\Big(\sum_{\substack{\mu=1,\dots,n\\ \mu\neq v}}[A_\mu, A_v]\frac{da_\mu - da_v}{a_\mu - a_v}\Big).$$

Hence our equations (4.21) are integrable. □

Proposition 4.27. *The solution $Y(x, a)$ satisfying the set of linear PDE* (4.20) *is sufficient for a deformation of the system of linear differential equations* (4.19) *to be isomonodromic.*

Proof. It remains to prove the other direction, namely, condition (4.20) is sufficient. We assume equation (4.20) to be true and need to show the following

$$\boldsymbol{\delta}A_0^{(v)} = 0,$$
$$\boldsymbol{\delta}C_v = 0.$$

This would mean that $A_0^{(v)}$ and C_v are independent of variation in the singularities a_v and hence a deformation of the system (4.19) is isomonodromic.

Suppose the solutions A_v of (4.21) are defined on some domain $\mathcal{D}$. We make the assumption that conditions 4.16 and 4.17 hold on this domain so then solutions $Y(x, a)$ of (4.19) and (4.20) exist.

We now show $\boldsymbol{\delta}A_0^{(v)} = 0$ for $v = 1, ..., n, \infty$.

Let $Y(x,a)$ and some set of $A_v(a)$'s be a solution of (4.19), (4.20) and (4.21) and let $s \in \mathbb{C}$ be a complex number not belonging to the spectrum of A_v, meaning its set of eigenvalues. Using the matrix identity

$$\partial \log\det M = trace(M^{-1}\partial M), \tag{4.25}$$

we obtain for $v = 1, ..., n$

$$\boldsymbol{\delta} \log\det(A_v - s) = \sum_{\substack{\mu=1,...,n \\ \mu\neq v}} \frac{da_\mu - da_v}{a_\mu - a_v} trace((A_v - s)^{-1}[A_\mu, A_v]).$$

The trace on the right hand-side all vanish using linearity and cycle property of trace. Hence $\boldsymbol{\delta}\det(A_v - s) = 0$ which means that the spectrum of A_v does not depend on the singularities a_v's and hence

$$\boldsymbol{\delta} A_0^{(v)} = 0, \;\; v = 1, ..., n.$$

We are left to show $\boldsymbol{\delta} C_v = 0$. Making use of (4.13) and (4.24) which gives

$$\boldsymbol{\delta} A_\infty = \sum_{\substack{\mu,v=1,...,n \\ \mu\neq v}} [A_v, A_\mu] \frac{da_v - da_\mu}{a_v - a_\mu}$$

Noting that the quantity which is summed up in the right hand-side changes sign when exchanging μ and v tells us that

$$\boldsymbol{\delta} A_\infty = 0$$

From Assumption 4.16, $A_\infty(a)$ is diagonal for any $a \in \mathcal{D}$ and so its diagonalization matrices are trivial meaning $G_\infty(a) = 1$ and hence

$$\boldsymbol{\delta} A_0^{(\infty)} = \boldsymbol{\delta} G_\infty^{-1} A_\infty G_\infty = \boldsymbol{\delta} A_\infty = 0.$$

Now we just need to prove that the C_v's are independent of the singularities a. Applying the exterior differential $\boldsymbol{\delta}$ to the diagonalization relation for the A_v's gives

$$\boldsymbol{\delta} A_v = G_v[G_v^{-1}\boldsymbol{\delta} G_v, A_0^{(v)}]G_v^{-1} \;\; v = 1, ..., n.$$

When compared with (4.24) which can be written alternatively as

$$\boldsymbol{\delta} A_v = G_v[-G_v^{-1} \sum_{\substack{\mu=1,...,n \\ \mu\neq v}} A_\mu \frac{da_v - da_\mu}{a_v - a_\mu} G_v, A_0^{(v)}]G_v^{-1},$$

it becomes clear that

$$G_v^{-1}\boldsymbol{\delta} G_v = -G_v^{-1} \sum_{\substack{\mu=1,...,n \\ \mu\neq v}} A_\mu \frac{da_v - da_\mu}{a_v - a_\mu} G_v + d_v,$$

for some d_v matrix which commutes with $A_0^{(v)}$. However, we can take d_v to be zero since G_v is defined up to such matrix. Then

$$\boldsymbol{\delta} G_v G_v^{-1} = - \sum_{\substack{\mu=1,...,n \\ \mu\neq v}} A_\mu \frac{da_v - da_\mu}{a_v - a_\mu} \;\; v = 1, ..., n. \tag{4.26}$$

We recall the expansion of $\Omega(x,a)$ about a_v. This time we go one order further and include all the terms which don't vanish as $x \to a_v$. Then using (4.14), (4.15), (4.16) we get

$$\Omega(x,a) = \begin{cases} -G_v[\frac{A_0^{(v)}}{x-a_v} + A_1^{(v)}]G_v^{-1}da_v + YC_v^{-1}\boldsymbol{\delta}C_vY^{-1} + \boldsymbol{\delta}G_vG_v^{-1} + \mathcal{O}(x-a_v) & v = 1,...,n \\ YC_\infty^{-1}\boldsymbol{\delta}C_\infty Y^{-1} + \mathcal{O}(1/x) & v = \infty \end{cases} \tag{4.27}$$

where the $A_1^{(v)}$ matrix is given by

$$G_vA_1^{(v)}G_v^{-1} = \sum_{\substack{\mu=1,...,n \\ \mu\neq v}} \frac{A_\mu}{a_v - a_\mu}da_\mu \quad v = 1,...,n. \tag{4.28}$$

Then using (4.26) and (4.28), (4.27) becomes

$$\Omega(x,a) = \begin{cases} -\frac{A_v}{x-a_v}da_v + \sum_{\substack{\mu=1,...,n \\ \mu\neq v}} \frac{A_\mu}{a_\mu - a_v}da_v + YC_v^{-1}\boldsymbol{\delta}C_vY^{-1} + \mathcal{O}(x-a_v) & v = 1,...,n \\ YC_\infty^{-1}\boldsymbol{\delta}C_\infty Y^{-1} + \mathcal{O}(1/x) & v = \infty \end{cases}$$

which when compared with (4.23) it becomes clear that

$$\boldsymbol{\delta}C_v = 0 \quad v = 1,..,n,\infty$$

□

Remark 4.28. *A neat trick is that by applying a homographic transformation on x, we can fix the position of three singularities. Given that one singularity is at infinity, any two other singularities at finite distance can be fixed. In the case $n = 2$, there is no deformation parameter, since all singularities are fixed, thus Schlesinger's Theorem becomes trivial. In the simplest non-trivial case, $n = 3$, there is only one deformation parameter which corresponds to the position of the singularity not fixed. In this case, we are able to derive the Painlevé VI equation as a reduction of the Schlesinger equations* (4.21).

4.2.4 The isomonodromic deformation problem for *Painleve VI*

We now consider Schlesinger's equations (4.21) in the simplest non-trivial case which corresponds to the A_v matrices being 2×2 and there being three singularities at finite distance. We choose to two of them at $x = 0$ and $x = 1$ and the last one at $x = t$ for some unique deformation parameter t. Equations (4.19) and (4.20) become

$$\begin{aligned} \frac{\partial}{\partial x}Y(x,t) &= \Big(\frac{A_0(t)}{x} + \frac{A_1(t)}{x-1} + \frac{A_t(t)}{x-t}\Big)Y(x,t) \\ \frac{\partial}{\partial t}Y(x,t) &= -\frac{A_t}{x-t}Y(x,t) \end{aligned}$$

and equations (4.21) become

$$\dot{A}_0 = -\frac{1}{t}[A_0, A_t], \quad \dot{A}_1 = \frac{1}{1-t}[A_1, A_t], \quad \dot{A}_t = \frac{1}{t}[A_0, A_t] - \frac{1}{1-t}[A_1, A_t]$$

Using $A_\infty = -\sum_{v=1}^n A_v$ we obtain $A_0 + A_t + A_1 + A_\infty = 0$ and so $\dot{A}_0$, $\dot{A}_1$ reduce to

$$\dot{A}_0 = \frac{1}{t}[A_0, A_1 + A_\infty], \tag{4.29}$$

$$\dot{A}_1 = -\frac{1}{1-t}[A_1, A_0 + A_\infty]. \tag{4.30}$$

Now we need to parameterize the matrices A_0, A_1, A_t and A_∞. We choose them traceless with respective eigenvalues $\pm\theta_0/2, \pm\theta_1/2, \pm\theta_t/2$ and $\pm\theta_\infty/2$. From equation (4.29), we make use of the matrix identity (4.25) to obtain

$$\frac{\partial}{\partial t}\ln\det A_0 = \operatorname{tr} A_0^{-1}A_0 = \frac{1}{t}\operatorname{tr} A_0^{-1}[A_0, A_1 + A_\infty] = 0.$$

This means that $\det A_0$ and hence $\det A_1, \det A_t$ and $\det A_\infty$ are t independent and so we must have $\theta_0, \theta_1, \theta_t$ and θ_∞ are constant parameters.

We keep track of the eigenvalues of A_t via $\det(A_0 + A_1 + A_\infty) = -\frac{1}{4}\theta_t^2$. Using the identity $\det(A+B) = \det A + \det B - \operatorname{tr} AB$ for 2×2 matrices with at least one of them traceless, we obtain the equation

$$\operatorname{tr}(A_0A_1 + A_1A_\infty + A_\infty A_0) = \frac{1}{4}(\theta_t^2 - \theta_0^2 - \theta_1^2 - \theta_\infty^2). \tag{4.31}$$

From (4.31) we can infer a valid parametrization as

$$A_v = \frac{1}{2}\begin{pmatrix} z_v & u_v(\theta_v - z_v) \\ (\theta_v + z_v)/u_v & -z_v \end{pmatrix}, \quad v = \{0, 1, t\}, \quad A_\infty = \begin{pmatrix} \theta_\infty/2 & 0 \\ 0 & -\theta_\infty/2 \end{pmatrix},$$

where $z_0, z_1, z_t, u_0, u_1, u_t$ are functions of the parameter t. One can check that this parametrization does indeed satisfy (4.31).

For convenience, we replace u_0 and u_1 by two equivalent linear combinations k and y, defined from the component 12 of $A(x,t)$

$$A(x,t)_{12} = \frac{k(x-y)}{2x(x-1)(x-t)},$$

where

$$k = tu_0(z_0 - \theta_0) - (1-t)u_1(z_1 - \theta_1), \quad ky = tu_0(z_0 - \theta_0).$$

Introducing notation: $\zeta = t(1-y)z_0 + (1-t)yz_1$, the 11 and 12 components of (4.29) and (4.30) gives the following system

$$z_0' = -\frac{Z}{2t}, \tag{4.32}$$

$$z_1' = -\frac{Z}{2(1-t)}, \tag{4.33}$$

$$y' = \frac{(1-\theta_\infty)y(1-y) - \zeta}{t(1-t)}, \tag{4.34}$$

$$\frac{k'}{k} = \frac{(1-\theta_\infty)(y-t)}{t(1-t)}, \tag{4.35}$$

where

$$Z = -\Big(\frac{1}{t(1-y)} + \frac{1}{(1-t)y}\Big)\frac{\zeta^2}{y-t} + \frac{2\zeta(z_0+z_1)}{y-t} - \frac{t(1-y)}{(1-t)y}\theta_0^2 + \frac{(1-t)y\theta_1^2}{t(1-y)}. \tag{4.36}$$

Equation (4.31) writes as

$$\frac{\zeta^2}{t(1-t)y(1-y)} + 2\theta_\infty(z_0+z_1) = \theta_t^2 - \theta_\infty^2 - \Big(\frac{\theta_0^2}{(1-t)y} - \frac{\theta_1^2}{t(1-y)}\Big)(y-t). \tag{4.37}$$

We note that the elimination of any two of the three functions z_0, z_1, y between (4.32), (4.33), (4.34) leads to a second order differential equation for the third. This leads to the equation for y being linear in $\ddot{y}$. In view of this, we differentiate both sides of (4.34) with respect to t which gives

$$\ddot{y} = \frac{1}{t(1-t)(y-t)}\Big(\frac{Z}{2}(y-t) - \zeta(z_0+z_1) - \theta_\infty y(1-y)(z_0+z_1) + (1-y)\zeta + (y-t)[(1-\theta_\infty)(1-2y) - (1-2t)]\dot{y}\Big). \tag{4.38}$$

Then eliminating Z, ζ, and (z_0+z_1) between equations (4.34), (4.36), (4.37) and (4.38) we obtain a differential equation satisfied by $y(t)$

$$\ddot{y} = \frac{1}{2}\Big(\frac{1}{y} + \frac{1}{y-1} + \frac{1}{y-z}\Big)\dot{y}^2 - \Big(\frac{1}{t} + \frac{1}{t-1} + \frac{1}{y-t}\Big)\dot{y} + \frac{y(y-1)(y-t)}{t^2(t-1)^2}\Big(\alpha + \frac{\beta t}{y^2} + \frac{\gamma(t-1)}{(t-1)^2} + \frac{\delta t(t-1)}{(y-t)^2}\Big),$$

where

$$\alpha = \frac{(1-\theta_\infty)^2}{2}, \quad \beta = -\frac{\theta_0^2}{2}, \quad \gamma = \frac{\theta_1^2}{2}, \quad \delta = \frac{1-\theta_t^2}{2}.$$

Which is the ***Painleve VI Equation!***

This concludes our study of the Painlevé equations and their relationship to integrability. We have derived the Painlevé equation VI as a reduction of the Schlesinger equations (4.21) in the case of four regular singular points. The remaining Painlevé equations, I-V, can be derived by following the limiting procedure outlined in the coalescence cascade earlier. For $n \geq 4$ matrices A_v, the Schlesinger equations (4.21) are known to reduce to Garnier systems $\mathbb{G}_n$ [61].

5 Conclusion and Further Directions

5.1 Outline of Results

We introduced a blockchain mining model, recently proposed by Taylor et al. [1, 4]. In particular, we derived the Blockchain equation (1.11) directly from the defining Markov chain transition rates and an application of a Functional Law of Large Numbers due to Kurtz, Barbour and Luczak [5, 6]. By numerical observation, the Blockchain equation hinted at the existence of travelling wave solutions, which was originally conjectured in [1, 4].

We then introduced the modified non-linear Fisher-KPP equation (2.6), which was derived by Taylor expanding to second order the difference term in the Blockchain equation. We made clear that this expansion was analogous to the Kramers-Moyal expansion [7] and that the Pawula Theorem [8, 9] indicated that expanding to second order is sufficient for the evolution of a probability density. A minimal wave speed condition for the existence of a travelling wave solution by means of a standard phase-plane analysis. The technique of Painlevé integrability was used to determine an exact solution of this modified Fisher-KPP equation. We showed that the modified Fisher-KPP equation in travelling wave coordinates satisfied the Painlevé property for three different values of the wave speed v up to a choice of λ and ω. We assumed the choice of v which satisfied the minimal wave speed condition. This particular wave speed provided an exact analytic solution which was shown to be in agreement with the numerical blockchain solution in the fast mining regime.

We conducted a detailed numerical study of the Blockchain equation. Our numerical results indicated that solutions $\varphi_n(t)$ approach a travelling wave in the limit $n \to \infty$ for any choice of $\lambda, \omega > 0$. This was observed both in solution and the accompanying speed curve $s_n(p)$ flattening out. Following this, we studied the wave speed of this travelling wave. We assumed the form $v_{bc} = v_{min}(\lambda, \omega) + v_2(\omega)$ for the travelling wave speed and studied the behaviour of $v_2(\omega)$. The numerical observation was that $v_2 = \alpha\omega$ in the regime $\lambda \geq \omega$ for some $\alpha > 0$ within the numeric bound of (3.1). This observation formed Assumption 3.1 and further numerical analysis in the regime $\lambda \to 0$ gave us Assumption 3.2. Using these numerically motivated assumptions, we detailed a heuristic argument for the travelling wave speed v_{bc} of the Blockchain equation. Our argument concluded that the travelling wave speed is bounded as $v_{bc} \leq \lambda + \sqrt{2\lambda\omega} + \frac{9}{32}\omega$. By numerical observation, we found that the travelling wave speed coincided with $\lambda + \sqrt{2\lambda\omega} + \frac{9}{32}\omega$ in the fast mining regime $\lambda \geq \omega$, whereas in the slow mining regime $\lambda < \omega$, the travelling wave speed was bounded above by $\lambda + \sqrt{2\lambda\omega} + \frac{9}{32}\omega$, thus confirming the result of our heuristic analysis. We formalised our findings with with Conjecture 3.6. This conjecture, the numerical evidence surrounding it and the accompanying heuristic argument, forms the original key result of this thesis. Despite extensive study of the Fisher-KPP equation, this new result has not appeared in the literature as of current knowledge.

The fact that the modified Fisher-KPP equation was shown to be Painlevé integrable, (for certain values of v, as a function of λ and ω), motivated us to study in detail the connection between the Painlevé equations and integrability. We detailed the connection between the Painlevé equations and integrable systems, namely, similarity reductions and monodromy deformations, which lead us to study in detail the isomonodromy deformations of meromorphic linear systems. In particular, it was shown that the Schlesinger equations (4.21) govern the isomonodromy deformations of a Fuchsian system. We detailed the derivation of the Painlevé VI equation which was shown to reduce from the Schlesinger equations (4.21) in the case of four regular singular points.

5.2 Outlook

We outline some directions for future work.

5.2.1 A generalized wave speed conjecture

In Chapter 3, we conjectured a wave speed formula for the travelling wave speed of solutions $\varphi_n(t)$ of the Blockchain equation (2.5). The validity of our conjecture was supported by both numerical evidence and a detailed heuristic argument. A natural extension of this thesis would be a proof of Conjecture 3.6. Ideally the proof would involve sequence of arguments on the level of rigour of Kolmogorov et al. [12], due to his original analysis of the Fisher-KPP travelling wave speed.

Furthermore, we can generalize the non-linear term of the Blockchain equation (2.5) to obtain

$$\frac{d\varphi_n(t)}{dt} = -\lambda(\varphi_n(t) - \varphi_{n-1}(t)) - \omega f(\varphi_n(t)), \tag{5.1}$$

with $\varphi_n(0) = 1$ for $n \geq 0$ and $\varphi_{-1}(t) = 0$ for $t \geq 0$ and conditions on f as

$$\begin{aligned} f(0) = f(1) &= 0; \\ f(\varphi_n) &> 0, \;\; 0 < \varphi_n < 1; \\ f'(0) = 1 &> 0, \;\; f'(\varphi_n) <, \;\; 0 < \varphi_n \leq 1, \end{aligned}$$

which can be viewed as a generalized Blockchain equation. These conditions on f are analogous to those for the Fisher-KPP equation (2.2) which were generalized by Kolmogorov et al. [12] from the original Fisher equation (2.1).

Following the heuristic argument outlined in Chapter 3, we can only speculate that if solutions $\varphi_n(t)$ of the generalized Blockchain equation (5.1) approach a travelling wave in the limit $n \to \infty$, then the travelling wave speed v_{bc_g} should be bounded above as

$$v_{bc_g} \leq \lambda + \sqrt{2\lambda\omega} + \omega \max_{\varphi \in (0,1)} \left(\frac{1}{2} f(\varphi)^2 + f(\varphi) \right) \tag{5.2}$$

Conjecture 5.1. *(Generalized Wave Speed Conjecture) For all $\lambda, \omega > 0$, solutions $\varphi_n(t)$ of the generalized Blockchain equation* (5.1) *approach a travelling wave in the limit $n \to \infty$. The speed of this travelling wave v_{bc_g} is bounded above as* (5.2)*.*

The inequality (5.2) can be viewed as a generalized wave speed conjecture for the generalized Blockchain equation (5.1). If we set $f(\varphi_n) = \varphi_n(t)(1 - \varphi_n(t))$ then the generalized Blockchain equation (5.1) becomes the Blockchain equation (2.5), and the generalized Conjecture 5.1 becomes Conjecture 3.6. Again, a proof of Conjecture 5.1 would be a natural extension of this thesis which would imply Conjecture 3.6.

As of current knowledge, the travelling wave speed formulas of Conjecture 3.6 and Conjecture 5.1 are unknown in the literature. We have substantiated evidence for at least Conjecture 3.6, which included numerical evidence and heuristic analysis. Conjecture 5.1 is a generalization and, at the moment, speculative. A rigorous proof, of at least Conjecture 3.6, would be a seminal result and admit immediate applications in various areas of applied mathematics and mathematical physics.

5.2.2 An integrable Blockchain mining model?

The development of an integrable differential difference equation for $\varphi_n(t)$ is an obvious extension for this thesis. This would allow a direct analysis without having to settle for an approximation.

There are already many well known integrable differential-difference equations. For example, the discrete KdV equation:

$$\frac{d\nu_n}{dt} = \nu_n(t)(\nu_{n+1}(t) + \nu_{n-1}(t)), \tag{5.3}$$

is the set of ODE's for functions $\nu_n(t)$ where $n \in \mathbb{Z}$. Typical boundary conditions are either periodic $\nu_n = \nu_{n+N}$ for some $N \in \mathbb{Z}$, or Dirichlet $\nu_n = 0$ for $n \leq \alpha$ and $\nu_n = 0$ for $n \geq \beta$ where $\alpha < \beta$.

These kinds of equations, partial differential-difference equations, have an analogous Painlevé integrability criterion, called singularity confinement. This criterion was originally formulated as a test for integrability of discrete difference equations. For example, consider the following second-order difference equation

$$g_{n+1} = \frac{(g_n - k)(g_n + k)g_{n-1}}{k^2 - g_n^2 + 2\tau g_n g_{n-1}}, \tag{5.4}$$

with parameters $k \neq 0, \pm 1$ and $\tau \neq 0$. This initial value problem requires g_0 and g_1 so that g_n can be determined recursively from (5.4) for $n \geq 2$. We observe our system (5.4) having singular points $g_n = \pm k$, in the sense that if $g_n = \pm k$ then $g_{n+1} = 0$ is forced independently of g_{n-1}, given that $g_{n-1} \neq 0$. This is referred to as a loss of degree of freedom occurring when iterating through. If the discrete system is not integrable, then in general, the singularity will propagate in the sense that all subsequent values $g_{n+2}, g_{n+3}, ...$ are determined independently of g_{n-1}, and so this loss of degree of freedom is never recovered. In the context of system (5.4), we compute the next iterate as $g_{n+2} = \mp k$, at which we arrive at an indeterminacy giving g_{n+3} when $(g_{n+1}, g_{n+2}) = (0, \mp k)$. The trick is we now consider a perturbation of the singular value $g_n = \pm k$ by introducing a small perturbation ϵ, where we may compute the following in the limit $\epsilon \to 0$:

$$g_{n-1} \neq 0, \;\; g_n = \pm k + \mathcal{O}(\epsilon), \;\; g_{n+1} = \mathcal{O}(\epsilon), \;\; g_{n+2} = \mp k + \mathcal{O}(\epsilon), \;\; g_{n+3} = g_{n-1} + \mathcal{O}(\epsilon).$$

If we choose to define the value of the iterates as above in the limit $\epsilon \to 0$, then we are able to recover the lost degree of freedom in g_{n+3}. We say that the singularity at $g_n = \pm k$ is confined. It is in this sense that the system (5.4) is integrable. This singularity confinement process does not always work, however, when it does we say the discrete system is integrable by means of singularity confinement.

This technique has been extended to consider partial differential difference equations, like the discrete KdV equation (5.3). For example, Quispel et al. [62] applied this technique to (5.3) where is was shown to satisfy singularity confinement. The fact that the discrete KdV equation (5.3) is already known to be integrable eluded to the idea that, singularity confinement may also work as a test of integrability, for partial differential difference equations.

Following the analysis of [62], initial attempts indicate that the Blockchain equation (2.5) does not satisfy the singularity confinement property.

A natural extension of this thesis would be finding an integrable partial differential difference equation with solutions $\varphi_n(t)$ which model blockchain behaviour in the sense of Model 2, as introduced in Chapter 1. This would allow a direct analysis and exact solution for the distribution function $\varphi_n(t)$ of local blockchain heights at every height in the blockchain.

For those interested in this extension we recommend the following literature to get started; [62] for the application of singularity confinement to the discrete KdV; [63] for the application to the Kac–Moerbeke equation and the semi-discrete mKdV equation; [64] for review on symmetries as an integrability criteria for differential difference equations; and [65] for the application to delay-differential Painlevé equations .

Bibliography

[1] A.E. Krzesinski P.G. Taylor R.A Bowden, J. de Gier. A model for consensus in fast mining blockchains (draft). 2022.

[2] A.E. Krzesinski R. Bowden, H.P. Keeler and P.G. Taylor. Block arrivals in the bitcoin blockchain. 2018.

[3] A.E. Krzesinski J. Gobel, H.P. Keeler and P.G. Taylor. Bitcoin blockchain dynamics: the selfish-mine strategy in the presence of propagation delay. 2015.

[4] P.G. Taylor. The bitcoin blockchain: what can mathematical modelling teach us? *OPTIMA*, 2023.

[5] T Kurtz. Relationships between stochastic and deterministic population models. *Advances in Applied Probability*, 12(3):570 570, 1980.

[6] A. D. Barbour and M. J. Luczak. Laws of large numbers for epidemic models with countably many types. *The Annals of Applied Probability*, 18:2208 2238, 2008.

[7] Alan J. McKane. Stochastic processes. *Theory Group, School of Physics and Astronomy, University of Manchester*, 2009.

[8] Robert F. Pawula. Generalizations and extensions of the fokker-planck-kolmogorov equations. *California Institute of Technology Pasadena*, 1965.

[9] Robert F. Pawula. Approximation of the linear boltzmann equation by the fokker-planck equation. *Phys. Rev.*, 162(1):186 188, 1967.

[10] T. Kawano et al. Logistic models for simulating the growth of plants by defining the maximum plant size as the limit of information flow. *Plant Signal Behav.*, 15(2), 2020.

[11] M. J. Ablowitz & Anthony Zeppetella. Explicit solutions of fisher's equation for a special wave speed. *Bulletin of Mathematical Biology*, 41:835 840, 1979.

[12] A.N. Kolmogorov and N.S. Piskunov. Studies of the diffusion with the increasing quantity of the substance; its application to a biological problem*. *Bull. Univ. Moscow*, 1(6):1–26, 1937.

[13] R. A. Fisher. The wave of advance of advantageous genes. *Annals of Eugenics*, 7:355–369, 1937.

[14] D. G. Aronson and H. F. Weinberger. Nonlinear diffusion in population genetics, combustion, and nerve pulse propagation, in partial differential equations and related topics. *Springer*, pages 5–49, 1975.

[15] S. V. Petrovskii and B.-L. Li. Exactly solvable models of biological invasion, c. *CRC press*, 2005.

[16] G. Teschl. Ordinary differential equations and dynamical systems. *Graduate Studies in Mathematics*, 140, 2012.

[17] Jin X. Riedel-Kruse I.H. Glass, D.S. Nonlinear delay differential equations and their application to modeling biological network motifs. *Nat Commun*, 12:1788, 2021.

[18] D. A. Larson. Transient bounds and time-asymptotic behavior of solutions to nonlinear equations of fisher type. *Society for Industrial and Applied Mathematics*, 34:93 103, 1978.

[19] Pavel Levi, Decio. Winternitz. Painleve transcendents: Their asymptotics and physical applications. *Physics Series B*, 278, 1992.

[20] Scott McCue et al. Exact sharp-fronted travelling wave solutions of the fisher-kpp equation. *1School of Mathematical Sciences, Queensland University of Technology*, 2020.

[21] Mehdi Bastani et al. A numerical treatment of fisher equation. *Procedia Engineering*, 127: 1256 1262, 2015.

[22] Shahid Hasnain et al. Numerical study of one dimensional fishers kpp equation with finite difference schemes. *American Journal of Computational Mathematics*, 7(1), 2017.

[23] Murat Sari et al. High-order finite difference schemes for the solution of the generalized burgers–fisher equation. *Int. J. Numer. Meth. Biomed. Engng.*, 27:1296 1308, 2011.

[24] HINA MUJAHID et al. Numerical solution of fisher's equation by using meshless method of lines. *PJCIS.*, 1:29 42, 2016.

[25] Mehdi Bastani et al. A highly accurate method to solve fisher's equation. *Pramana-Journal of Physics*, 78:335 346, 2012.

[26] Weber R. Tang, S. Numerical study of fisher's equation by a petrov-galerkin finite element method. *The ANZIAM Journal*, 33(1):27 38, 1991.

[27] Kamel Al-Khaled. Numerical study of fisher's reaction–diffusion equation by the sinc collocation method. *Journal of Computational and Applied Mathematics*, 137(2):245 255, 2001.

[28] K.M. Agbavon et al. On the numerical solution of fisher's equation with coefficient of diffusion term much smaller than coefficient of reaction term. *Advances in Difference Equations*, 146, 2019.

[29] Julyan H. E. Cartwright Oreste Piro. The dynamics of runge–kutta methods. *Int. J. Bifurcation and Chaos*, 2:427 449,, 1992.

[30] M.E. Hosea and L.E Shampine. Analysis and implementation of tr-bdf2. *Applied Numerical Mathematics*, 20:21–37, 1996.

[31] P. Painlevé. Sur les équations différentielles du second ordre et d'ordre supérieur dont l'intégrale générale est uniforme. *Acta Math*, 25(1):1–85, 1902.

[32] B. Gambier. Sur les équations différentielles du second ordre et du premier degré dont l'intégrale générale est a points critiques fixes. *Acta Math*, 33(1):1–55, 1910.

[33] R. Fuchs. Über lineare homogene differentialgleichungen zweiter ordnung mit drei im endlichen gelegenen wesentlich singulären stellen. *Math. Ann.*, 63(3):301–321, 1907.

[34] R. Fuchs. Über lineare homogene differentialgleichungen zweiter ordnung mit drei im endlichen gelegenen wesentlich singulären stellen. *Math. Ann.*, 70(4):525–549, 1911.

[35] Edward L Ince. Ordinary differential equations. *Dover*, 1956.

[36] P. A. Clarkson. Orthogonal polynomials and special functions. *Lecture Notes in Mathematics*, 1817:331–400, 2003.

[37] C.A. Tracy and H. Widom. Level-spacing distributions and the airy kernel. *Comm. Math. Phys.*, 159:151–174, 1994.

[38] C.A. Tracy and H. Widom. Level-spacing distributions and the bessel kernel. *Comm. Math. Phys.*, 161:289–310, 1994.

[39] Y. Mori M. Jimbo, T. Miwa and M. Sato. Density matrix of an impenetrable bose gas and the fifth painlev´e transcendent. *Physica*, D1:80–158, 1980.

[40] K. Okamoto. Studies on the painlev´e equations iii. second and fourth painlev´e equations, pii and piv. *Math. Ann.*, 275:221–225, 1986.

[41] K. Okamoto. Studies on the painlev´e equations i. sixth painlev´e equation pvi. *Ann. Mat. Pura Appl.*, 146:337–381, 1987.

[42] K. Okamoto. Studies on the painlev´e equations ii. fifth painlev´e equation pv. *Japan. J. Math.*, 13:47–76, 1987.

[43] K. Okamoto. Studies on the painlev´e equations iv. third painlev´e equation piii. *Funkcial. Ekvac.*, 30:305–332, 1987.

[44] Maciej Dunajski. Integrable systems lecture notes. *Department of Applied Mathematics and Theoretical Physics University of Cambridge*, 2012.

[45] H. Flaschka and A. C. Newell. Monodromy- and spectrum-preserving deformations. i. *Comm. Math. Phys.*, 76:65–116, 1980.

[46] M. J. Ablowitz and P. A. Clarkson. Solitons, nonlinear evolution equations and inverse scattering. *London Mathematical Society Lecture Note Series*, 149, 1991.

[47] A. A. Kapaev A. S. Fokas, A. R. Its and V. Yu. Novokshenov. Painlevé transcendents: The riemann-hilbert approach, mathematical surveys and monographs. *Mathematical Surveys and Monographs*, 128, 2006.

[48] Ashok Das. Integrable models. *World Scientific Lecture Notes in Physics*, 30, 1989.

[49] M. J. Ablowitz and H. Segur. Exact linearization of a painlevé transcendent. *Phys. Rev. Lett.*, 38:1103–1106, 1977.

[50] A. Ramani M. J. Ablowitz and H. Segur. A connection between nonlinear evolution equations and ordinary differential equations of p-type. i. *J. Math. Phys.*, 21:715–721, 1980.

[51] A. Ramani M. J. Ablowitz and H. Segur. A connection between nonlinear evolution equations and ordinary differential equations of p-type. ii. *J. Math. Phys.*, 21:1006–1015, 1980.

[52] P. A. Clarkson A. P. Bassom and A. C. Hicks. On the application of solutions of the fourth painlevé equation to various physically motivated nonlinear partial differential equations. *Adv. Differential Equations*, 1:175–198, 1996.

[53] A. Ramani H. Segur M. J. Ablowitz. Nonlinear evolution equations and ordinary differential equations of painlevè type. *Lettere al Nuovo Cimento*, 23:333–338, 1978.

[54] G. Mahoux. Introduction to the theory of isomonodromic deformations of linear ordinary differential equations with rational coefficients. *The Painlevé Property. CRM Series in Mathematical Physics. Springer, New York, NY*, page 35–76, 1999.

[55] Philip Boalch. Symplectic manifolds and isomonodromic deformations. *Advances in Mathematics*, 163(2):137–205, 2001.

[56] Charles F. Doran. Algebraic and geometric isomonodromic deformations. *Journal of Differential Geometry*, 59(1):33–85, 2001.

[57] E.L. Ince. Ordinary differential equations. *Longmans, London*, 1927.

[58] Fedoryuk. Isomonodromy deformations of equations with irregular singularities. *Sbornik: Mathematics*, 71:463–479, 1992.

[59] Michio Jimbo et al. Monodromy preserving deformation of linear ordinary differential equations with rational coefficients. *Physica 2D*, pages 306–352, 1981.

[60] Ludwig Schlesinger. Über eine klasse von differentialsystemen beliebiger ordnung mit festen kritischen punkten. *Journal für die reine und angewandte Mathematik*, pages 96–145, 1912.

[61] K. Okamoto. Isomonodromic deformations, painlevé equations and the garnier system. *J. Fac. Sci. Univ. Tokyo, Sect. 1A, Math.*, 33:576–618, 1986.

[62] G.R.W. Quispel et al. Continuous symmetries of differential—difference equations: the kac—van moerbeke equation and painlevé reduction. *Physics Letters A*, 170:379—383, 1992.

[63] K M Tamizhmani et al. Integrability criteria for differential-difference systems: a comparison of singularity confinement and low-growth requirements. *J. Phys. A: Math. Gen.*, 32: 6679–6685, 1999.

[64] Ravil Yamilov. Symmetries as integrability criteria for differential difference equations. *J. Phys. A: Math. Gen.*, 39:541—623, 2006.

[65] Alexander Stokes. Singularity confinement in delay-differential painleve equations. *J. Phys. A: Math. Theor.*, 53, 2020.